

Astronomical Journal, submitted

***UBVRI* PHOTOMETRIC STANDARD STARS AROUND THE SKY AT -50 DEGREES DECLINATION**

Arlo U. Landolt¹

*Department of Physics & Astronomy, Louisiana State University, Baton Rouge, LA
70803-4001*

landolt@phys.lsu.edu

ABSTRACT

UBVRI photoelectric observations have been made of 109 stars around the sky, and centered more or less at -50 degrees declination. The majority of the stars fall in the magnitude range $10.4 < V < 15.5$, and in the color index range $-0.33 < (B - V) < +1.66$. These new broad-band photometric standard stars average 16.4 measures each from data taken on 116 different nights over a period of four years. Similar data are tabulated for 19 stars of interest, but which were not observed often enough to make them well-defined standard stars.

Subject headings: stars: standard — photometry: broad-band — photometry: standardization

1. Introduction

Accurate and readily accessible standard star sequences are necessary for the calibration of intensity and color data obtained for objects projected against the celestial sphere. Toward this end, this author has published sequences around the sky centered on the celestial equator (Landolt 1973, 1983, 1992).

¹Visiting Astronomer, Cerro Tololo Inter-American Observatory, National Optical Astronomical Observatories, which are operated by the Association of Universities for Research in Astronomy, under contract with the National Science Foundation.

Far southern declination photometric sequences, including Cousins early work, as summarized by Menzies et al. (1980), were published by Graham (1982), Menzies et al. (1989), and Kilkenny et al. (1998). A more complete history may be found in Landolt (2007). *UBVRI* photometry for a number of spectrophotometric standard stars has appeared in Landolt & Uomoto (2007).

2. Observations

The CTIO 1.5-m telescope together with a GaAs photomultiplier was assigned on 168 nights for the program in the time interval 1998-2001. Useful data were obtained on 116 whole or partial different nights, wherein 55% of the possible observing hours were photometric.

These broad-band *UBVRI* photometric observations all were obtained with the same RCA 31034A-02 photomultiplier mounted in KPNO cold box #53. The photomultiplier was operated at -1600 V . The sensitivity function of the photomultiplier was unavailable. Data for the same brand photomultiplier has been tabulated in Landolt (1992), Appendix B, Table 11, Figures 52-54.

The filter set was CTIO's *UBVRI* filter set #3. Information describing the composition of that filter set may be found in Landolt (1983, Table III). The transmission characteristics of those filters are tabulated in Landolt (1992, Appendix B).

Between 20 and 25 *UBVRI* standard stars, as defined by Landolt (1992), were observed each night together with the program stars. A night's observations began and ended with a group of four or five standard stars. Similar groups were observed periodically throughout the night. Each of these groups contained stars closely spaced on the sky, and possessing as wide a color range as possible. A more complete outline of the author's observing philosophy has been given in Landolt (2007).

A complete data set for a star consisted of a series of measures: *VBU_IIIRUBV*. A $14.0''$ diaphragm was used throughout the observing program. The integration or counting time depended upon the faintness of a particular star. The counting time never was less than ten seconds per filter, and was as long as 60 s for the faintest stars. Data reduction procedures followed the precepts outlined by Schulte & Crawford (1961) and by Landolt (2007).

Extinction coefficients were calculated from three or four standard stars possessing a range in color index that were followed from near the meridian over to an air mass of 2.1, or so. Each night's data were reduced using the primary extinction coefficients derived from

that night, whenever possible. Average secondary extinction coefficients for a given run were used. Examples of the range in extinction coefficients which an observer in fact encounters have been tabulated in Landolt (2007). Such tabulations should remind any observer of the perils in using mean extinction coefficients.

The final computer printout for each night’s reductions contained the magnitude and color indices for each of the standard stars. Since the time of observation was recorded for each measurement, it was possible to plot the residuals in the V magnitude and in the different color indices for each standard star against Universal Time for a given night. These plots permitted small corrections to be made to all program star measures. The corrections usually were less than a few hundredths of a magnitude. Such corrections took into account small changes in both atmospheric and instrumental conditions that occurred during the course of a night’s observations.

3. Discussion

A total of 128 stars, distributed around the sky, and more or less centered at -50 degrees declination, comprised this program. The data were reduced night by night. The results were tied into the $UBVRI$ photometric system defined by Landolt (1992).

A check on the accuracy of the magnitude and color index transformations was made via a comparison of the magnitudes and color indices of the stars from Landolt (1992) that were used as standard stars in this paper, with the magnitudes and color indices of these same standard stars obtained during this current program. The comparisons, the delta quantities, were in the sense of data from this program *minus* the corresponding magnitudes and color indices from Landolt (1992).

The V magnitude for the standard star Feige 108 shows an appreciable deviation in Figure 1 from the past. A suspected variable star number, NSV 26050, has been assigned based on a comment in Bergeron et al. (1984).

The V magnitude for the standard star G 163-51 shows an approximate 0.02 mag difference from the past. No suspected variable star number has been assigned, insofar as is known.

Figures 1 - 6 illustrate the plots of the delta quantities on the ordinates versus the color indices on the abscissas. Nonlinearities are apparent in the figures. Inspection of each figure allowed the nonlinear “break points” to be chosen. They are indicated below in association with the appropriate nonlinear transformation relation, which were derived by least-squares

fitting from the data appearing in Figures 1 - 6.

The non-linear transformation relations had the form, where a subscript “c” indicates “catalog” and subscript “obs” indicates “observed”, as follows:

$$\begin{aligned}
 (B - V)_c &= +0.00127 + 1.06192(B - V)_{obs} & (B - V) < +0.1, \\
 &\quad \pm 0.00154 \pm 0.00880 \\
 (B - V)_c &= +0.01091 + 0.99029(B - V)_{obs} & + 0.1 < (B - V) < +1.0, \\
 &\quad \pm 0.00106 \pm 0.00202 \\
 (B - V)_c &= +0.00781 + 0.99172(B - V)_{obs} & (B - V) > +1.0, \\
 &\quad \pm 0.00624 \pm 0.00485 \\
 (U - B)_c &= -0.03057 + 0.94734(U - B)_{obs} & (U - B) < -0.2, \\
 &\quad \pm 0.00923 \pm 0.01053 \\
 (U - B)_c &= -0.02134 + 1.02212(U - B)_{obs} & - 0.2 < (U - B) < +0.5, \\
 &\quad \pm 0.00157 \pm 0.00948 \\
 (U - B)_c &= -0.01422 + 1.02218(U - B)_{obs} & (U - B) > +0.5, \\
 &\quad \pm 0.01110 \pm 0.00868 \\
 V_c &= +0.00068 - 0.00536(B - V)_c + V_{obs} & (B - V) < +0.1, \\
 &\quad \pm 0.00129 \pm 0.00750 \\
 V_c &= +0.00002 + 0.00123(B - V)_c + V_{obs} & + 0.1 < (B - V) < +1.0, \\
 &\quad \pm 0.00114 \pm 0.00216 \\
 V_c &= -0.00244 + 0.00106(B - V)_c + V_{obs} & (B - V) > +1.0, \\
 &\quad \pm 0.00633 \pm 0.00515
 \end{aligned}$$

$(V - R)_c = +0.00030 + 1.00034(V - R)_{obs}$	$(V - R) < +0.1,$
$\pm 0.00052 \pm 0.00588$	
$(V - R)_c = -0.00052 + 1.00150(V - R)_{obs}$	$+ 0.1 < (V - R) < +0.5,$
$\pm 0.00101 \pm 0.00334$	
$(V - R)_c = -0.00387 + 1.00617(V - R)_{obs}$	$(V - R) > +0.5,$
$\pm 0.00237 \pm 0.00335$	
$(R - I)_c = -0.00129 + 0.99863(R - I)_{obs}$	$(R - I) < +0.1,$
$\pm 0.00098 \pm 0.00963$	
$(R - I)_c = -0.00118 + 1.00367(R - I)_{obs}$	$+ 0.1 < (R - I) < +0.5,$
$\pm 0.00114 \pm 0.00369$	
$(R - I)_c = -0.00254 + 1.00343(R - I)_{obs}$	$(R - I) > +0.5,$
$\pm 0.00185 \pm 0.00277$	
$(V - I)_c = -0.00215 + 0.98744(V - I)_{obs}$	$(V - I) < +0.1,$
$\pm 0.00289 \pm 0.01413$	
$(V - I)_c = +0.00014 + 0.99962(V - I)_{obs}$	$+ 0.1 < (V - I) < +1.0,$
$\pm 0.00123 \pm 0.00219$	
$(V - I)_c = -0.00587 + 1.00431(V - I)_{obs}$	$(V - I) > +1.0.$
$\pm 0.00310 \pm 0.00227$	

After the above relations were applied to the recovered magnitudes and color indices of the standard stars used in this project, the data were on the broadband *UBVRI* photometric system defined by the standard stars in Landolt (1992). Next the standard star magnitudes and color indices, now corrected for nonlinear transformation, once again were compared

to the published values in the sense of corrected values minus published magnitudes and color indices. The fact that the nonlinear effects were corrected successfully is illustrated in Figures 7 - 12. Therefore, the data in this paper have been transformed to the photometric system defined in Landolt (1992).

The final magnitudes and color indices for the new standard stars resulting from this program are tabulated in Table 1. Each star was observed an average of 16.4 times on an average 9 nights. Finding charts are provided via Figures 13 - 27. The coordinates in Table 1 were taken from the UCAC2 catalog (Zacharias et al. 2004) when possible. Positions for stars not in the UCAC2 catalog were taken from the 2MASS Point Source Catalog which coordinates came from the Two Micron All Sky survey (2MASS; Skrutskie et al. 2006).

Columns (4)-(9) in Table 1 give the final magnitude and color indices in the *UBVRI* photometric system as defined by Landolt (1992). Column (10) indicates the number of times n that each star was observed. Column (11) gives the number of nights m that each star was observed. The numbers in columns (4)-(9) are mean magnitudes and color indices. Hence, the errors tabulated in columns (12)-(17) are mean errors of the mean magnitude and color indices (see Landolt 1983, p. 450).

The stars in the WD 1153-484 sequence are of interest because they encompass a good range in color. However, there are insufficient measures, on average, for the stars to make the sequence as robust as one would like. The number of measures is fewer than had been anticipated because during the reduction and analysis, two nights of data had to be rejected apparently due to thin cirrus.

The numerical size of the average mean error of a single observation of a V magnitude or a color index for the 109 new standard stars in Table 1 is given in the second column of Table 2. The last column shows the average mean error of the mean observed magnitude or color index. Errors in the second column for a single observation are as large as they are for $(U - B)$, $(R - I)$, and $(V - I)$ since red stars are faint in U and blue stars are faint in I .

While accurate coordinates for individual stars are necessary in many circumstances, modern area detectors need knowledge of the coordinate center of a photometric sequence. Table 3 provides the coordinate centers for the new *UBVRI* photometric sequences listed in Table 1. The field name is based on a blue star chosen from the literature, or recommended by a colleague, with the exception of the T Phe field. T Phe is a Mira variable (= HD 2725 = CD-47 131 = CPD-47 50 = GSC 08024-01000). The current T Phe sequence has been enlarged from the sequence initially published in Landolt (1992).

Isolated stars were measured on occasion as potential standard stars. Several of them have just enough measures to be usable as standard stars, but a sequence never materialized

in their vicinity. Others have just too few data to be used as standards. However, their *UBVRI* magnitudes and color indices may be of use for other purposes. Final data for these stars are given in Table 4, where the column headings have the same explanation and their content the same basis as in Table 1. Finding charts for these isolated stars may be found in Figures 28 - 46.

The magnitude distribution of all the stars studied in this paper, that is, a combination of stars in Tables 1 and 4, is plotted in Figure 47 in 0.25 *V* magnitude bins. Figure 48 shows the (*B* − *V*) color index range in 0.1 magnitude bins for all the stars studied in this paper.

Figures 49 - 55 have been plotted using data for the new standard stars in Table 1. These figures show the mean error of a mean magnitude or color index, plotted as a function of magnitude or color index.

Figures 56 and 57 illustrate the [(*U* − *B*), (*B* − *V*)] and [(*V* − *R*), (*R* − *I*)] color-color plots for all stars measured in this paper, respectively, with stars from Table 1 plotted as filled circles and stars from Table 4 as open circles.

Cross-identifications are provided in Table 5. On occasion the very best coordinate and proper motion information is needed for standard stars. Hence, Table 5 presents the most recent coordinates and proper motions for the new standard stars in Table 1 and the isolated stars in Table 4. All coordinates are for the epoch J2000.0. The 2MASS Point Source Catalog (PSC) positions come from The Two Micron All Sky Survey (2MASS; Skrutskie et al. 2006). The UCAC2 positions come from The Second USNO CCD Astrograph Catalog (Zacharias et al. 2004). Spectral types are given where available.

4. Comments on Individual Stars

The numbering system for the stars labeled with LB (Luyten Blue) is described in Luyten (1956).

The numbering system for the stars labeled with JL arises from the observations of Jaidee & Lynga (1969). These authors provide coordinates and star charts resulting from their search for ‘faint violet stars.’

The LSE numbering system originated with Drilling (1983).

The LSS numbering system originated with the publication of the catalog Luminous Stars in the Southern Milky Way (Stephenson & Sanduleak 1971).

The MCT stars (Montreal-Cambridge-Tololo) initially were discussed by Demers et al.

(1986) and Demers et al. (1987). CCD sequences used to calibrate the MCT fields appeared in Demers et al. (1993a,b). An initial set of photometry and charts for a selected subset of the MCT stars themselves appeared in Lamontagne et al. (2000). However, a final summary paper listing all the MCT stars discovered in the survey has not appeared, because a large number of these stars lack spectroscopic data (Demers 2007; Lamontagne 2007).

The nomenclature for the EC stars was defined in the Edinburgh-Cape survey (Kilkenny et al. 1991).

The nomenclature GJ pertains to stars in the Gliese & Jahreiß (1979) catalog of nearby stars.

The *Hubble Space Telescope* Guide Star Catalog (GSC) acronym first appeared in Lasker et al. (1990).

The NVS terminology began with the New Catalog of Suspected Variable Stars (Kukarkin & Kholopov 1982). One most easily now can access variable and suspected variable star information by entering the Sternberg Astronomical Institute's webpage at <http://www.sai.msu.edu>, and clicking on the “GCVS Research Group” (General Catalog of Variable Stars), and then going to the appropriate catalog.

The WD numbering system exists for white dwarf stars. Excellent online sources of information for white dwarf stars include Jay Holberg's website at <http://procyon.lpl.arizona.edu/WD/> and G. McCook and E. Sion's website at <http://www.astronomy.villanova.edu/WDCatalog/index.html>. A print description of the latter is in McCook & Sion (1999).

Expanded comments, in the sense of increasing right ascension, follow for individual stars which appear in both Tables 1 and 4:

JL 163B [= USNO-B1.0 0397-0001111 = USNO-A2.0 0375-00050408 = GSC2.2 S0120011284]

JL 163 [= GSC 08028-00524]

JL 166 [= GSC 08022-01020]

T Phe B [= RW Phe = AN 409.1929 = CD-47 128 = GSC 08024-00363] See note 1, Table 2 in Landolt (1992). Discovered by Dartayet (1929). T Phe B is sequence star “h” for variable star T Phe in Fleming & Pickering (1907) and Campbell & Pickering (1913).

T Phe F [= GSC 08024-00830 = NSV 184] See comment by Dartayet (1929) that the T Phe sequence star “h¹” might be variable. The sequence is in Fleming & Pickering (1907) and Campbell & Pickering (1913). The AAVSO (d) chart for T Phe (002546), plotted at a scale of 20'' = 1mm, is based on Fleming & Pickering (1907) and Campbell & Pickering (1913).

T Phe F here is the star marked as 132 on the AAVSO chart.

JL 194 [= CD-48 106 = LB 1559 = GSC 08024-00844 = HIP 2499] Found to be a blue star by Luyten & Anderson (1958). The *Hipparcos* Catalog flagged JL 194 as a variable star, indicating a variability range between 0.06 and 0.60 magnitude. The flag indicates that the photometry quoted was ground-based. The photometry of Hill & Hill (1966) differs from that herein (with their $V = 12.36$), but one could say that their and the current photometry agrees, given Hill and Hill's quoted errors of 0.04 magnitude in V and 0.03 magnitude in the color indices. A more concordant value of $V = 12.41$ is given in Kilkenny & Hill (1975). A “near V ” magnitude of 12.33 is quoted by Newell (1973). Newell & Graham (1976) present a Strömgren y magnitude of 12.45. UBV photometry of Wegner (1980) essentially agrees with the current results. After a review of the literature, then, and given that the current photometry was obtained over a two year interval, JL 194 appears to be constant in brightness.

JL 202 [= CPD-55 142 = LB 1566 = GSC 08469-00387] Found to be a blue star by Luyten & Anderson (1958). A search for nebular emission around JL 202 (Mendez et al. 1988) found none. Nevertheless, Kohoutek (1997) indicated that JL 202 might be a possible post-planetary nebulae, citing only Mendez et al. Photometry from Hill & Hill (1966) and from Wegner (1980) bracket the new photometry herein, thereby indicating the likelihood of long term constancy in brightness for JL 202.

GD 679 [BPM 46934 = BPS CS 30316-0011 = GSC 06999-02080 = WD 0104-33] Appeared in the “Bruce Proper Motion Survey” (Luyten 1963). Identified as a white dwarf suspect (Giclas et al. 1972). Appears in Lamontagne et al. (2000) as MCT 0104-3336.

JL 236 [= GSC 08474-00031]

JL 261 [= LB 3229 = GSC 08047-00420] Initially cataloged as a blue star by Luyten & Anderson (1959). Wegner (1980) has photometry in fair agreement, considering his quoted errors, compared with the new photometry herein. However, the photometry herein consists only of one measurement.

LB 3241 [= GSC 08045-00656 = JL 285 = NSV 759] Identified as a faint blue star by Luyten & Anderson (1959). The first measured proper motion for LB 3241 was recorded by Luyten (1962). Kilkenny & Hill (1975) found a variation of 0.12 mag in V .

JL 286 [= GSC 08048-00322]

LB 1735 [= EC 04300-5341 = USNO-A1.0 0300-01365856] Identified as a faint blue star by Luyten & Anderson (1958). The first measured proper motion for LB 1735 was recorded by Luyten (1962). Beers et al. (2001) classify LB 1735 as a horizontal-branch B-type (HBB)

star. They report UBV photometry of $V = 13.66$, $(B - V) = -0.17$, and $(U - B) = -0.59$, with errors of two to three percent.

LB 1735 E The mean error of a single observation in V is 0.038, a bit high. The star may bear watching for possible variability.

L745-46A [= LPM 269 = GJ 283A] Discovered by Luyten (1941) to be a high proper motion star, and cataloged by Luyten as L745-46 in the “Bruce Proper Motion Survey”, and as BPM 72393 (Luyten 1963). Now known to be a common proper motion pair with modern astrometric information ($\mu = 1.2613''/yr$ at a position angle of 116.3°) published by Costa et al. (2005). Inspection showed that their V magnitude is some 0.03 mag fainter than the author’s in Table 4 in this paper. Another example of photometry in the literature is by Eggen (1969): $V = 12.98$, $(B - V) = +0.29$, $(U - B) = -0.61$. The fainter red member, L745-46B, was not measured in this program. Both components are identified in Figure 36 with a straight line at a position angle of 116° indicating their approximate direction of motion, but not the size of the motion. L745-46A will move along this line a distance equal to the length of the scale marked at the bottom of the figure in 48 years. The epoch of the image in Figure 36 is 1983.02 (The author is indebted to B. Skiff (2007) for ferreting this information from the literature.).

LSS 982 [= CD-40 3927 = CPD-40 2185] First was identified in a survey of luminous stars in the southern Milky Way (Stephenson & Sanduleak 1971).

WD 0830-535 [= GSC 08568-02947 = L 245-50 (Luyten & Smith 1958) = BPM 19061 (Luyten 1963)] Eggen (1969) gave $V = 14.47$, $(B - V) = -0.15$, and $(U - B) = -1.15$ in reasonable agreement with the values in Table 1 herein. Luyten (1963) found proper motion components $\mu = 0.167''$ and $\theta = 166^\circ$.

LSS 1275 [= CD-45 5058 = CPD-45 3655 = HIP 45789 = GSC 08166-01456] This paper only has two photometric measurements made on one night for LSS 1275, but since the star is bright at $V = 11.417$, those two measures should have value. Also, the logbook noted that the night was photometric. However, photometry in the literature indicates considerable differences as compared with that in Table 4 herein. Klare & Neckel (1977) found $V = 11.33$, $(B - V) = -0.31$, $(U - B) = -1.21$; Denoyelle (1977) found $V = 11.36$, $(B - V) = -0.32$, $(U - B) = -1.24$; and, Schild et al. (1983) found $V = 11.32$, $(B - V) = -0.32$, $(U - B) = -1.19$. The *Hipparcos Catalog* (HIP 45789) provides a variability range of 0.2 mag. A comparison of these various magnitudes indicates the possibility of variability. One must remember, though, that each of the magnitudes quoted is based on only a couple measures.

LSS 1362 [= PN G273.6+06.1] Found by Drilling (1983) to be a subluminous O star. Heber & Drilling (1984) found it to be a planetary nebula, further studied by Mendez et al.

(1988).

WD 1056-384 [= GSC 07724-01874 = 2RE J105818-384423 (Mason et al. 1995) = EUVE J1058-387 (Vennes et al. 1996)] Pye et al. (1995) give a DA spectral type. Mason et al. (1995) quote $V = 13.5$ from the *HST* Guide Star Catalog V.1.1, which Vennes et al. (1996) convert to a “photoelectric” $V = 14.08$.

WD 1153-484 [= L 325-214 (Luyten & Smith 1958) = BPM 36430 (Luyten 1963) = UCAC2 10852635] (Hintzen & Jensen 1979) determined a DA spectral type. Eggen (1969) found $V = 12.85$, $(B - V) = -0.205$, and $(U - B) = -1.01$.

LSE 44 [= GSC 08267-02418] Found by Drilling (1983) to be a subluminous O star.

LSE 153 [= CD-46 8926 = CPD-46 6542 = GSC 08263-02213] Found by Drilling (1983) to be a subluminous O star.

LSE 125 [= GSC 07837-01483 = PN G335.5+12.4 (planetary nebula)] Found by Drilling (1983) to be a subluminous O star.

LSE 259 [= GSC 08730-00028] Found by Drilling (1983) to be a subluminous O star.

LSE 234 [= CPD-64 3829 = GSC 09063-01610 = NSV 24315] Found by Drilling (1983) to be a subluminous O star. With regard to NSV 24315, Kukarkin & Kholopov (1982) online at <http://www.sai.msu.su/groups/cluster/gcvs/gcvs/nsvsup/ref.txt> only lead to a preprint not locatable.

LSE 263 [= CD-51 11879 = GSC 08386-01370] Found by Drilling (1983) to be a subluminous O star.

JL 25 [= GSC 09459-01325]

MCT 2019-4339 [= CS 22943-127 (Beers et al. 1992)] Beers et al. (1992) give a spectral type of sdO.

JL 82 [= GSC 09331-00373 = EC 21313-7301]

JL 117 [= GSC 09340-00915]

LB 1516 [= GSC 08451-00403 = UCAC2 11226102] Identified as a faint blue star by Luyten & Anderson (1958). The first measured proper motion for LB 1516 was recorded by Luyten (1962).

It always is a pleasure to acknowledge the staff of the CTIO for their hospitality and assistance! Individuals always available to help in anyway include A. Alvarez, E. Cosgrove, M. Fernandez, A. Gomez, A. Guerra, R. Leiton, D. Maturana, A. Perez, S. Pizarro, D.

Rojas, O. Saa, N. Saavedra, E. Schmidt, H. Tirado, P. Ugarte, R. Venegas, and A. Zuniga. Thanks go to John Drilling for calling the blue LSE stars to the author's attention, and to Serge Demers for providing preliminary charts for the MCT star fields. Todd J. Henry and Wei-Chen Jao provided a modern finding chart for L745-46A. Brian Skiff updated the author with techniques to ensure that the coordinates and proper motions are modern and accurate. The appearance of this paper's figures and tables are due to the skills of James L. Clem. The author is indebted to the referee, M. S. Bessell, for his helpful comments. This observational program has been supported by NSF grants AST 9528177, AST-0097895, and AST-0503871.

REFERENCES

- Beers, T. C., Doinidis, S. P., Griffin, K. E., Preston, G. W., & Shectman, S. A. 1992, AJ, 103, 267
- Beers, T. C., Rossi, S., O'Donoghue, D., Kilkenny, D., Stobie, R. S., Koen, C., & Wilhelm, R. 2001, MNRAS, 320, 451
- Bergeron, P., Fontaine, G., Lacombe, P., Wesemael, F., Crawford, D. L., & Jakobsen, A. M. 1984, AJ, 89, 374
- Campbell, L., & Pickering, E. C. 1913, Annals of Harvard College Observatory, 63, 143
- Costa, E., Méndez, R. A., Jao, W.-C., Henry, T. J., Subasavage, J. P., Brown, M. A., Ianna, P. A., & Bartlett, J. 2005, AJ, 130, 337
- Dartayet, M. 1929, AN, 237, 220
- Demers, S. 2007, private communication
- Demers, S., Beland, S., Kibblewhite, E. J., Irwin, M. J., & Nithakorn, D. S. 1986, AJ, 92, 878
- Demers, S., Fontaine, G., Wesemael, F., Lamontagne, R., & Irwin, M. J. 1987, IAU Colloq. 95: Second Conference on Faint Blue Stars, 497
- Demers, S., Lamontagne, R., Wesemael, F., Fontaine, G., Barneoud, R., & Irwin, M. J. 1993a, A&AS, 99, 437
- Demers, S., Lamontagne, R., Wesemael, F., Fontaine, G., Barneoud, R., & Irwin, M. J. 1993b, A&AS, 99, 461

- Denoyelle, J. 1977, A&AS, 27, 343
- Drilling, J. S. 1983, ApJ, 270, L13
- Eggen, O. J. 1969, ApJ, 157, 287
- Fleming, W. P. S. M., & Pickering, E. C. 1907, Annals of Harvard College Observatory, 47, 1
- Giclas, H. L., Burnham, R., & Thomas, N. G. 1972, Lowell Observatory Bulletin, 7, 217
- Gliese, W., & Jahreiß, H. 1979, A&AS, 38, 423
- Graham, J. A. 1982, PASP, 94, 244
- Greenstein, J. L., & Sargent, A. I. 1974, ApJS, 28, 157
- Heber, U., & Drilling, J. S. 1984, Mitteilungen der Astronomischen Gesellschaft Hamburg, 62, 252
- Hill, P. W., & Hill, S. R. 1966, MNRAS, 133, 205
- Hintzen, P., & Jensen, E. 1979, PASP, 91, 492
- Jaidee, S., & Lynga, G., 1969, Arkiv for Astronomi, 5, 345
- Kilkenny, D. 1987, MNRAS, 228, 713
- Kilkenny, D., Heber, U., & Drilling, J. S. 1988, South African Astronomical Observatory Circular, 12, 1
- Kilkenny, D., & Hill, P. W. 1975, MNRAS, 173, 625
- Kilkenny, D., & Muller, S. 1989, South African Astronomical Observatory Circular, 13, 69
- Kilkenny, D., O'Donoghue, D., & Stobie, R. S. 1991, MNRAS, 248, 664
- Kilkenny, D., van Wyk, F., Roberts, G., Marang, F., & Cooper, D. 1998, MNRAS, 294, 93
- Klare, G., & Neckel, T. 1977, A&AS, 27, 215
- Kohoutek, L. 1997, Astronomische Nachrichten, 318, 35
- Kukarkin, B. V., & Kholopov, P. N. 1982, Moscow: Publication Office “Nauka”, 1982
- Lamontagne, R. 2007, private communication

- Lamontagne, R., Demers, S., Wesemael, F., Fontaine, G., & Irwin, M. J. 2000, AJ, 119, 241
- Landolt, A. U. 1973, AJ, 78, 959
- Landolt, A. U. 1983, AJ, 88, 439
- Landolt, A. U. 1992, AJ, 104, 340
- Landolt, A. U. 2007, The Future of Photometric, Spectrophotometric, and Polarimetric Standardization, C. Sterken, Editor, ASP Conference Series, 364, 27
- Landolt, A. U., & Uomoto, A. K. 2007, AJ, 133, 768
- Lasker, B. M., Sturch, C. R., McLean, B. J., Russell, J. L., Jenkner, H., & Shara, M. M. 1990, AJ, 99, 2019
- Luyten, W. J. 1941, Publications of the Astronomical Observatory University of Minnesota, 3, 1
- Luyten, W. J. 1956, AJ, 61, 261
- Luyten, W. J. 1962, A Search for Faint Blue Stars, No. 29 (Minneapolis: University of Minnesota)
- Luyten, W. J. 1963, Bruce proper motion survey. The general catalog (vol 1,2). (1963)
- Luyten, W. J., & Anderson, J. H. 1958, A Search for Faint Blue Stars, No. 12 (Minneapolis: University of Minnesota)
- Luyten, W. J., & Smith, J. A. 1958, A Search for Faint Blue Stars, No. 16 (Minneapolis: University of Minnesota)
- Luyten, W. J., & Anderson, J. H. 1959, A Search for Faint Blue Stars, No. 18 (Minneapolis: University of Minnesota)
- Mason, K. O., et al. 1995, MNRAS, 274, 1194
- McCook, G. P., & Sion, E. M. 1999, ApJS, 121, 1
- Mendez, R. H., Gathier, R., Simon, K. P., & Kwitter, K. B. 1988, A&A, 198, 287
- Menzies, J. W., Banfield, R. M., & Laing, J. D. 1980, South African Astronomical Observatory Circular, 1, 149

- Menzies, J. W., Cousins, A. W. J., Banfield, R. M., & Laing, J. D. 1989, South African Astronomical Observatory Circular, 13, 1
- Monet, D. G., et al. 2003, AJ, 125, 984
- Newell, E. B. 1973, ApJS, 26, 37
- Newell, B., & Graham, J. A. 1976, ApJ, 204, 804
- Platais, I., et al. 1998, AJ, 116, 2556
- Platais, I., Melo, C., Mermilliod, J.-C., Kozhurina-Platais, V., Fulbright, J. P., Méndez, R. A., Altmann, M., & Sperauskas, J. 2007, A&A, 461, 509
- Pye, J. P., et al. 1995, MNRAS, 274, 1165
- Schulte, D. H. & Crawford, D. L. 1961, Kitt Peak Nat. Obs. Cont., No 10, 1.
- Schild, R. E., Garrison, R. F., & Hiltner, W. A. 1983, ApJS, 51, 321
- Skiff, B. 2007, private communication
- Skrutskie, M. F., et al. 2006, AJ, 131, 1163
- Stephenson, C. B., & Sanduleak, N. 1971, Publications of the Warner & Swasey Observatory, 1, 1
- Vennes, S., Thejll, P. A., Wickramasinghe, D. T., & Bessell, M. S. 1996, ApJ, 467, 782
- Wegner, G. 1980, AJ, 85, 538
- Zacharias, N., Urban, S. E., Zacharias, M. I., Wycoff, G. L., Hall, D. M., Monet, D. G., & Rafferty, T. J. 2004, AJ, 127, 3043

Table 1. *UBVRI* Photometry of Standard Stars Near -50° Degrees Declination

Star	α (2000)			δ $^{\circ}$ $'$ $''$	V	$B - V$	$U - B$	$V - R$	$R - I$	$V - I$	n	m	V	Mean Error of the Mean				
	h	m	s											$B - V$	$U - B$	$V - R$	$R - I$	$V - I$
JL 163B	00	10	24.88	$-50^{\circ} 13' 55.6''$	15.554	+1.077	+1.053	+0.665	+0.560	+1.226	24	13	0.0033	0.0065	0.0241	0.0037	0.0094	0.0096
JL 163A	00	10	26.309	$-50^{\circ} 15' 03.52''$	12.927	+0.524	-0.058	+0.317	+0.315	+0.632	21	12	0.0033	0.0028	0.0041	0.0020	0.0022	0.0028
JL 163	00	10	33.221	$-50^{\circ} 15' 24.37''$	12.963	-0.240	-1.006	-0.122	-0.158	-0.278	20	11	0.0027	0.0020	0.0042	0.0016	0.0027	0.0036
JL 163C	00	10	38.238	$-50^{\circ} 15' 26.39''$	14.391	+0.828	+0.369	+0.458	+0.433	+0.892	21	11	0.0017	0.0046	0.0096	0.0022	0.0050	0.0061
JL 163D	00	10	41.62	$-50^{\circ} 13' 45.6''$	14.300	+0.896	+0.695	+0.520	+0.444	+0.967	21	11	0.0022	0.0044	0.0098	0.0022	0.0041	0.0050
JL 163E	00	10	58.017	$-50^{\circ} 14' 17.44''$	13.544	+0.699	+0.218	+0.389	+0.362	+0.752	18	10	0.0038	0.0049	0.0111	0.0019	0.0042	0.0035
JL 163F	00	11	00.225	$-50^{\circ} 12' 53.81''$	12.638	+0.808	+0.361	+0.448	+0.430	+0.881	18	9	0.0012	0.0021	0.0052	0.0009	0.0019	0.0021
TPhe I	00	30	04.593	$-46^{\circ} 28' 10.17''$	14.820	+0.764	+0.338	+0.422	+0.395	+0.817	25	13	0.0026	0.0032	0.0072	0.0036	0.0098	0.0110
TPhe A	00	30	09.594	$-46^{\circ} 31' 28.91''$	14.651	+0.793	+0.380	+0.435	+0.405	+0.841	29	12	0.0028	0.0046	0.0071	0.0019	0.0035	0.0032
TPhe H	00	30	09.683	$-46^{\circ} 27' 24.30''$	14.942	+0.740	+0.225	+0.425	+0.425	+0.851	23	12	0.0029	0.0029	0.0071	0.0035	0.0077	0.0098
TPhe B	00	30	16.313	$-46^{\circ} 27' 58.57''$	12.334	+0.405	+0.156	+0.262	+0.271	+0.535	29	17	0.0115	0.0026	0.0039	0.0020	0.0019	0.0035
TPhe C	00	30	16.98	$-46^{\circ} 32' 21.4''$	14.376	-0.298	-1.217	-0.148	-0.211	-0.360	39	23	0.0022	0.0024	0.0043	0.0038	0.0133	0.0149
TPhe D	00	30	18.342	$-46^{\circ} 31' 19.85''$	13.118	+1.551	+1.871	+0.849	+0.810	+1.663	37	23	0.0033	0.0030	0.0118	0.0015	0.0023	0.0030
TPhe E	00	30	19.768	$-46^{\circ} 24' 35.60''$	11.631	+0.443	-0.103	+0.276	+0.283	+0.564	38	10	0.0017	0.0013	0.0025	0.0007	0.0016	0.0020
TPhe J	00	30	23.02	$-46^{\circ} 23' 51.6''$	13.434	+1.465	+1.229	+0.980	+1.063	+2.043	28	15	0.0023	0.0043	0.0059	0.0011	0.0015	0.0011
TPhe F	00	30	49.820	$-46^{\circ} 33' 24.07''$	12.475	+0.853	+0.534	+0.492	+0.437	+0.929	19	10	0.0008	0.0024	0.0095	0.0005	0.0014	0.0029
TPhe K	00	30	56.315	$-46^{\circ} 23' 26.04''$	12.935	+0.806	+0.402	+0.473	+0.429	+0.909	2	2	0.0007	0.0007	0.0163	0.0007	0.0001	0.0007
TPhe G	00	31	04.303	$-46^{\circ} 22' 51.35''$	10.447	+1.545	+1.910	+0.934	+1.086	+2.025	20	10	0.0008	0.0011	0.0049	0.0008	0.0016	0.0017
MCT 0401–4017E	04	02	28.087	$-40^{\circ} 09' 35.57''$	10.636	+0.527	+0.040	+0.307	+0.299	+0.606	20	10	0.0020	0.0011	0.0027	0.0011	0.0011	0.0016
MCT 0401–4017F	04	02	29.559	$-40^{\circ} 10' 21.19''$	12.990	+0.790	+0.380	+0.441	+0.400	+0.841	20	9	0.0013	0.0018	0.0042	0.0011	0.0022	0.0018
MCT 0401–4017D	04	02	55.219	$-40^{\circ} 15' 52.60''$	11.947	+0.549	+0.045	+0.319	+0.304	+0.623	20	11	0.0020	0.0018	0.0029	0.0013	0.0020	0.0020
MCT 0401–4017	04	03	04.540	$-40^{\circ} 09' 41.05''$	14.418	-0.272	-1.180	-0.141	-0.156	-0.291	21	11	0.0022	0.0017	0.0055	0.0035	0.0131	0.0151
MCT 0401–4017A	04	03	05.195	$-40^{\circ} 11' 02.88''$	10.709	+0.562	+0.001	+0.328	+0.321	+0.649	21	11	0.0024	0.0013	0.0041	0.0011	0.0022	0.0022
MCT 0401–4017B	04	03	29.846	$-40^{\circ} 10' 58.46''$	12.654	+0.506	-0.092	+0.315	+0.319	+0.633	20	11	0.0025	0.0031	0.0056	0.0013	0.0020	0.0020
MCT 0401–4017C	04	03	34.273	$-40^{\circ} 07' 02.53''$	12.395	+0.906	+0.589	+0.551	+0.524	+1.075	21	11	0.0028	0.0020	0.0041	0.0011	0.0020	0.0022
LB 1735	04	31	11.090	$-53^{\circ} 35' 27.06''$	13.634	-0.142	-0.632	-0.059	-0.098	-0.157	27	15	0.0017	0.0023	0.0029	0.0017	0.0064	0.0067
LB 1735A	04	31	19.438	$-53^{\circ} 34' 38.22''$	13.906	+0.589	-0.004	+0.339	+0.334	+0.672	20	11	0.0025	0.0036	0.0051	0.0018	0.0029	0.0034
LB 1735B	04	31	22.810	$-53^{\circ} 36' 36.85''$	14.542	+0.675	+0.126	+0.379	+0.361	+0.741	17	9	0.0032	0.0046	0.0051	0.0022	0.0053	0.0063
LB 1735F	04	31	37.11	$-53^{\circ} 36' 53.4''$	15.205	+0.402	-0.206	+0.265	+0.290	+0.556	27	14	0.0035	0.0031	0.0052	0.0046	0.0106	0.0131
LB 1735E	04	31	42.303	$-53^{\circ} 36' 18.48''$	13.759	+0.706	+0.242	+0.399	+0.362	+0.760	21	11	0.0083	0.0028	0.0063	0.0020	0.0044	0.0055
LB 1735C	04	31	49.652	$-53^{\circ} 34' 37.52''$	12.765	+0.459	-0.052	+0.290	+0.297	+0.587	20	11	0.0034	0.0034	0.0047	0.0016	0.0022	0.0029
LB 1735D	04	31	58.253	$-53^{\circ} 34' 52.52''$	14.184	+0.657	+0.099	+0.383	+0.383	+0.765	17	9	0.0034	0.0024	0.0051	0.0022	0.0063	0.0078
LB 1735G	04	31	46.194	$-53^{\circ} 39' 47.89''$	13.446	+1.276	+1.241	+0.815	+0.701	+1.516	26	14	0.0020	0.0071	0.0008	0.0018	0.0008	0.0018
MCT 0436–4616A	04	38	20.929	$-46^{\circ} 09' 27.54''$	12.089	+0.504	-0.014	+0.296	+0.285	+0.581	5	3	0.0009	0.0040	0.0063	0.0018	0.0036	0.0027
MCT 0436–4616	04	38	27.320	$-46^{\circ} 10' 52.69''$	13.823	-0.213	-1.153	-0.032	-0.015	-0.048	8	5	0.0032	0.0032	0.0053	0.0021	0.0120	0.0117
MCT 0436–4616B	04	38	47.374	$-46^{\circ} 10' 08.74''$	13.522	+0.448	-0.194	+0.284	+0.312	+0.596	5	3	0.0040	0.0049	0.0089	0.0049	0.0058	0.0089
MCT 0550–4911E	05	51	43.660	$-49^{\circ} 10' 48.59''$	13.671	+1.300	+1.429	+0.831	+0.711	+1.544	16	8	0.0040	0.0078	0.0935	0.0022	0.0025	0.0040
MCT 0550–4911D	05	51	49.207	$-49^{\circ} 11' 18.95''$	14.592	+0.732	+0.217	+0.406	+0.383	+0.701	15	9	0.0075	0.0065	0.0256	0.0044	0.0116	0.0127
MCT 0550–4911B	05	51	59.105	$-49^{\circ} 11' 25.06''$	14.683	+0.856	+0.530	+0.483	+0.427	+0.910	14	8	0.0067	0.0086	0.0061	0.0032	0.0061	0.0083
MCT 0550–4911	05	52	02.712	$-49^{\circ} 11' 22.38''$	14.355	-0.270	-1.219	-0.114	-0.175	-0.288	18	11	0.0057	0.0035	0.0042	0.0040	0.0139	0.0156
MCT 0550–4911C	05	52	03.98	$-49^{\circ} 09' 37.6''$	13.019	+0.588	+0.058	+0.343	+0.327	+0.670	14	8	0.0035	0.0032	0.0072	0.0024	0.0029	0.0045
MCT 0550–4911A	05	52	04.104	$-49^{\circ} 10' 48.55''$	14.255	+0.606	+0.020	+0.351	+0.340	+0.690	14	9	0.0032	0.0051	0.0059	0.0035	0.0045	0.0064
LSS 982G	08	10	19.984	$-40^{\circ} 31' 57.19''$	13.374	+0.542	+0.040	+0.329	+0.317	+0.647	15	8	0.0057	0.0036	0.0065	0.0023	0.0031	0.0036
LSS 982F	08	10	21.386	$-40^{\circ} 31' 30.31''$	11.623	+0.376	+0.035	+0.231	+0.228	+0.458	15	8	0.0057	0.0021	0.0031	0.0015	0.0026	0.0034

Table 1—Continued

Star	α (2000)			δ	V	$B - V$	$U - B$	$V - R$	$R - I$	$V - I$	n	m	V	Mean Error of the Mean						
	h	m	s	$^{\circ}$										$B - V$	$U - B$	$V - R$	$R - I$	$V - I$		
LSS 982E	08	10	29.667	-40	30	06.85	11.297	+1.086	+0.567	+0.494	+1.059	15	8	0.0039	0.0021	0.0046	0.0013	0.0026	0.0026	
LSS 982	08	10	31.719	-40	32	47.07	12.258	-0.331	-1.233	-0.143	-0.181	-0.323	20	11	0.0036	0.0018	0.0031	0.0016	0.0036	0.0042
LSS 982A	08	10	32.719	-40	31	14.52	12.292	+0.470	-0.009	+0.290	+0.287	+0.577	16	9	0.0022	0.0030	0.0038	0.0012	0.0028	0.0038
LSS 982B	08	10	34.325	-40	30	49.16	12.435	+0.468	-0.049	+0.297	+0.291	+0.587	16	9	0.0025	0.0018	0.0040	0.0018	0.0030	0.0038
LSS 982D	08	10	38.089	-40	28	20.84	11.648	+1.204	+0.934	+0.671	+0.626	+1.298	17	9	0.0044	0.0027	0.0056	0.0010	0.0029	0.0032
LSS 982C	08	10	38.222	-40	30	09.95	12.571	+1.660	+1.745	+0.937	+0.849	+1.787	19	11	0.0032	0.0025	0.0112	0.0011	0.0023	0.0021
WD 0830-535J	08	31	41.877	-53	37	28.27	13.484	+1.256	+1.078	+0.698	+0.650	+1.348	16	8	0.0025	0.0030	0.0132	0.0018	0.0025	0.0030
WD 0830-535K	08	31	42.960	-53	39	19.33	14.085	+0.635	+0.037	+0.383	+0.390	+0.774	12	7	0.0055	0.0081	0.0098	0.0032	0.0055	0.0069
WD 0830-535I	08	31	45.769	-53	37	35.34	13.172	+0.575	+0.014	+0.363	+0.366	+0.729	8	5	0.0057	0.0060	0.0085	0.0028	0.0042	0.0060
WD 0830-535C	08	31	50.421	-53	43	51.16	13.529	+0.628	+0.089	+0.387	+0.381	+0.768	10	5	0.0054	0.0057	0.0111	0.0016	0.0051	0.0054
WD 0830-535	08	31	51.91	-53	40	32.5	14.497	-0.227	-1.119	-0.134	-0.161	-0.293	18	12	0.0049	0.0040	0.0054	0.0040	0.0203	0.0224
WD 0830-535B	08	31	54.356	-53	42	37.91	13.847	+0.654	+0.181	+0.392	+0.389	+0.780	10	7	0.0057	0.0032	0.0076	0.0022	0.0057	0.0076
WD 0830-535A	08	31	54.454	-53	40	48.08	14.123	+0.719	+0.205	+0.415	+0.414	+0.829	11	6	0.0075	0.0048	0.0118	0.0048	0.0103	0.0130
WD 0830-535H	08	32	03.822	-53	37	50.36	12.790	+0.566	+0.136	+0.364	+0.371	+0.734	9	5	0.0030	0.0030	0.0050	0.0017	0.0020	0.0023
WD 0830-535D	08	32	04.970	-53	44	14.80	12.599	+0.514	+0.006	+0.327	+0.335	+0.661	9	5	0.0043	0.0027	0.0050	0.0013	0.0040	0.0037
WD 0830-535G	08	32	08.190	-53	40	30.15	14.009	+0.577	+0.270	+0.368	+0.357	+0.725	8	5	0.0035	0.0067	0.0088	0.0039	0.0053	0.0074
WD 0830-535F	08	32	08.639	-53	40	44.59	14.509	+0.618	+0.134	+0.377	+0.376	+0.752	7	4	0.0053	0.0060	0.0110	0.0060	0.0098	0.0083
WD 0830-535E	08	32	11.137	-53	41	58.54	13.225	+0.769	+0.199	+0.462	+0.473	+0.932	9	5	0.0043	0.0037	0.0083	0.0013	0.0030	0.0027
WD 1056-384D	10	58	08.051	-38	46	22.33	13.132	+0.521	+0.032	+0.307	+0.309	+0.615	12	6	0.0049	0.0029	0.0023	0.0020	0.0038	0.0049
WD 1056-384C	10	58	11.053	-38	41	50.97	13.326	+0.649	+0.164	+0.367	+0.357	+0.724	13	8	0.0050	0.0028	0.0047	0.0017	0.0033	0.0039
WD 1056-384B	10	58	18.691	-38	41	56.56	12.471	+1.156	+1.003	+0.611	+0.548	+1.159	14	8	0.0027	0.0027	0.0083	0.0016	0.0064	0.0078
WD 1056-384	10	58	20.11	-38	44	25.1	14.047	-0.187	-1.085	-0.132	-0.174	-0.303	14	8	0.0032	0.0021	0.0032	0.0045	0.0187	0.0187
WD 1056-384A	10	58	23.720	-38	44	01.19	12.375	+1.132	+0.916	+0.616	+0.581	+1.197	14	8	0.0016	0.0029	0.0056	0.0013	0.0013	0.0021
WD 1153-484G	11	55	53.78	-48	42	01.3	13.531	+0.911	+0.562	+0.504	+0.509	+1.010	4	2	0.0080	0.0140	0.0755	0.0065	0.0160	0.0200
WD 1153-484H	11	55	53.886	-48	41	24.93	14.276	+0.478	-0.036	+0.298	+0.277	+0.576	6	3	0.0122	0.0131	0.0082	0.0057	0.0265	0.0302
WD 1153-484F	11	55	56.276	-48	42	03.51	13.329	+0.489	+0.005	+0.298	+0.286	+0.583	4	2	0.0070	0.0060	0.0170	0.0015	0.0050	0.0040
WD 1153-484D	11	55	57.027	-48	37	23.50	13.275	+0.754	+0.221	+0.431	+0.406	+0.837	4	2	0.0080	0.0035	0.0050	0.0030	0.0065	0.0080
WD 1153-484C	11	56	01.765	-48	38	32.38	12.687	+1.179	+1.156	+0.617	+0.550	+1.168	2	2	0.0007	0.0049	0.0092	0.0014	0.0042	0.0064
WD 1153-484B	11	56	05.105	-48	38	50.36	13.282	+1.362	+1.633	+0.699	+0.590	+1.292	7	4	0.0049	0.0147	0.0189	0.0019	0.0053	0.0064
WD 1153-484A	11	56	10.834	-48	39	48.51	12.633	+0.700	+0.154	+0.415	+0.389	+0.803	4	2	0.0080	0.0055	0.0060	0.0035	0.0060	0.0060
WD 1153-484	11	56	11.427	-48	40	03.30	12.915	-0.215	-1.023	-0.098	-0.130	-0.228	6	3	0.0065	0.0029	0.0029	0.0020	0.0029	0.0016
WD 1153-484E	11	56	13.505	-48	42	16.00	13.440	+0.511	0.000	+0.308	+0.297	+0.605	4	2	0.0050	0.0045	0.0060	0.0020	0.0065	0.0070
LSE 44F	13	52	34.466	-48	06	59.26	12.013	+1.194	+1.172	+0.620	+0.560	+1.180	19	10	0.0034	0.0028	0.0044	0.0064	0.0028	0.0069
LSE 44A	13	52	39.573	-48	10	04.92	13.743	+1.435	+1.634	+0.791	+0.719	+1.511	21	10	0.0033	0.0057	0.0238	0.0017	0.0022	0.0035
LSE 44	13	52	40.779	-48	08	22.75	12.459	-0.265	-1.152	-0.112	-0.145	-0.255	20	11	0.0040	0.0018	0.0027	0.0011	0.0034	0.0034
LSE 44B	13	52	43.784	-48	11	34.04	12.632	+1.039	+0.774	+0.567	+0.538	+1.105	18	9	0.0033	0.0021	0.0061	0.0007	0.0012	0.0014
LSE 44C	13	52	51.850	-48	09	56.32	13.437	+1.426	+1.559	+0.793	+0.738	+1.531	17	9	0.0082	0.0053	0.0155	0.0017	0.0068	0.0075
LSE 44D	13	52	52.115	-48	08	38.43	13.140	+1.360	+1.598	+0.728	+0.626	+1.354	15	8	0.0049	0.0062	0.0238	0.0010	0.0018	0.0023
LSE 44E	13	52	55.514	-48	08	19.58	13.554	+0.827	+0.440	+0.454	+0.413	+0.866	16	8	0.0048	0.0045	0.0062	0.0020	0.0048	0.0060
LSE 259C	16	53	30.037	-56	00	54.62	10.866	+1.025	+0.700	+0.561	+0.525	+1.087	15	8	0.0021	0.0021	0.0039	0.0010	0.0013	0.0013
LSE 259D	16	53	41.607	-55	59	08.96	11.719	+0.331	+0.183	+0.191	+0.209	+0.400	15	8	0.0041	0.0026	0.0026	0.0008	0.0013	0.0015
LSE 259E	16	53	43.240	-55	58	30.06	11.922	+0.613	+0.118	+0.362	+0.362	+0.725	17	9	0.0034	0.0022	0.0036	0.0012	0.0012	0.0012
LSE 259B	16	53	44.377	-56	01	32.85	13.596	+0.888	+0.468	+0.506	+0.482	+0.991	18	10	0.0045	0.0064	0.0151	0.0019	0.0024	0.0040
LSE 259H	16	53	48.077	-56	00	42.24	14.164	+1.317	+1.272	+0.699	+0.614	+1.314	15	8	0.0046	0.0036	0.0336	0.0026	0.0044	0.0062
LSE 259A	16	53	53.147	-56	02	02.58	13.545	+1.692	+1.980	+0.993	+1.013	+2.006	19	12	0.0028	0.0044	0.0695	0.0014	0.0018	0.0023

Table 1—Continued

Star	α h m s			δ $^{\circ}$ $'$ $''$			V	$B - V$	$U - B$	$V - R$	$R - I$	$V - I$	n	m	V	$B - V$	$U - B$	$V - R$	Mean Error of the Mean		
LSE 259	16 53 54.573	-56 01 54.76	12.551	-0.127	-1.123	-0.019	-0.026	-0.046	22	14	0.0023	0.0019	0.0043	0.0013	0.0028	0.0034					
LSE 259F	16 53 55.538	-55 59 26.16	13.580	+0.615	+0.052	+0.374	+0.375	+0.749	17	9	0.0027	0.0032	0.0068	0.0024	0.0032	0.0034					
LSE 259G	16 54 00.237	-55 59 20.05	14.092	+0.841	+0.241	+0.515	+0.514	+1.029	14	7	0.0035	0.0043	0.0144	0.0024	0.0061	0.0067					
MCT 2019-4339E	20 22 38.910	-43 31 17.07	13.693	+1.029	+0.788	+0.566	+0.530	+1.096	28	15	0.0017	0.0025	0.0064	0.0009	0.0028	0.0030					
MCT 2019-4339D	20 22 40.476	-43 27 26.39	13.205	+0.924	+0.748	+0.518	+0.434	+0.953	19	11	0.0018	0.0023	0.0050	0.0014	0.0023	0.0028					
MCT 2019-4339A	20 22 45.332	-43 29 43.33	13.055	+0.521	-0.011	+0.307	+0.295	+0.602	20	11	0.0025	0.0025	0.0040	0.0016	0.0031	0.0036					
MCT 2019-4339B	20 22 46.726	-43 28 10.88	13.923	+0.671	+0.208	+0.369	+0.347	+0.716	19	11	0.0028	0.0030	0.0044	0.0032	0.0041	0.0067					
MCT 2019-4339	20 22 49.056	-43 30 11.53	13.685	-0.288	-1.212	-0.115	-0.149	-0.261	24	13	0.0029	0.0020	0.0065	0.0027	0.0067	0.0069					
MCT 2019-4339C	20 23 02.134	-43 28 22.40	12.440	+0.939	+0.726	+0.547	+0.466	+1.011	20	11	0.0018	0.0020	0.0051	0.0009	0.0011	0.0016					
MCT 2019-4339F	20 23 03.99	-43 31 21.9	13.936	+0.647	+0.097	+0.369	+0.360	+0.729	20	11	0.0031	0.0029	0.0060	0.0022	0.0047	0.0054					
JL 82C	21 35 45.005	-72 50 12.76	13.440	+0.612	+0.041	+0.357	+0.358	+0.715	19	10	0.0037	0.0023	0.0053	0.0028	0.0034	0.0055					
JL 82B	21 35 59.34	-72 50 15.1	13.507	+0.705	+0.121	+0.411	+0.414	+0.825	19	10	0.0037	0.0032	0.0053	0.0021	0.0037	0.0048					
JL 82	21 36 01.289	-72 48 27.21	12.389	-0.208	-0.947	-0.098	-0.115	-0.211	21	11	0.0031	0.0020	0.0041	0.0013	0.0035	0.0037					
JL 82D	21 36 15.362	-72 45 27.21	12.371	+1.062	+0.865	+0.551	+0.509	+1.061	19	10	0.0034	0.0025	0.0053	0.0016	0.0018	0.0021					
JL 82A	21 36 17.052	-72 50 08.57	11.226	+1.050	+0.803	+0.543	+0.503	+1.048	21	11	0.0031	0.0013	0.0022	0.0007	0.0015	0.0015					
JL 117A	22 54 13.332	-72 23 04.33	14.061	+0.629	+0.072	+0.362	+0.354	+0.717	6	3	0.0029	0.0037	0.0069	0.0024	0.0147	0.0159					
JL 117	22 54 38.002	-72 23 09.68	14.469	-0.336	-1.233	-0.152	-0.128	-0.272	12	6	0.0032	0.0023	0.0023	0.0055	0.0271	0.0297					
JL 117B	22 54 51.021	-72 23 23.61	14.961	+0.806	+0.471	+0.444	+0.334	+0.779	4	2	0.0045	0.0035	0.0120	0.0165	0.9590	0.0755	1				
JL 117C	22 55 00.471	-72 22 41.35	14.398	+0.797	+0.385	+0.436	+0.395	+0.834	6	4	0.0045	0.0151	0.0033	0.0061	0.0065	0.0027	QO				
JL 117D	22 55 37.574	-72 22 34.28	12.550	+0.657	+0.159	+0.369	+0.360	+0.731	5	2	0.0027	0.0018	0.0058	0.0018	0.0022	0.0027					

Table 2. Error Analysis for 109 New Standards Stars in Table 1.

	Mean Errors of a Single Observation	Mean Errors of the Mean
V	0.0161 ± 0.0101	0.0035 ± 0.0021
$B - V$	0.0137 ± 0.0070	0.0033 ± 0.0024
$U - B$	0.0368 ± 0.0488	0.0091 ± 0.0135
$V - R$	0.0091 ± 0.0055	0.0021 ± 0.0019
$R - I$	0.0206 ± 0.0202	0.0048 ± 0.0071
$V - I$	0.0240 ± 0.0233	0.0060 ± 0.0093

Table 3. Field Centers for Sequences.

Field Name	$\alpha(2000.0)$	$\delta(2000.0)$
JL 163	00 10 42.6	-50 14 10
T Phe	00 30 34.4	-46 28 08
MCT 0401-4017	04 03 01.2	-40 11 28
LB 1735	04 31 34.7	-53 37 13
MCT 0436-4616	04 38 34.2	-46 10 10
MCT 0550-4911	05 51 53.9	-49 10 31
LSS 982	08 10 29.1	-40 30 34
WD 0830-535	08 31 56.5	-53 40 52
WD 1056-384	10 58 15.9	-38 44 07
WD 1153-484	11 56 03.6	-48 39 50
LSE 44	13 52 45.0	-48 09 17
LSE 259	16 53 45.1	-56 00 16
MCT 2019-4339	20 22 51.5	-43 29 24
JL 82	21 36 01.0	-72 47 51
JL 117	22 54 55.5	-72 22 59

Table 4. *UBVRI* Photometry of Isolated Stars

Star	α (2000)			δ	Mean Error of the Mean													
	h	m	s		V	$B - V$	$U - B$	$V - R$	$R - I$	$V - I$	n	m	V	$B - V$	$U - B$	$V - R$	$R - I$	$V - I$
JL 166	00	12	43.023	-45 51 15.48	15.341	-0.281	-1.122	-0.069	+0.184	+0.116	2	1	0.0021	0.0014	0.0021	0.0021	0.0361	0.0339
JL 194	00	31	41.651	-47 25 20.03	12.397	-0.234	-0.947	-0.122	-0.157	-0.279	5	3	0.0040	0.0018	0.0027	0.0022	0.0054	0.0076
JL 202	00	40	13.303	-55 01 52.20	13.087	-0.296	-1.195	-0.138	-0.184	-0.321	5	3	0.0022	0.0009	0.0031	0.0027	0.0089	0.0098
GD 679	01	06	51.07	-33 20 31.3	13.537	-0.278	-1.083	-0.137	-0.156	-0.289	6	3	0.0006	0.0004	0.0027	0.0007	0.0099	0.0117
JL 236	01	14	06.692	-52 44 02.19	13.376	-0.242	-1.005	-0.129	-0.132	-0.264	1	1
JL 261	01	47	17.465	-51 33 39.18	13.589	-0.299	-1.191	-0.123	-0.206	-0.329	1	1
LB 3241	02	13	11.934	-49 44 53.76	12.763	-0.304	-1.166	-0.131	-0.179	-0.309	2	2	0.0014	0.0007	0.0078	0.0070	0.0127	0.0127
JL 286	02	13	12.410	-50 04 40.02	14.291	-0.207	-0.982	-0.103	-0.150	-0.253	1	1
L745-46A	07	40	20.794	-17 24 49.20	13.034	+0.248	-0.652	+0.165	+0.161	+0.326	5	3	0.0022	0.0022	0.0036	0.0013	0.0067	0.0063
LSS 1274	09	18	56.013	-57 04 25.42	12.959	-0.212	-1.187	-0.070	-0.092	-0.166	2	1	0.0021	0.0007	0.0007	0.0014	0.0127	0.0113
LSS 1275	09	20	10.130	-45 31 54.96	11.417	-0.322	-1.263	-0.135	-0.170	-0.306	2	1	0.0007	0.0007	0.0007	0.0001	0.0028	0.0028
LSS 1349	09	46	57.109	-50 12 16.05	13.379	+0.028	-0.986	+0.062	+0.079	+0.140	2	1	0.0001	0.0014	0.0049	0.0028	0.0007	0.0042
LSS 1362	09	52	44.524	-46 16 47.47	12.533	-0.222	-1.189	-0.064	-0.075	-0.141	2	1	0.0001	0.0014	0.0021	0.0007	0.0014	0.0007
LSE 153	13	53	08.214	-46 43 42.32	11.379	-0.275	-1.218	-0.107	-0.146	-0.251	4	2	0.0100	0.0015	0.0030	0.0015	0.0020	0.0030
LSE 125	15	43	05.042	-39 18 14.59	12.372	-0.153	-1.119	-0.027	-0.049	-0.074	4	2	0.0075	0.0040	0.0045	0.0030	0.0015	0.0040
LSE 234	18	13	15.853	-64 55 16.86	12.705	-0.280	-1.231	-0.086	-0.118	-0.205	4	2	0.0100	0.0030	0.0095	0.0085	0.0070	0.0125
LSE 263	19	02	11.740	-51 30 09.54	11.771	-0.278	-1.245	-0.091	-0.122	-0.211	2	1	0.0007	0.0007	0.0021	0.0001	0.0035	0.0035
JL 25	19	39	38.960	-76 01 17.25	13.321	-0.188	-1.129	-0.017	+0.040	+0.018	4	2	0.0010	0.0015	0.0020	0.0035	0.0115	0.0085
LB 1516	23	01	56.152	-48 03 48.46	12.967	-0.241	-0.981	-0.117	-0.128	-0.244	4	2	0.0035	0.0020	0.0020	0.0015	0.0055	0.0080

Table 5. Accurate Coordinates and Proper Motions for the Stars in Tables 1 and 4.

Star Name	α h m s	(2000)	δ $^{\circ}$ $'$ $''$	UCAC2	2MASS-PSC	μ_{α} (mas/yr)	μ_{δ} (mas/yr)	μ Ref.	Sp. Type	Sp. Type Ref.
JL 163B	00 10 24.88	-50 13 55.6	...	J00102488-5013556	-4	-20	1
JL 163A	00 10 26.309	-50 15 03.52	10092905	J00102631-5015034	13.3	9.1	2
JL 163	00 10 33.221	-50 15 24.37	10092907	J00103322-5015243	7.2	7.3	2	sdB	3,4	...
JL 163C	00 10 38.238	-50 15 26.39	10092908	J00103824-5015263	11.4	-0.6	2
JL 163D	00 10 41.62	-50 13 45.6	...	J00104162-5013456
JL 163E	00 10 58.017	-50 14 17.44	10092916	J00105801-5014175	9.0	-0.6	2
JL 163F	00 11 00.225	-50 12 53.81	10092918	J00110022-5012539	7.7	-3.5	2
JL 166	00 12 43.023	-45 51 15.48	12134270	J00124302-4551153	2.0	-15.8	2	sdOB	5	...
TPhε I	00 30 04.593	-46 28 10.17	11909220	J00300459-4628102	13.6	-8.5	2
TPhε A	00 30 09.594	-46 31 28.91	11679110	J00300959-4631289	8.3	-2.0	2
TPhε H	00 30 09.683	-46 27 24.30	11909222	J00300968-4627243	11.2	-8.1	2
TPhε B	00 30 16.313	-46 27 58.57	11909226	J00301631-4627586	1.0	-5.4	2
TPhε C	00 30 16.98	-46 32 21.4	...	J00301697-4632214
TPhε D	00 30 18.342	-46 31 19.85	11679116	J00301834-4631198	2.3	1.3	2
TPhε E	00 30 19.768	-46 24 35.60	11909227	...	51.4	1.6	2
TPhε J	00 30 23.02	-46 23 51.6	...	J00302301-4623516
TPhε F	00 30 49.820	-46 33 24.07	11679132	J00304980-4633239	80.6	-10.2	2
TPhε K	00 30 56.315	-46 23 26.04	11909244	J00305632-4623260	-11.2	-1.6	2
TPhε G	00 31 04.303	-46 22 51.35	11909246	J00310430-4622513	14.3	5.6	2
JL 194	00 31 41.651	-47 25 20.03	11454707	J00314165-4725200	21.2	-25.8	2	sdB	5	...
JL 202	00 40 13.303	-55 01 52.20	07669947	J00401329-5501520	18.9	3.6	2	sdO	5	...
GD 679	01 06 51.07	-33 20 31.3	...	J01065106-3320313	sdB	6,5	...
JL 236	01 14 06.692	-52 44 02.19	08932516	J01140669-5244021	13.3	-7.7	2	sdB	5	...
JL 261	01 47 17.465	-51 33 39.18	09398888	J01471747-5133391	16.2	-4.4	2	sdO:He	4	...
LB 3241	02 13 11.934	-49 44 53.76	10323959	J02131193-4944537	1.1	-6.7	2	sdOB	4	...
JL 286	02 13 12.410	-50 04 40.02	10095692	J02131241-5004399	-6.0	1.4	2	sdB	4	...
MCT 0401-4017E	04 02 28.087	-40 09 35.57	14539866	J04022808-4009355	13.0	40.7	2
MCT 0401-4017F	04 02 29.559	-40 10 21.19	14539867	J04022955-4010211	24.3	-3.9	2
MCT 0401-4017D	04 02 55.219	-40 15 52.60	14539878	J04025522-4015525	5.9	-2.5	2
MCT 0401-4017	04 03 04.540	-40 09 41.05	14539887	J04030453-4009409	-15.6	-9.1	2
MCT 0401-4017A	04 03 05.195	-40 11 02.88	14539888	J04030519-4011029	19.2	19.9	2
MCT 0401-4017B	04 03 29.846	-40 10 58.46	14539898	J04032984-4010585	-11.0	12.3	2
MCT 0401-4017C	04 03 34.273	-40 07 02.53	14539899	J04033426-4007025	-12.5	-100.7	2
LB 1735	04 31 11.090	-53 35 27.06	08436787	J04311106-5335270	11.6	-20.6	2	sdB?	4,5,7	...
LB 1735A	04 31 19.438	-53 34 38.22	08436790	J04311942-5334382	-14.9	16.5	2
LB 1735B	04 31 22.810	-53 36 36.85	08436792	J04312279-5336369	0.3	26.9	2
LB 1735F	04 31 37.11	-53 36 53.4	...	J04313710-5336534
LB 1735E	04 31 42.303	-53 36 18.48	08436802	J04314228-5336185	4.2	5.6	2
LB 1735G	04 31 46.194	-53 39 47.89	08436803	J04314617-5339477	7.4	27.4	2
LB 1735C	04 31 49.652	-53 34 37.52	08436806	J04314963-5334375	3.1	8.3	2
LB 1735D	04 31 58.253	-53 34 52.52	08436811	J04315824-5334524	-5.0	16.6	2
MCT 0436-4616A	04 38 20.929	-46 09 27.54	11916012	J04382091-4609276	4.2	8.5	2
MCT 0436-4616	04 38 27.320	-46 10 52.69	11916019	J04382730-4610527	8.9	3.2	2
MCT 0436-4616B	04 38 47.374	-46 10 08.74	11916039	J04384737-4610087	42.4	52.6	2
MCT 0550-4911E	05 51 43.660	-49 10 48.59	10562675	J05514366-4910485	18.0	21.7	2
MCT 0550-4911D	05 51 49.207	-49 11 18.95	10562687	J05514921-4911188	8.8	10.4	2
MCT 0550-4911B	05 51 59.105	-49 11 25.06	10562695	J05515910-4911250	11.7	2.0	2
MCT 0550-4911	05 52 02.712	-49 11 22.38	10562698	J05520271-4911223	-2.9	11.7	2
MCT 0550-4911C	05 52 03.98	-49 09 37.6	...	J05520398-4909376
MCT 0550-4911A	05 52 04.104	-49 10 48.55	10562700	J05520411-4910485	0.0	4.0	2
L745-46A	07 40 20.794	-17 24 49.20	25277198	J07402064-1724481	1148.7	-540.6	2
LSS 982G	08 10 19.984	-40 31 57.19	14358563	J08101998-4031571	1.1	9.4	2
LSS 982F	08 10 21.386	-40 31 30.31	14358565	J08102139-4031302	-7.0	-0.6	2
LSS 982E	08 10 29.667	-40 30 06.85	14358602	J08102966-4030068	-6.5	5.1	2
LSS 982	08 10 31.719	-40 32 47.07	14358605	J08103171-4032469	26.9	-39.9	2	sdO	5	...
LSS 982A	08 10 32.719	-40 31 14.52	14358607	J08103271-4031145	-8.4	17.1	2
LSS 982B	08 10 34.325	-40 30 49.16	14358613	J08103432-4030491	-4.9	5.3	2
LSS 982D	08 10 38.089	-40 28 20.84	14569244	J08103808-4028209	-1.1	6.0	2
LSS 982C	08 10 38.222	-40 30 09.95	14358632	J08103822-4030100	-8.7	1.3	2
WD0830-535J	08 31 41.877	-53 37 28.27	08458552	J08314187-5337281	-3.5	11.0	2
WD0830-535K	08 31 42.960	-53 39 19.33	08458557	J08314296-5339192	-9.4	4.3	2
WD0830-535I	08 31 45.769	-53 37 35.34	08458569	J08314576-5337352	1.1	4.3	2
WD0830-535C	08 31 50.421	-53 43 51.16	08458589	J08315042-5343511	-9.1	5.1	2
WD0830-535	08 31 51.91	-53 40 32.5	...	J08315191-5340324	+33.1	-133.8	10
WD0830-535B	08 31 54.356	-53 42 37.91	08458600	J08315435-5342379	-11.2	6.6	2
WD0830-535A	08 31 54.454	-53 40 48.08	08458601	J08315445-5340481	1.1	8.5	2

Table 5—Continued

Star Name	α h m s	(2000) δ ° ′ ″	UCAC2	2MASS-PSC	μ_α (mas/yr)	μ_δ (mas/yr)	μ Ref.	Sp. Type	Sp. Type Ref.
WD0830-535H	08 32 03.822	-53 37 50.36	08458638	J08320382-5337504	1.4	11.0	2
WD0830-535D	08 32 04.970	-53 44 14.80	08458647	J08320497-5344147	-5.3	-3.0	2
WD0830-535G	08 32 08.190	-53 40 30.15	08458656	J08320818-5340301	-8.7	5.9	2
WD0830-535F	08 32 08.639	-53 40 44.59	08458658	J08320863-5340446	-0.2	16.7	2
WD0830-535E	08 32 11.137	-53 41 58.54	08458669	J08321113-5341585	-5.9	0.0	2
LSS 1274	09 18 56.013	-57 04 25.42	06750679	J09185601-5704254	2.6	-8.9	2	sdO	5
LSS 1275	09 20 10.130	-45 31 54.96	12183510	J09201013-4531549	-19.5	-1.1	2	sdO	5
LSS 1349	09 46 57.109	-50 12 16.05	10140464	J09465710-5012160	-10.9	8.7	2	sdO	5
LSS 1362	09 52 44.524	-46 16 47.47	11964358	J09524453-4616474	-5.3	16.4	2	sdO	8
WD1056-384D	10 58 08.051	-38 46 22.33	15265422	J10580804-3846222	-14.5	-11.1	2
WD1056-384C	10 58 11.053	-38 41 50.97	15265430	J10581105-3841509	-10.2	1.7	2
WD1056-384B	10 58 18.691	-38 41 56.56	15265449	J10581868-3841565	-7.9	-1.0	2
WD1056-384	10 58 20.111	-38 44 25.1	...	J10582010-3844251	-158.0	32.4	9
WD1056-384A	10 58 23.720	-38 44 01.19	15265461	J10582371-3844011	-16.1	14.5	2
WD1153-484G	11 55 53.78	-48 42 01.3	...	J11555377-4842013
WD1153-484H	11 55 53.886	-48 41 24.93	10852585	J11555388-4841248	-32.2	10.5	2
WD1153-484F	11 55 56.276	-48 42 03.51	10852592	J11555628-4842034	4.5	-2.9	2
WD1153-484D	11 55 57.027	-48 37 23.50	10852595	J11555702-4837234	-62.7	-8.3	2
WD1153-484C	11 56 01.765	-48 38 32.38	10852612	J11560176-4838322	-10.8	3.4	2
WD1153-484B	11 56 05.105	-48 38 50.36	10852620	J11560511-4838502	-7.5	3.5	2
WD1153-484A	11 56 10.834	-48 39 48.51	10852634	J11561083-4839484	-11.8	-7.5	2
WD1153-484	11 56 11.427	-48 40 03.30	10852635	J11561142-4840031	-57.9	14.2	2
WD1153-484E	11 56 13.505	-48 42 16.00	10852642	J11561350-4842158	-4.9	3.2	2
LSE 44F	13 52 34.466	-48 06 59.26	11101888	J13523446-4806592	-9.3	-6.5	2
LSE 44A	13 52 39.573	-48 10 04.92	11101903	J13523957-4810049	-4.4	-2.9	2
LSE 44	13 52 40.779	-48 08 22.75	11101909	J13524078-4808226	-27.3	-6.9	2	sdO	8
LSE 44B	13 52 43.784	-48 11 34.04	11101921	J13524378-4811340	-9.7	1.8	2
LSE 44C	13 52 51.850	-48 09 56.32	11101947	J13525185-4809563	-9.6	-0.2	2
LSE 44D	13 52 52.115	-48 08 38.43	11101949	J13525211-4808384	-8.9	-0.9	2
LSE 44E	13 52 55.514	-48 08 19.58	11101960	J13525550-4808195	-0.3	-1.8	2
LSE 153	13 53 08.214	-46 43 42.32	11776514	J13530821-4643422	-24.4	-20.6	2	sdO	8
LSE 125	15 43 05.042	-39 18 14.59	15080788	J15430504-3918145	-12.1	-14.2	2
LSE 259C	16 53 30.037	-56 00 54.62	07384133	J16533002-5600544	1.6	-5.9	2
LSE 259D	16 53 41.607	-55 59 08.96	07623191	J16534160-5559089	-6.3	-0.6	2
LSE 259E	16 53 43.240	-55 58 30.06	07623206	J16534323-5558300	-8.2	0.5	2
LSE 259B	16 53 44.377	-56 01 32.85	07384228	J16534436-5601328	5.3	3.7	2
LSE 259H	16 53 48.007	-56 00 42.24	07384247	J16534807-5600422	-8.7	-2.2	2
LSE 259A	16 53 53.147	-56 02 02.58	07384280	J16535314-5602025	0.8	-6.8	2
LSE 259	16 53 54.573	-56 01 54.76	07384295	J16535458-5601547	0.3	-14.4	2	sdO	8
LSE 259F	16 53 55.538	-55 59 26.16	07623288	J16535554-5559261	-16.3	-6.4	2
LSE 259G	16 54 00.237	-55 59 20.05	07623325	J16540027-5559199	-3.4	-2.4	2
LSE 234	18 13 15.853	-64 55 16.86	03401203	J18131583-6455168	-5.0	-29.2	2	sdO	8
LSE 263	19 02 11.740	-51 30 09.54	09610773	J19021174-5130094	-11.8	0.0	2	sdO	8
JL 25	19 39 38.960	-76 01 17.25	00667985	J19393895-7601172	2.5	-22.3	2	sdOB	4
MCT 2019-4339E	20 22 38.910	-43 31 17.07	13255341	J20223890-4331171	9.7	-7.3	2
MCT 2019-4339D	20 22 40.476	-43 27 26.39	13472188	J20224047-4327264	30.6	-39.1	2
MCT 2019-4339A	20 22 45.332	-43 29 43.33	13472194	J20224532-4329433	3.9	-23.4	2
MCT 2019-4339B	20 22 46.726	-43 28 10.88	13472198	J20224672-4328108	5.2	-4.1	2
MCT 2019-4339	20 22 49.056	-43 30 11.53	13255356	J20224905-4330116	-3.7	-12.3	2
MCT 2019-4339C	20 23 02.134	-43 28 22.40	13472215	J20230213-4328224	47.8	-11.4	2
MCT 2019-4339F	20 23 03.99	-43 31 21.9	...	J20230398-4331219
JL 82C	21 35 45.005	-72 50 12.76	01156348	J21354498-7250127	-3.5	9.1	2
JL 82B	21 35 59.34	-72 50 15.1	...	J21355933-7250150
JL 82	21 36 01.289	-72 48 27.21	01156353	J21360128-7248272	13.1	-15.7	2	sdB	4
JL 82D	21 36 15.362	-72 45 27.21	01156358	J21361534-7245272	-2.6	3.5	2
JL 82A	21 36 17.052	-72 50 08.57	01156361	J21361703-7250084	2.4	4.0	2
JL 117A	22 54 13.332	-72 23 04.33	01245946	J22541335-7223043	15.2	-10.4	2
JL 117	22 54 38.002	-72 23 09.68	01245961	J22543801-7223097	0.8	10.7	2	sdO	5
JL 117B	22 54 51.021	-72 23 23.61	01245972	J22545102-7223236	16.4	-22.2	2
JL 117C	22 55 00.471	-72 22 41.35	01245977	J22550047-7222413	7.7	-7.2	2
JL 117D	22 55 37.574	-72 22 34.28	01245986	J22553759-7222343	22.5	-2.1	2
LB 1516	23 01 56.152	-48 03 48.46	11226102	J23015616-4803484	3.2	3.5	2	sdB	5

1. (Monet et al. 2003)[USNO-B1.0 catalog]

2. (Zacharias et al. 2004)[UCAC2]

3. (Kilkenny 1987)
4. (Kilkenny & Muller 1989)
5. (Kilkenny et al. 1988)
6. (Greenstein & Sargent 1974)
7. (Kilkenny & Hill 1975)
8. (Drilling 1983)
9. (Platais et al. 1998)
10. (Platais et al. 2007)

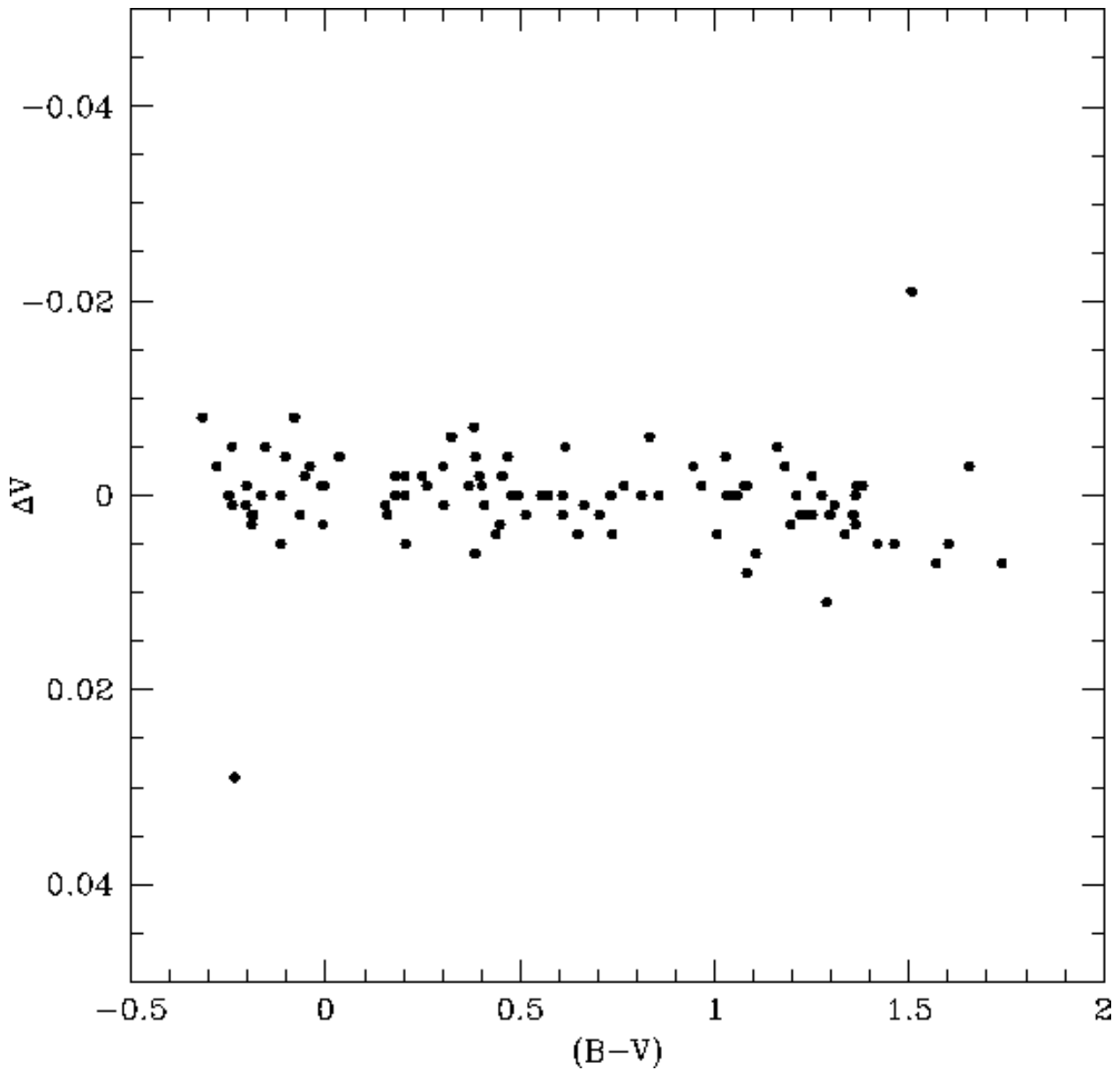


Fig. 1.— Comparison of the V magnitudes tied into Landolt (1992) standard stars as a function of the Landolt (1992) equatorial standard star's $(B - V)$ color indices. The two discrepant points are the white dwarf Feige 108 and the M-dwarf G163-51 (see text).

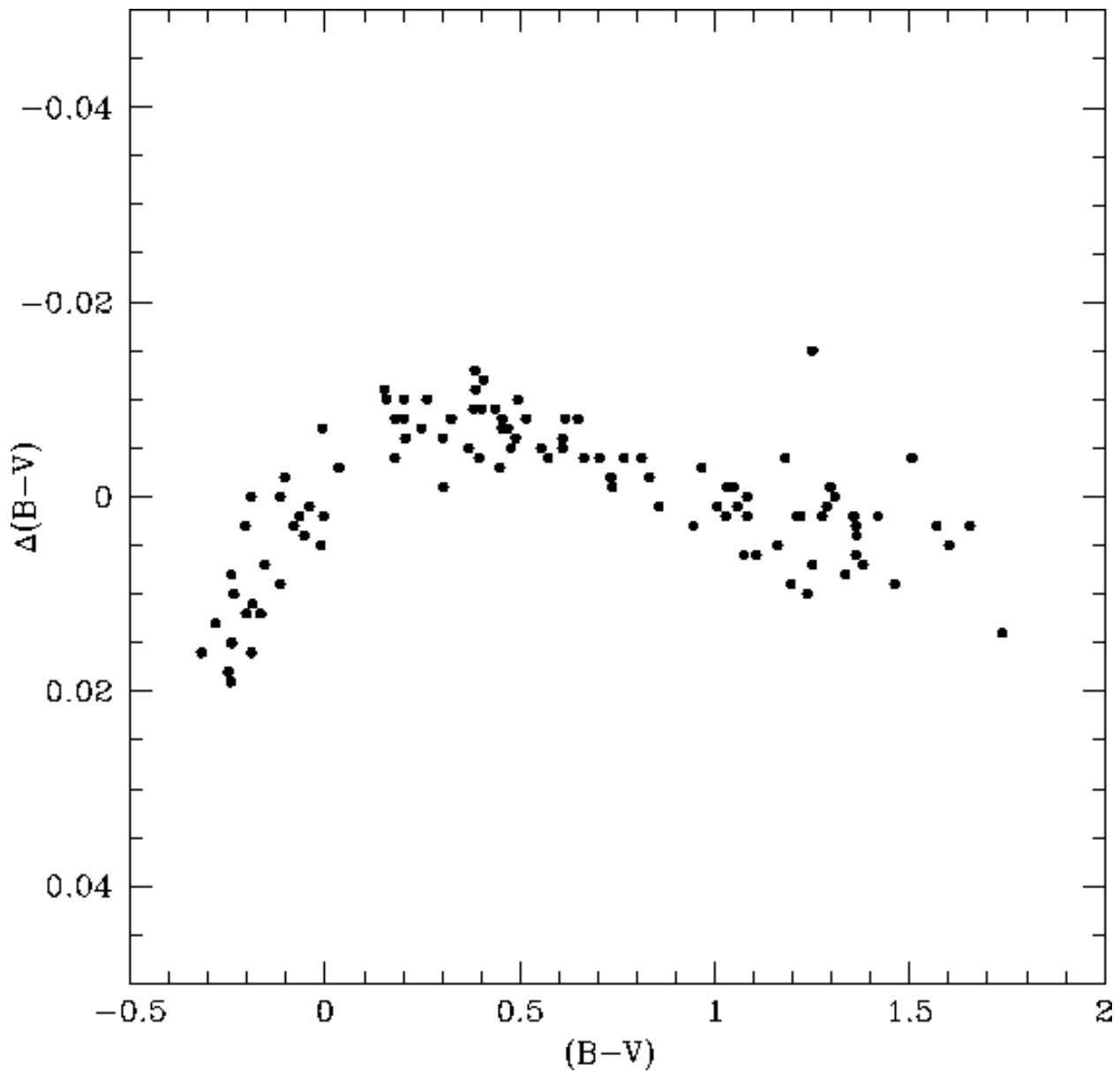


Fig. 2.— Comparison of the $(B - V)$ magnitudes tied into Landolt (1992) standard stars as a function of the Landolt (1992) equatorial standard star's $(B - V)$ color indices.

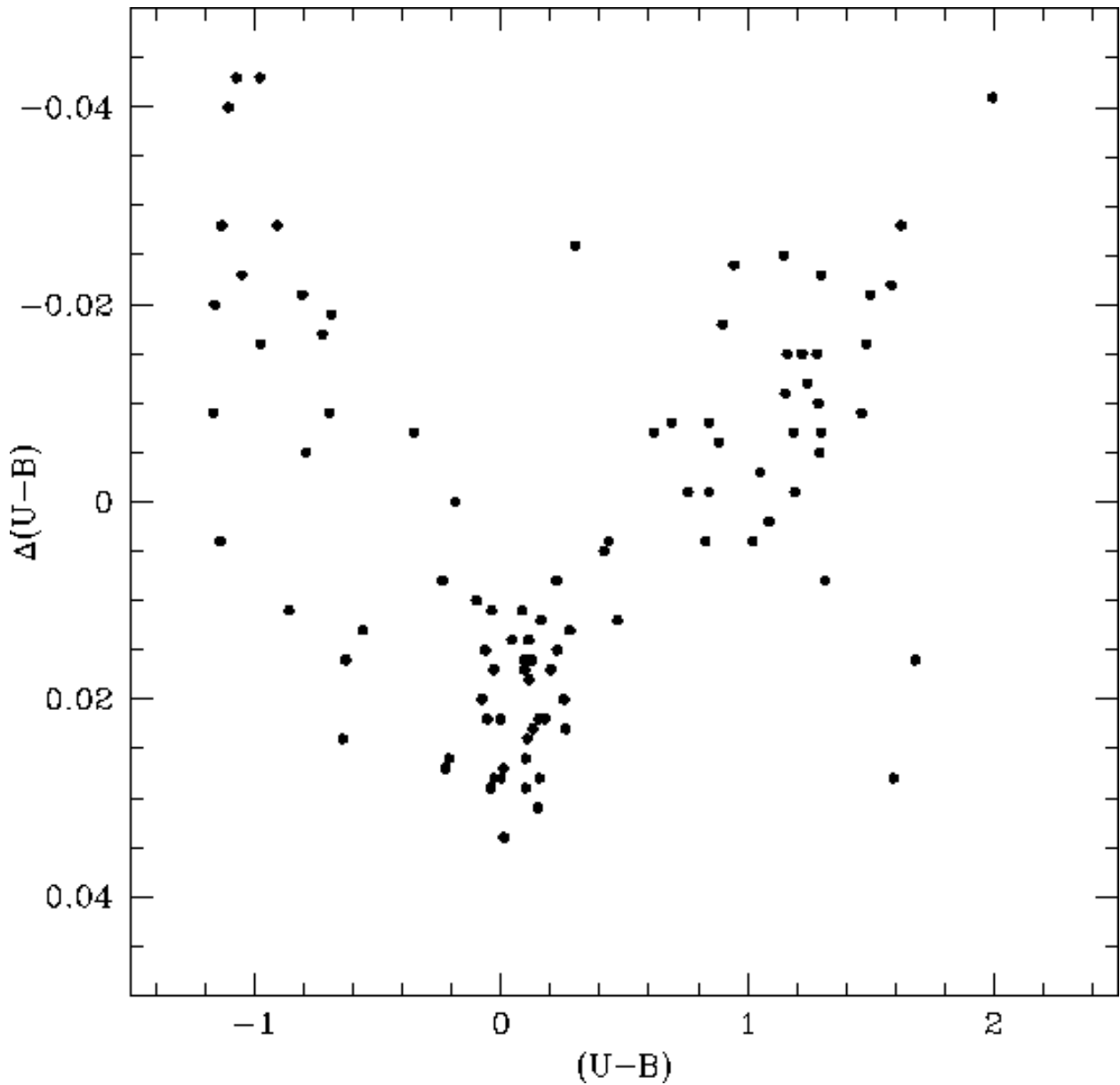


Fig. 3.— Comparison of the $(U - B)$ magnitudes tied into Landolt (1992) standard stars as a function of the Landolt (1992) equatorial standard star's $(U - B)$ color indices.

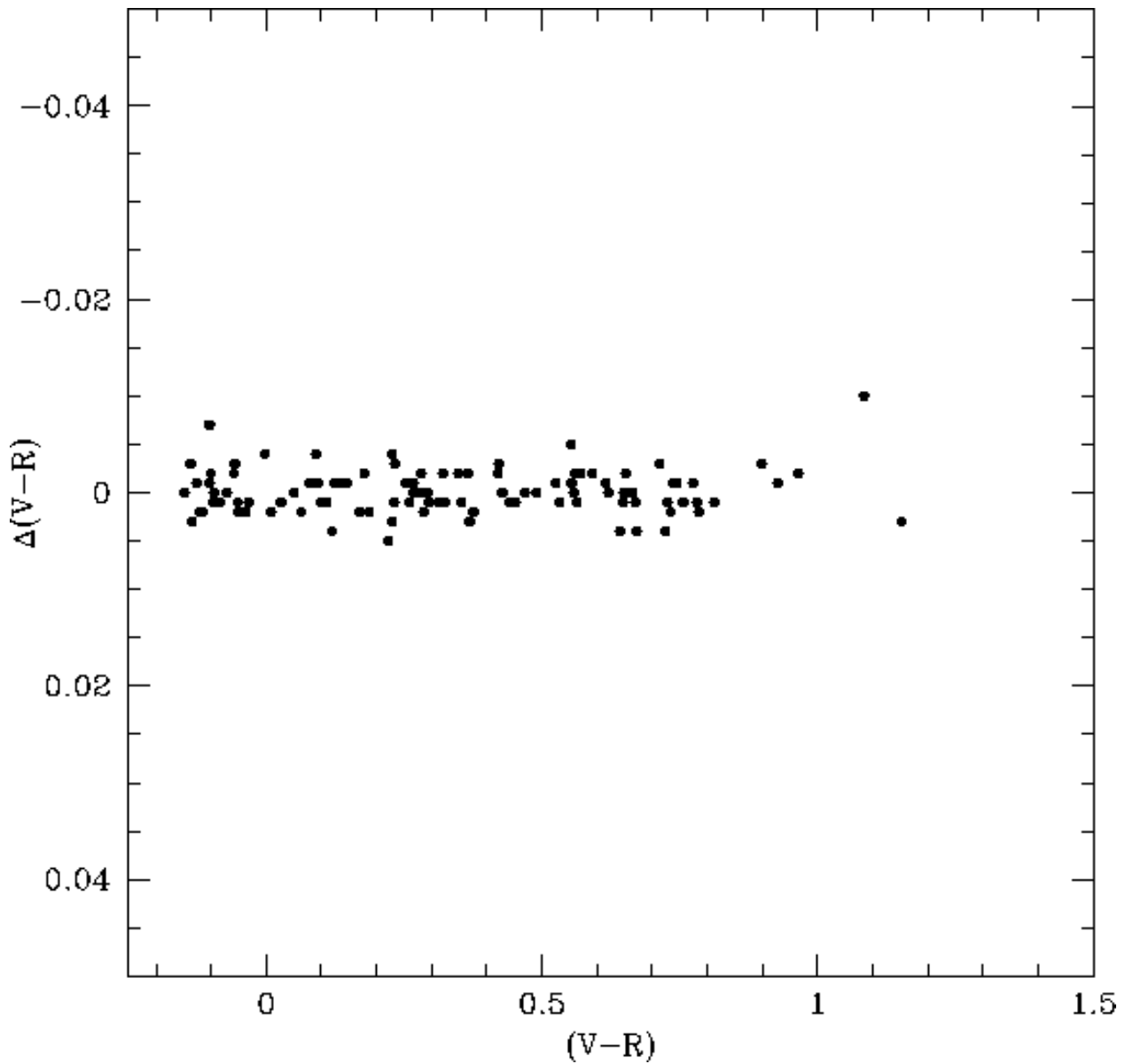


Fig. 4.— Comparison of the $(V - R)$ magnitudes tied into Landolt (1992) standard stars as a function of the Landolt (1992) equatorial standard star's $(V - R)$ color indices.

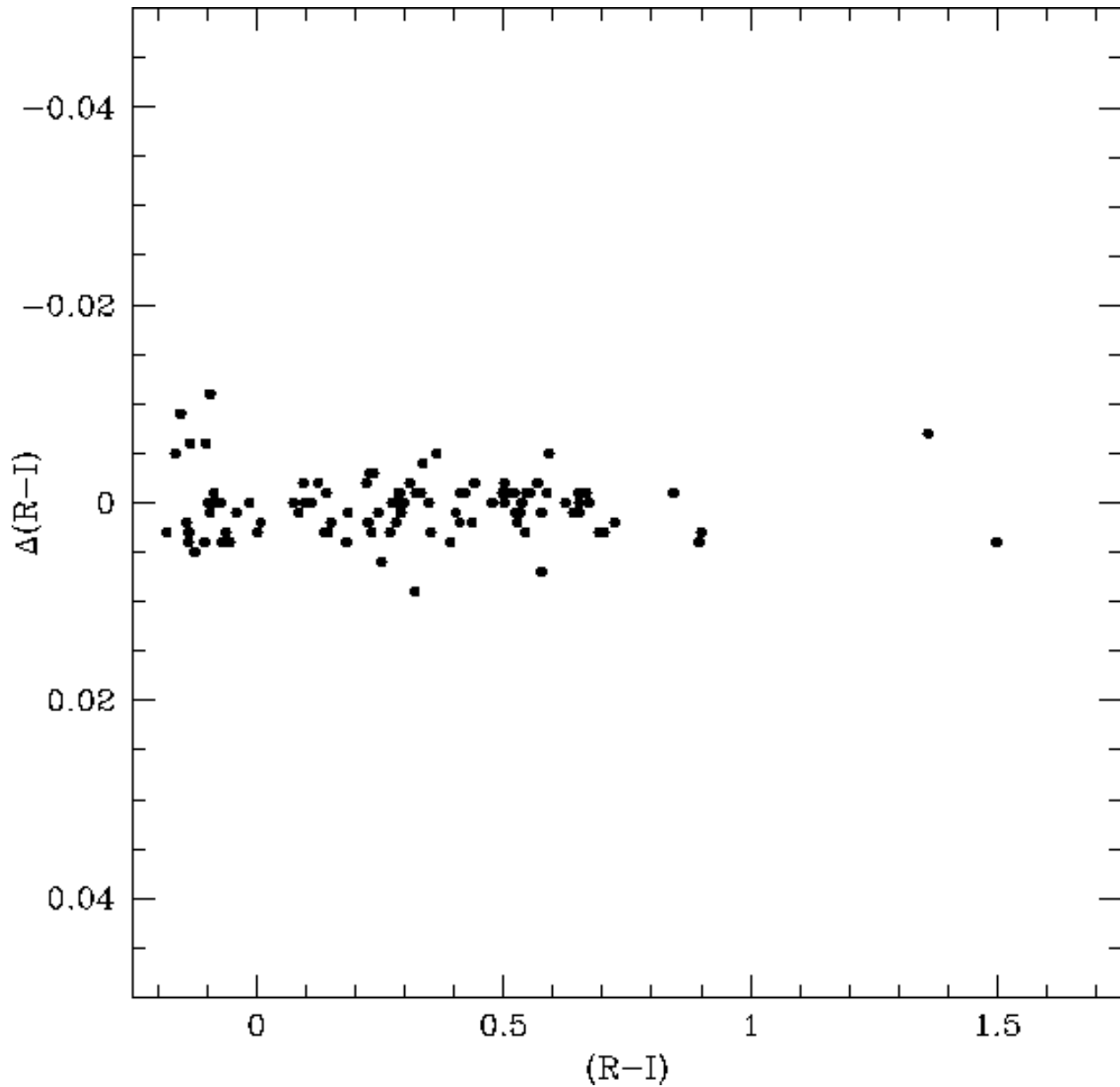


Fig. 5.— Comparison of the $(R - I)$ magnitudes tied into Landolt (1992) standard stars as a function of the Landolt (1992) equatorial standard star's $(R - I)$ color indices.

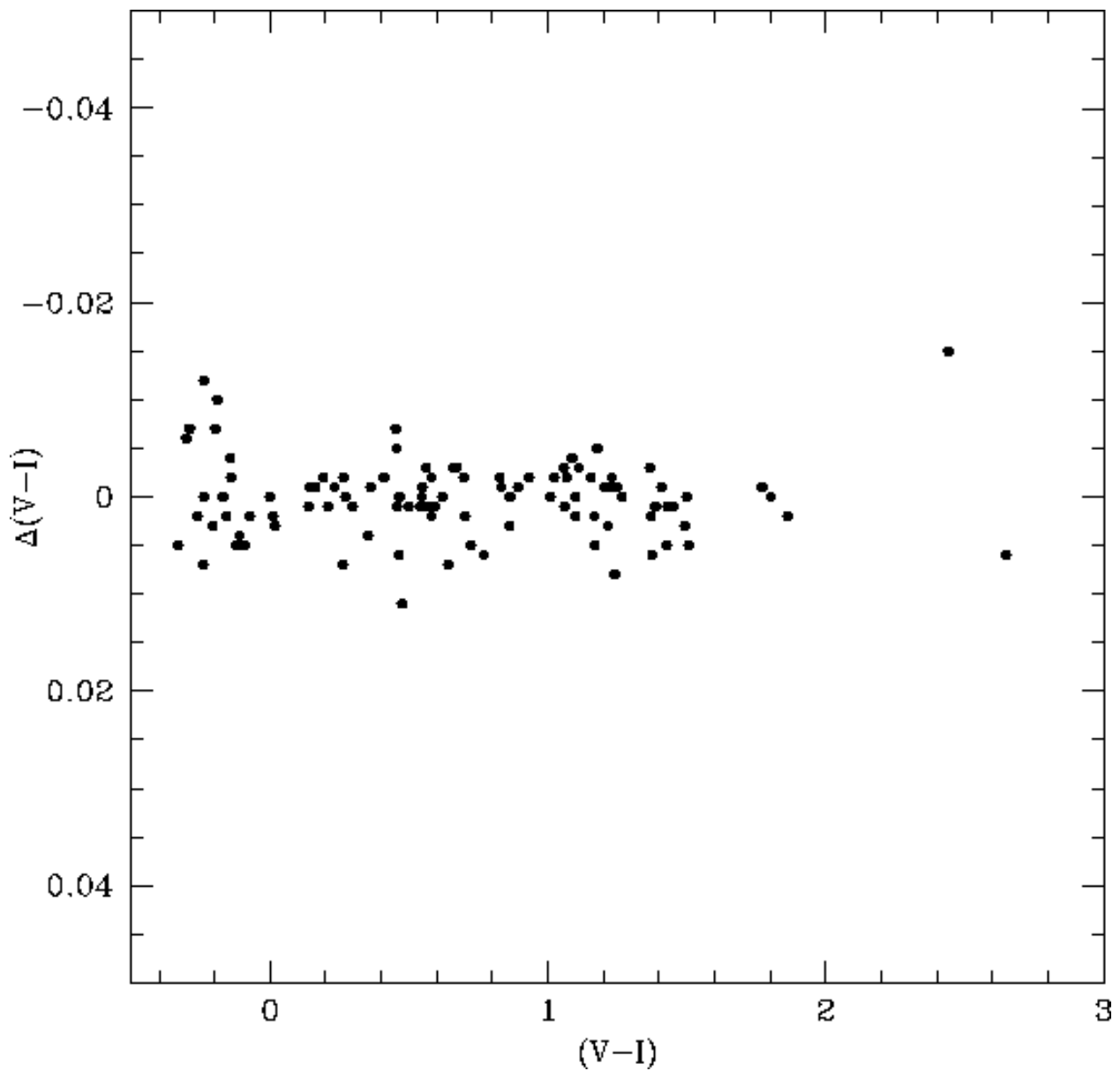


Fig. 6.— Comparison of the $(V - I)$ magnitudes tied into Landolt (1992) standard stars as a function of the Landolt (1992) equatorial standard star's $(V - I)$ color indices.

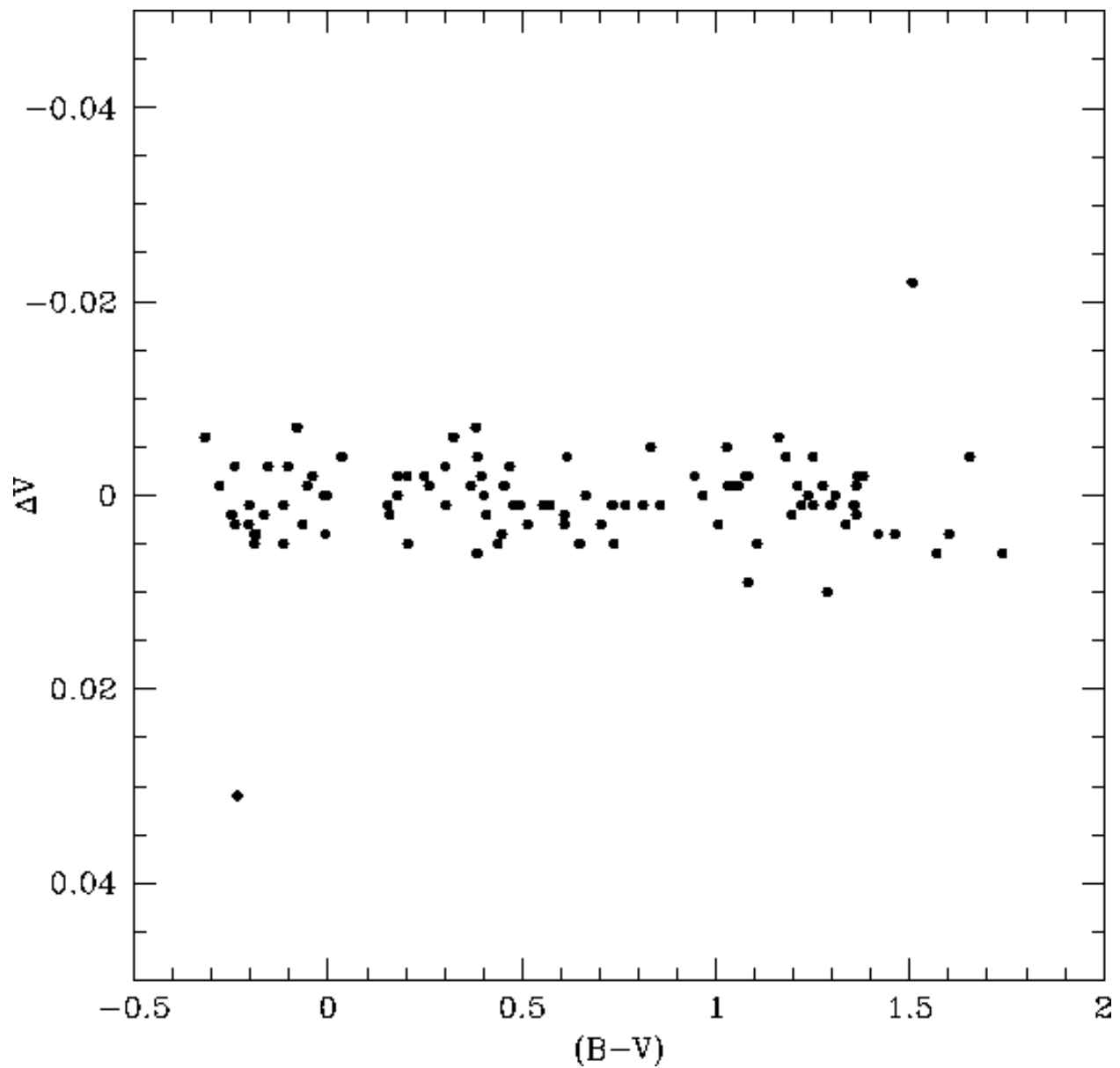


Fig. 7.— Comparison of the V magnitudes after removal of the transformation nonlinearity as a function of the Landolt (1992) equatorial standard star's $(B - V)$ color index.

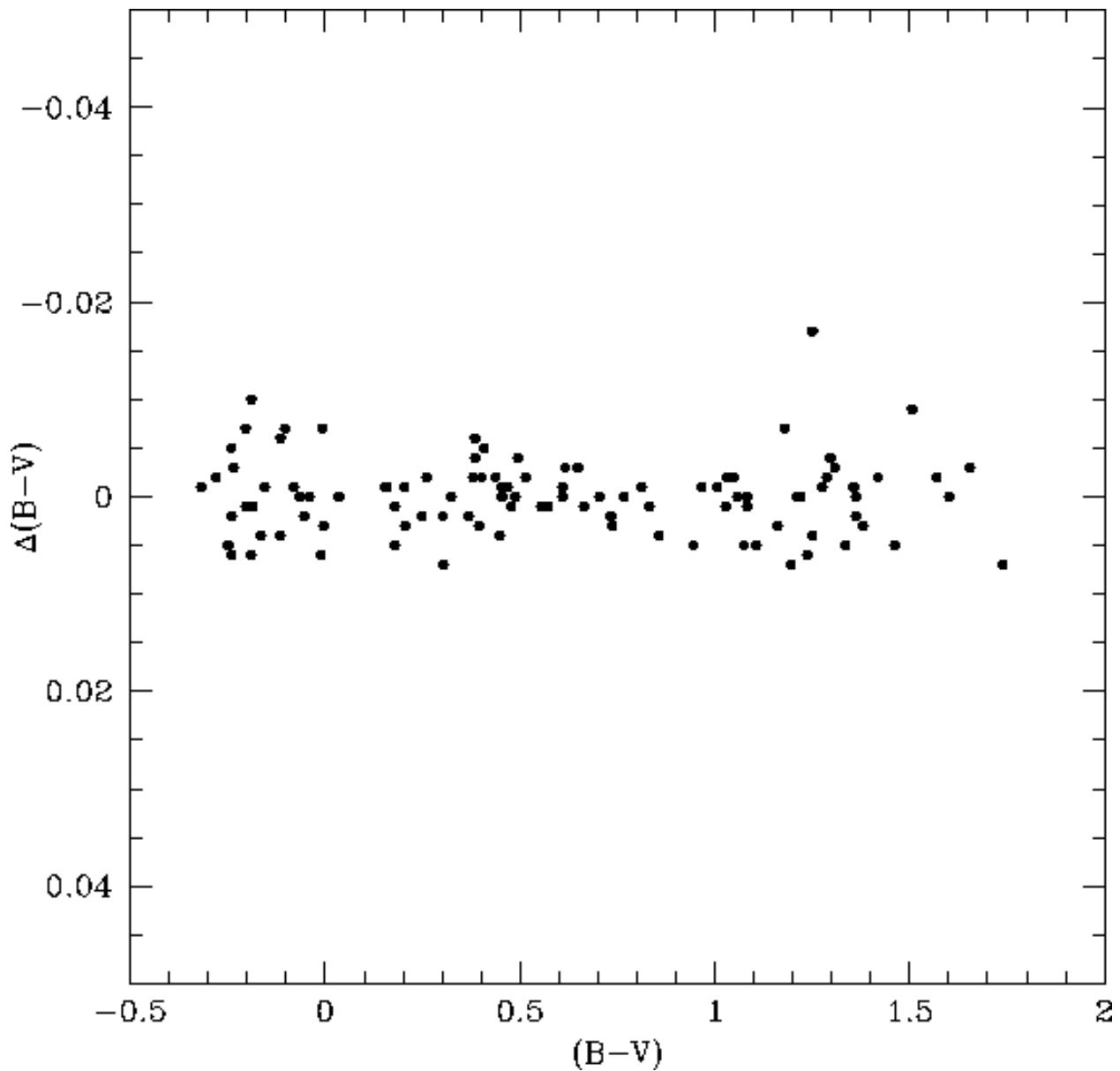


Fig. 8.— Comparison of the $(B - V)$ magnitudes after removal of the transformation non-linearity as a function of the Landolt (1992) equatorial standard star's $(B - V)$ color index.

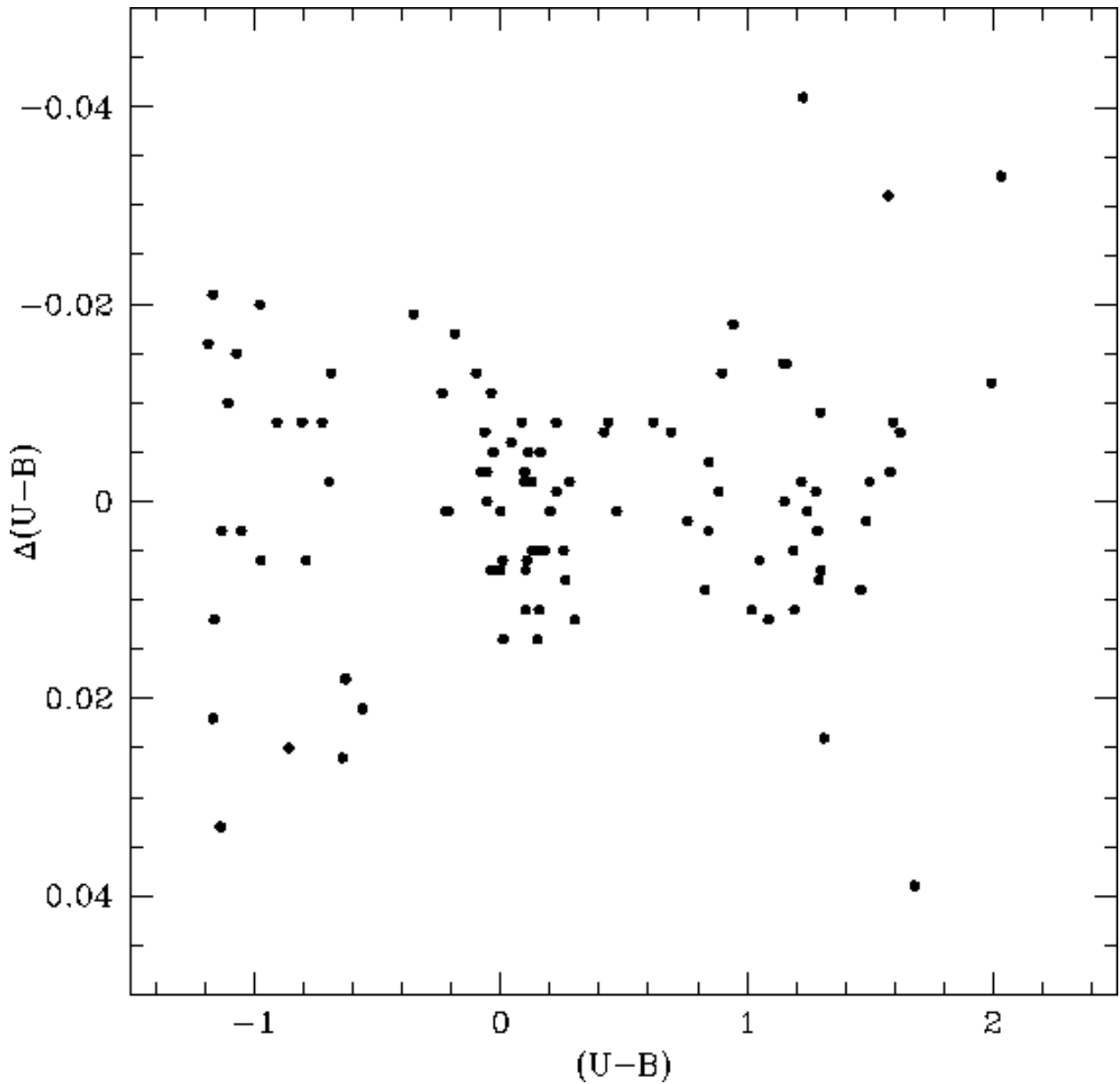


Fig. 9.— Comparison of the $(U - B)$ magnitudes after removal of the transformation non-linearity as a function of the Landolt (1992) equatorial standard star's $(U - B)$ color index.

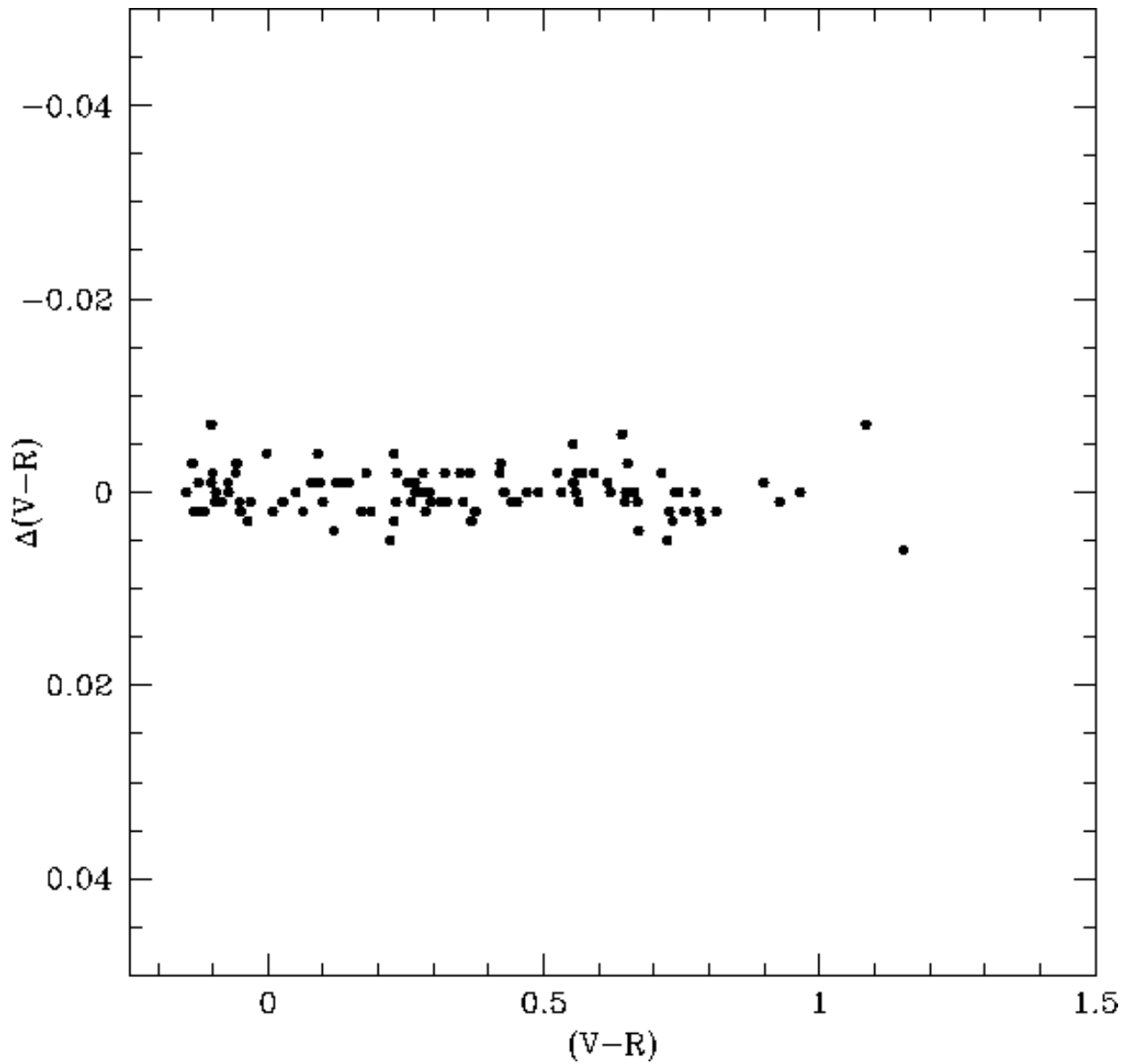


Fig. 10.— Comparison of the $(V - R)$ magnitudes after removal of the transformation nonlinearity as a function of the Landolt (1992) equatorial standard star's $(V - R)$ color index.

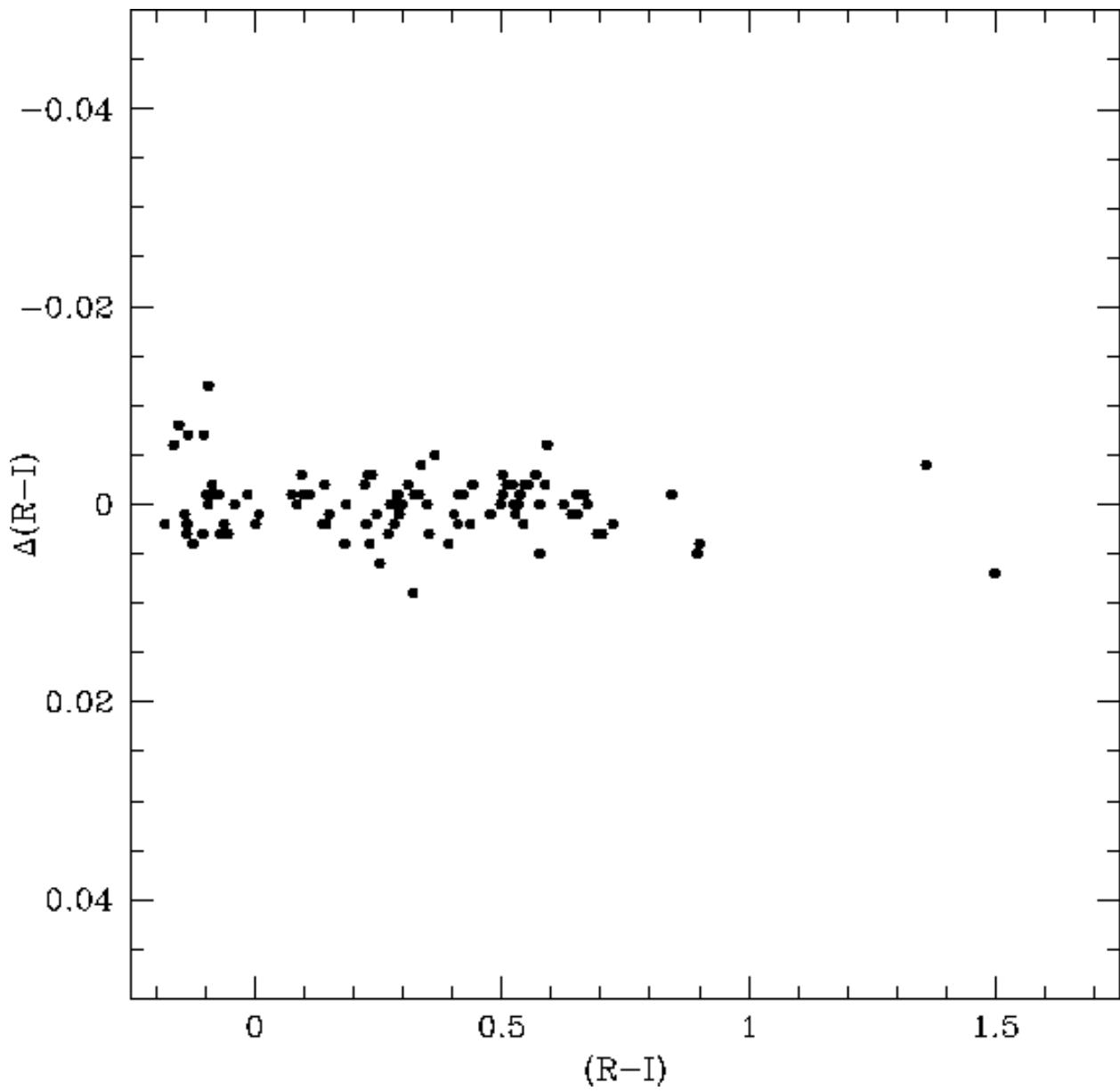


Fig. 11.— Comparison of the $(R - I)$ magnitudes after removal of the transformation nonlinearity as a function of the Landolt (1992) equatorial standard star's $(R - I)$ color index.

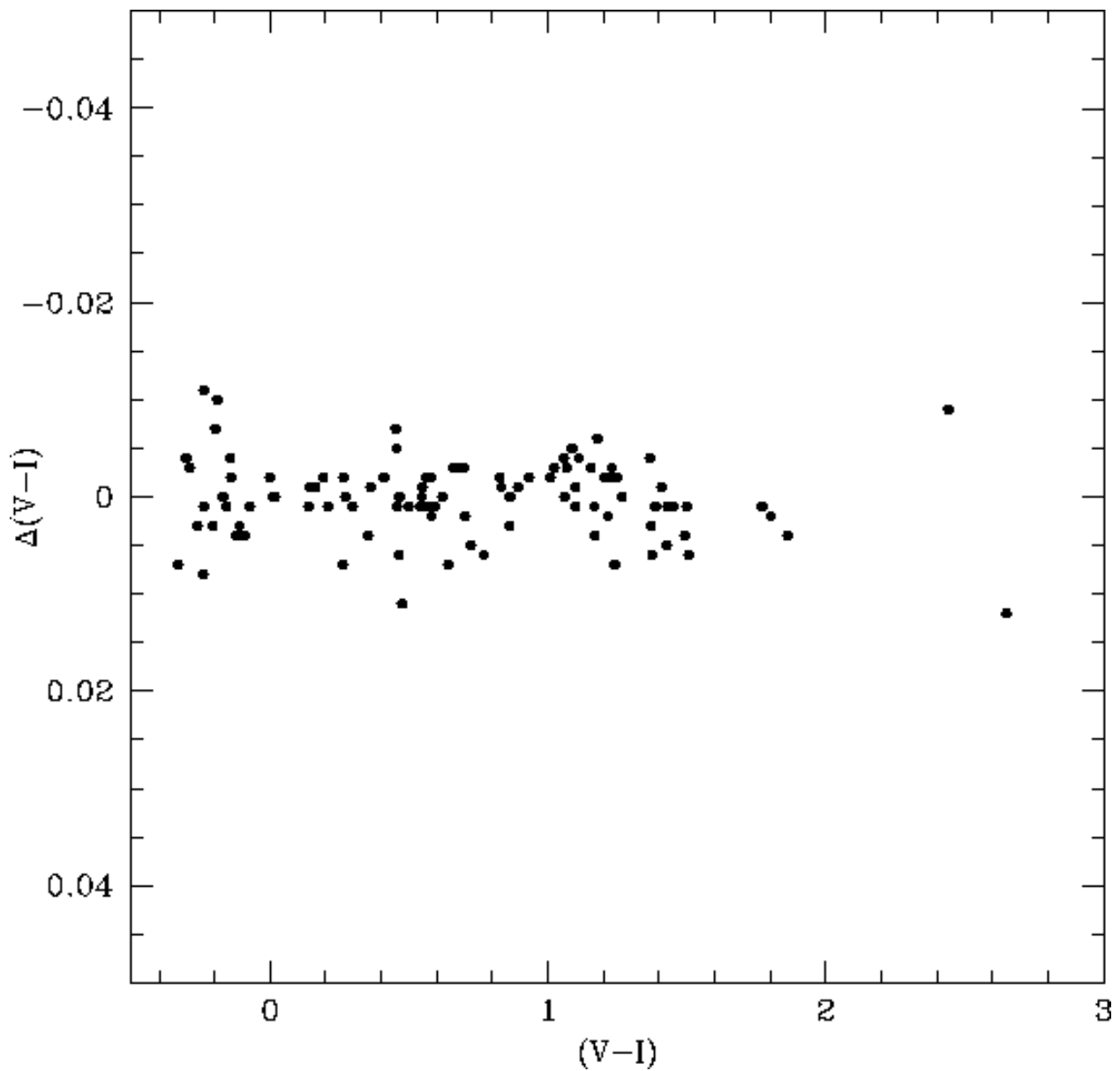


Fig. 12.— Comparison of the $(V - I)$ magnitudes after removal of the transformation nonlinearity as a function of the Landolt (1992) equatorial standard star's $(V - I)$ color index.

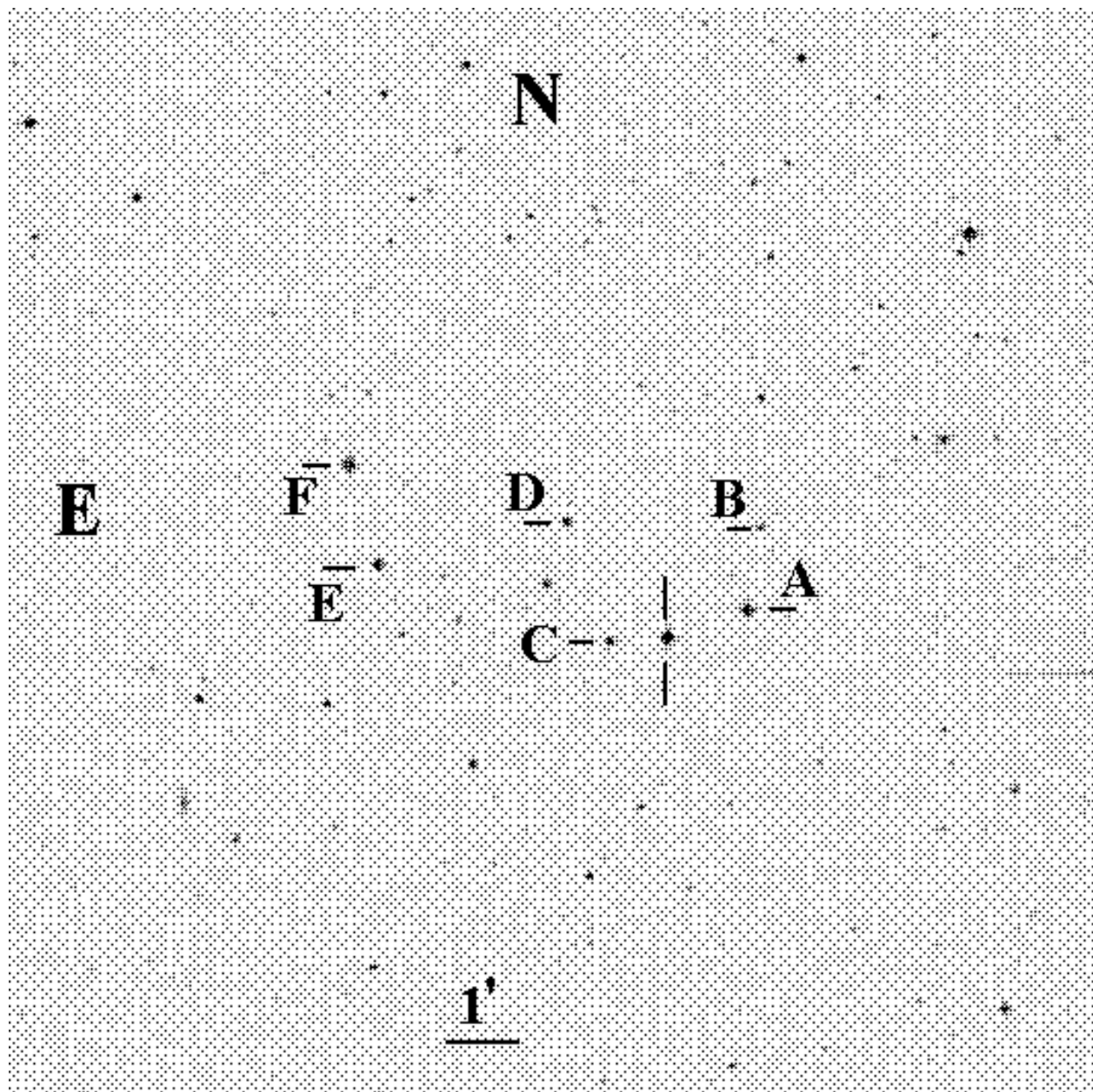


Fig. 13.— Field, 15' on a side, of the sequence in the vicinity of the star JL 163.

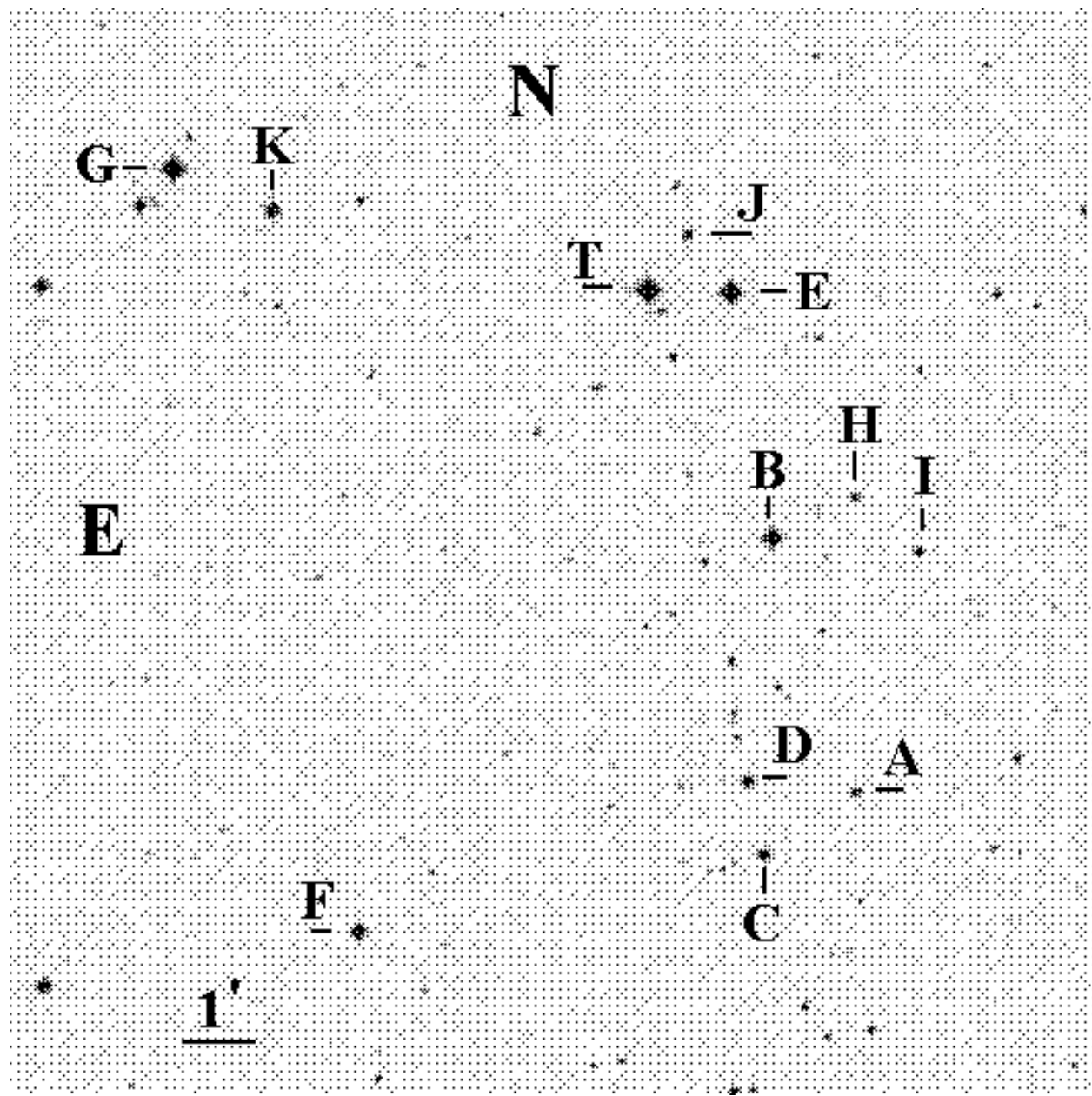


Fig. 14.—Field, 15' on a side, of the sequence in the vicinity of the Mira variable star T Phe, marked as "T" in the figure.

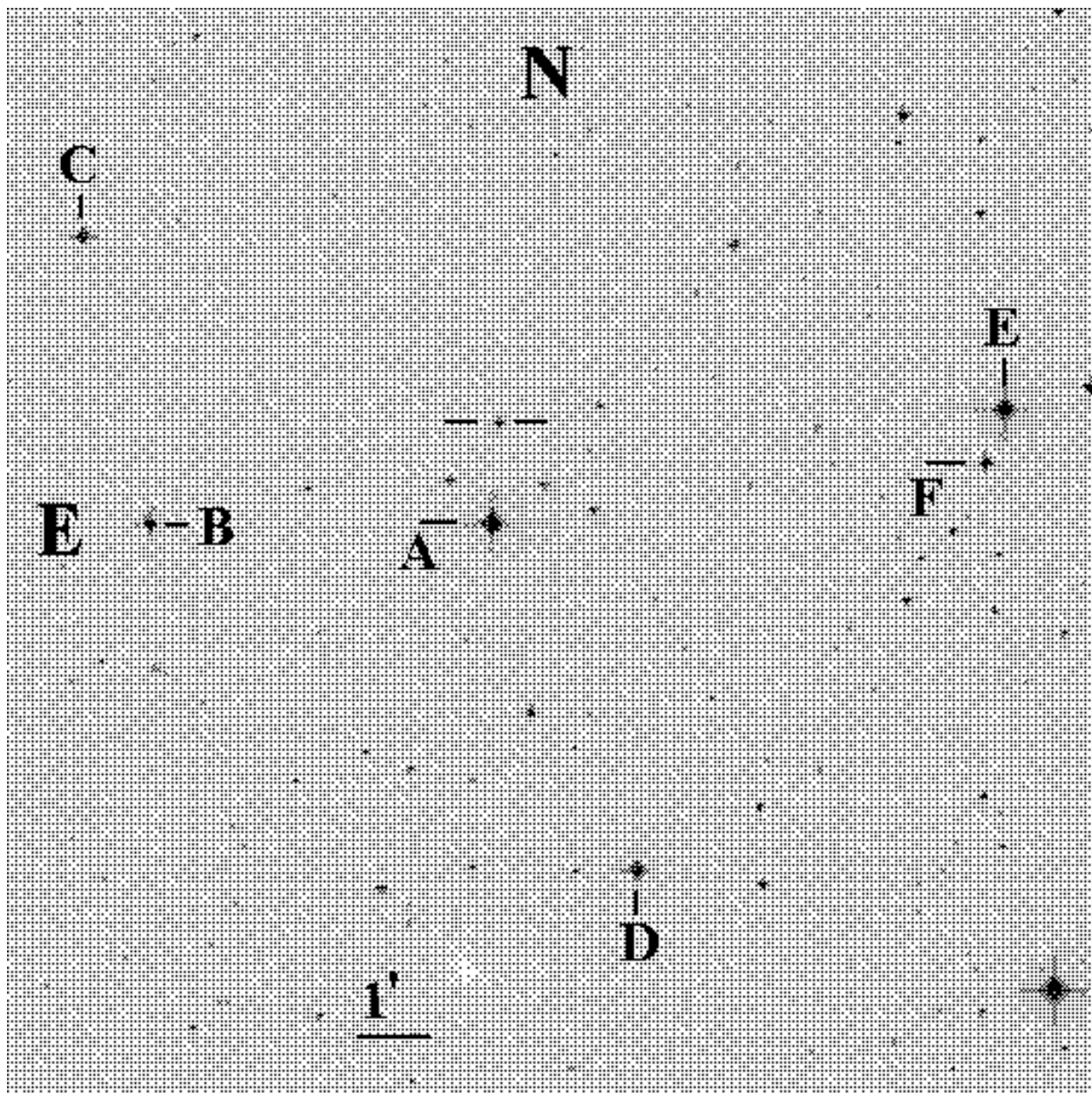


Fig. 15.—Field, 15' on a side, of the sequence in the vicinity of the star MCT 0401-4017.

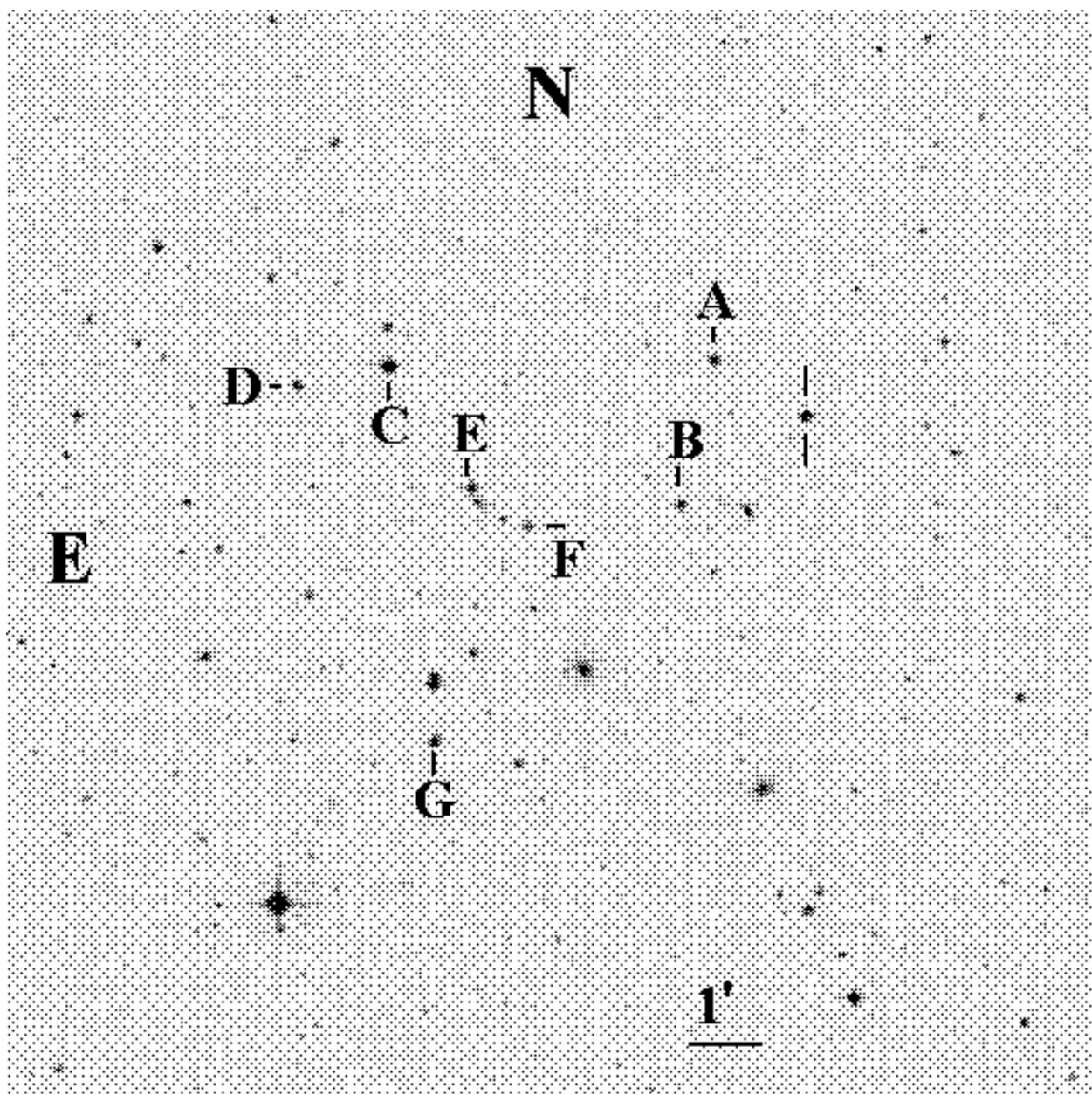


Fig. 16.—Field, 15' on a side, of the sequence in the vicinity of the star LB 1735.

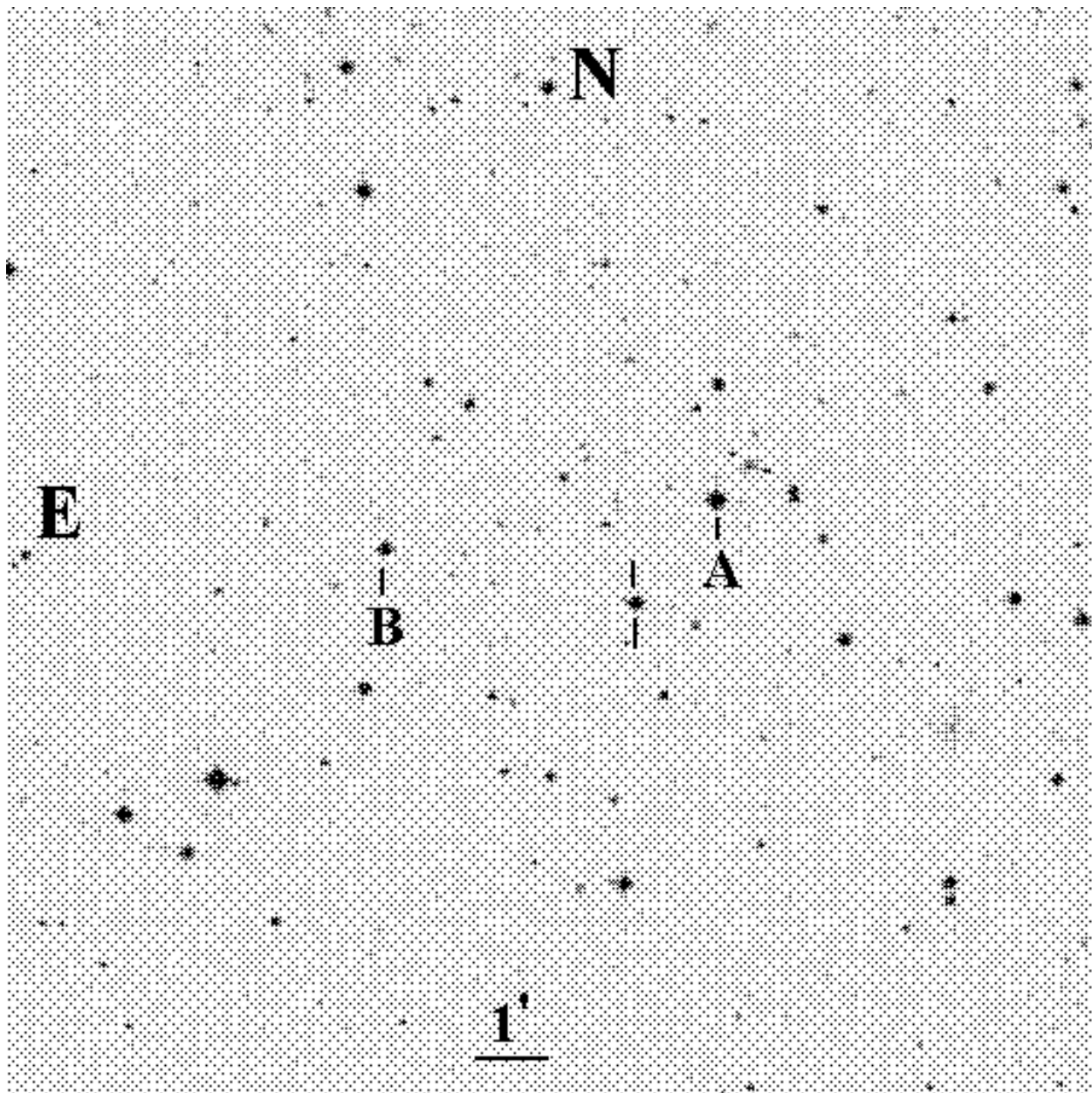


Fig. 17.—Field, 15' on a side, of the sequence in the vicinity of the star MCT 0436-4616.

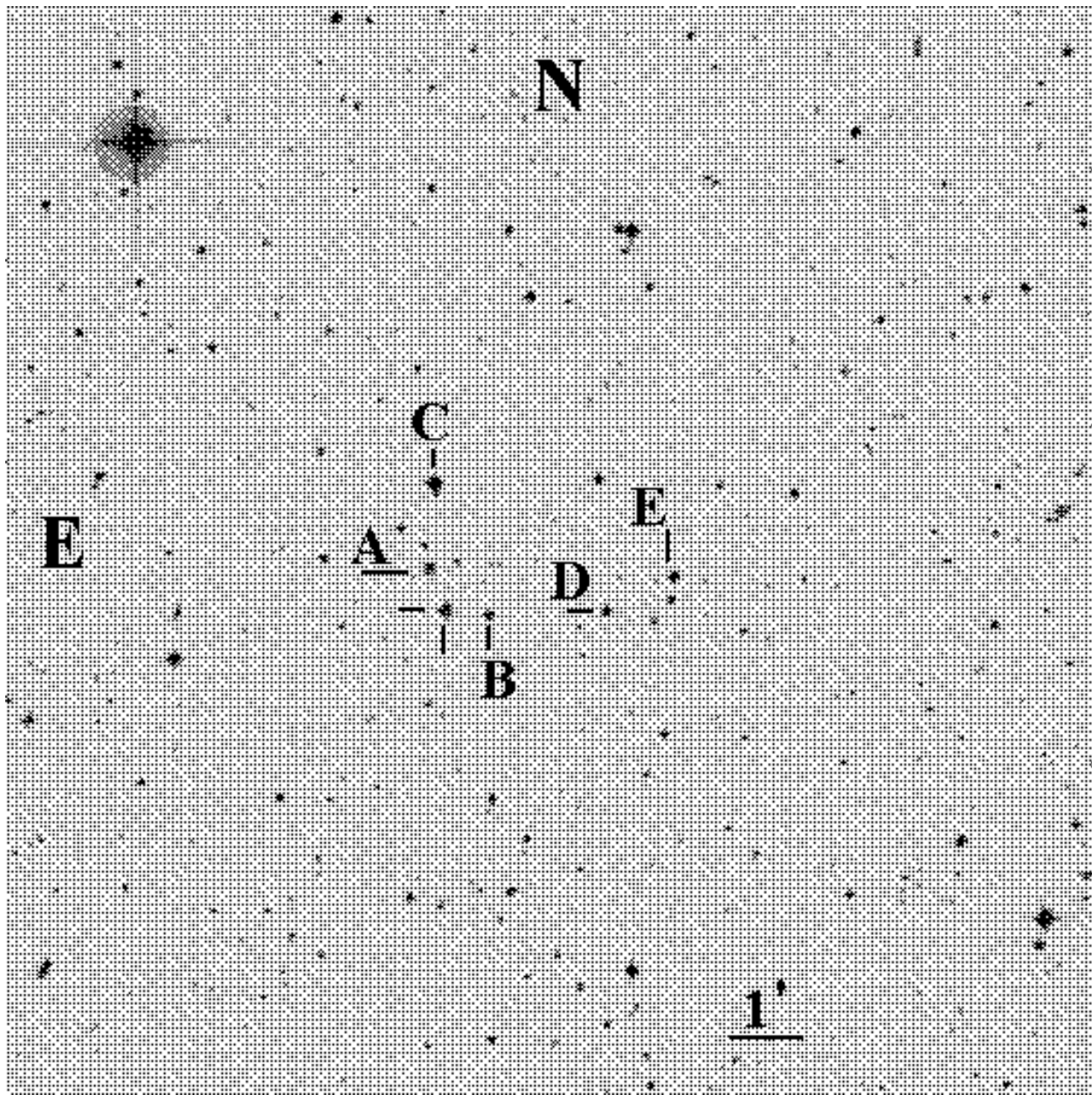


Fig. 18.—Field, 15' on a side, of the sequence in the vicinity of the star MCT 0550-4911.

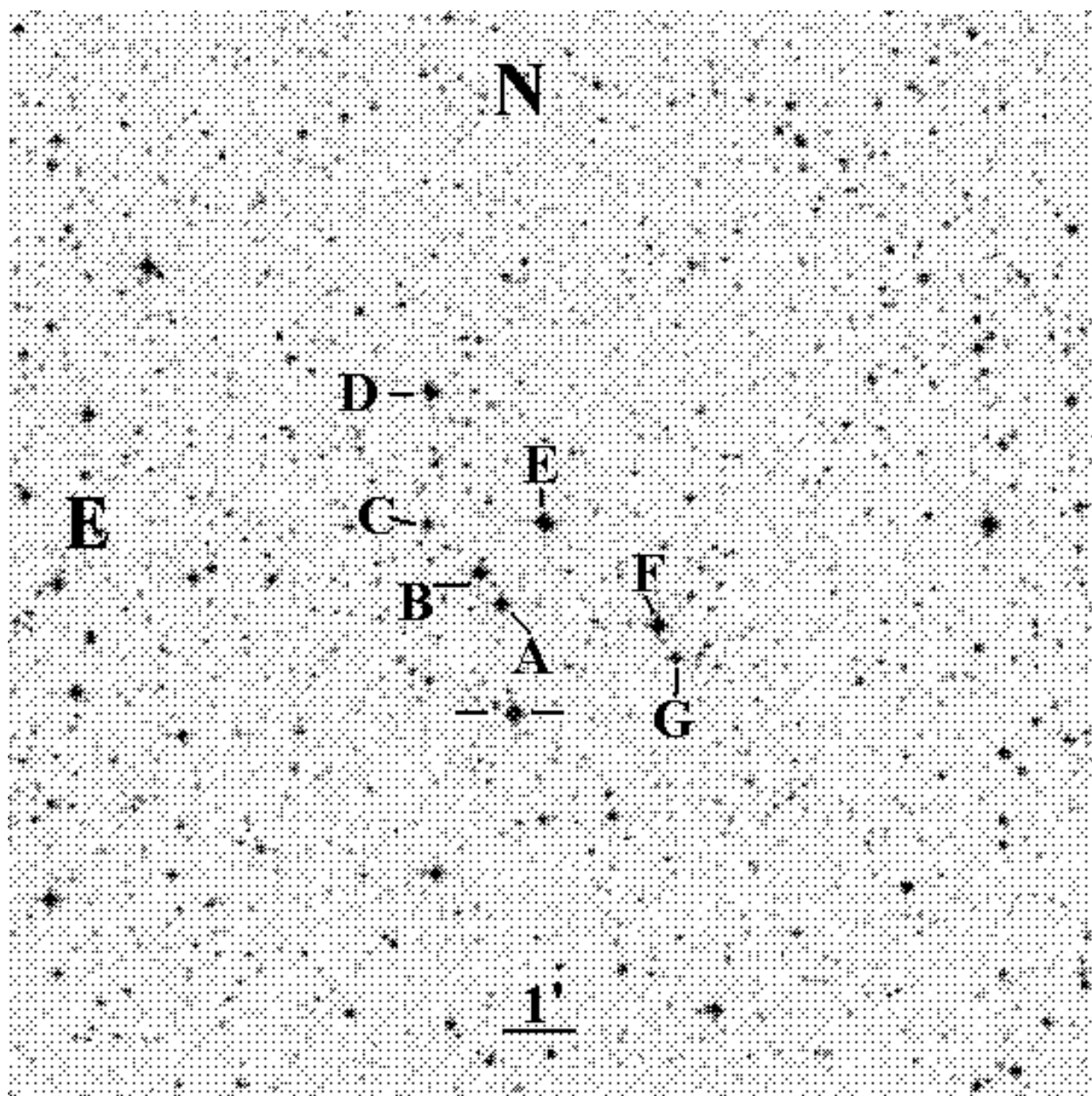


Fig. 19.— Field, 15' on a side, of the sequence in the vicinity of the star LSS 982.

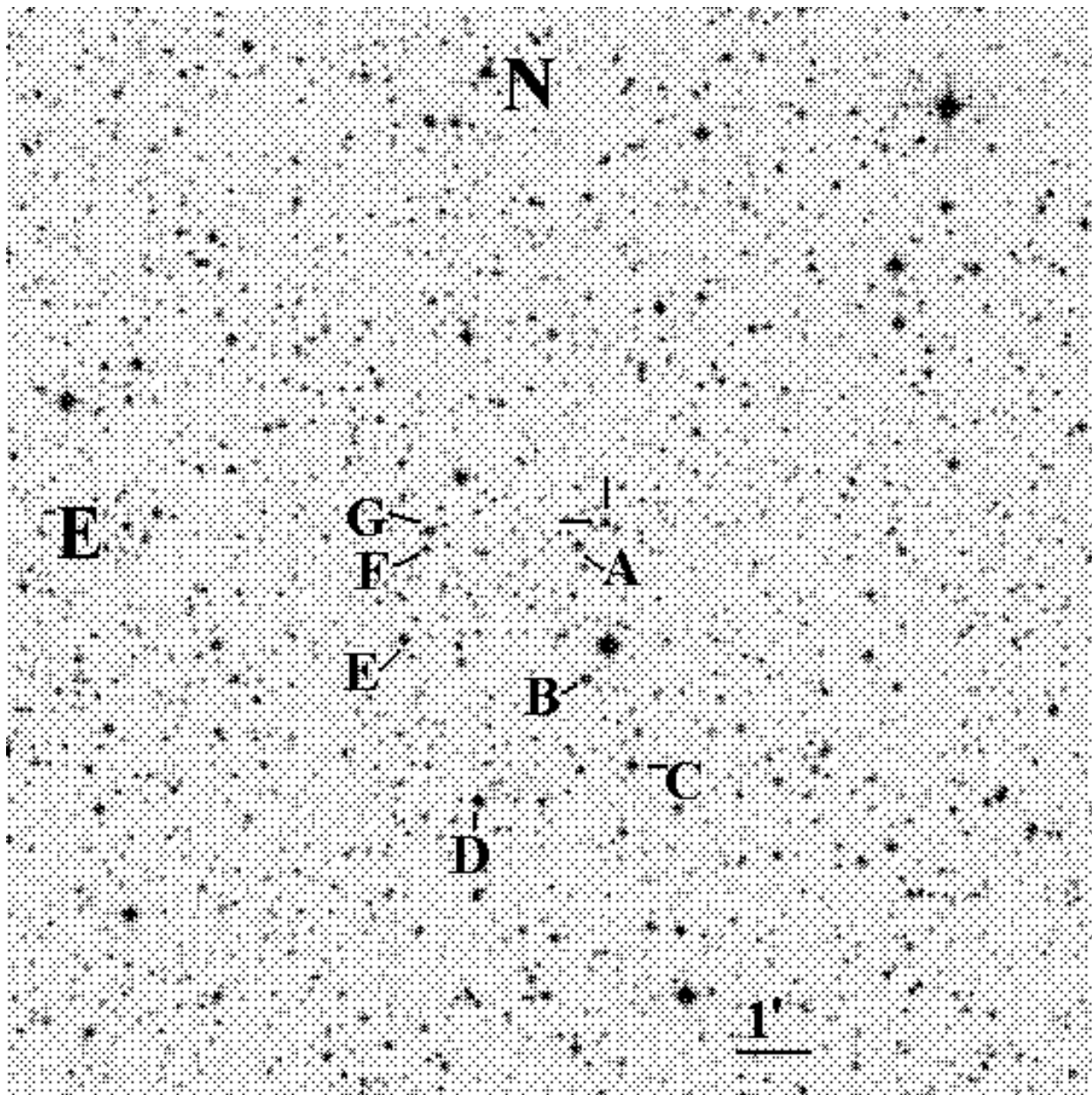


Fig. 20.— Field, 15' on a side, of the sequence in the vicinity of the star WD 0830-535.

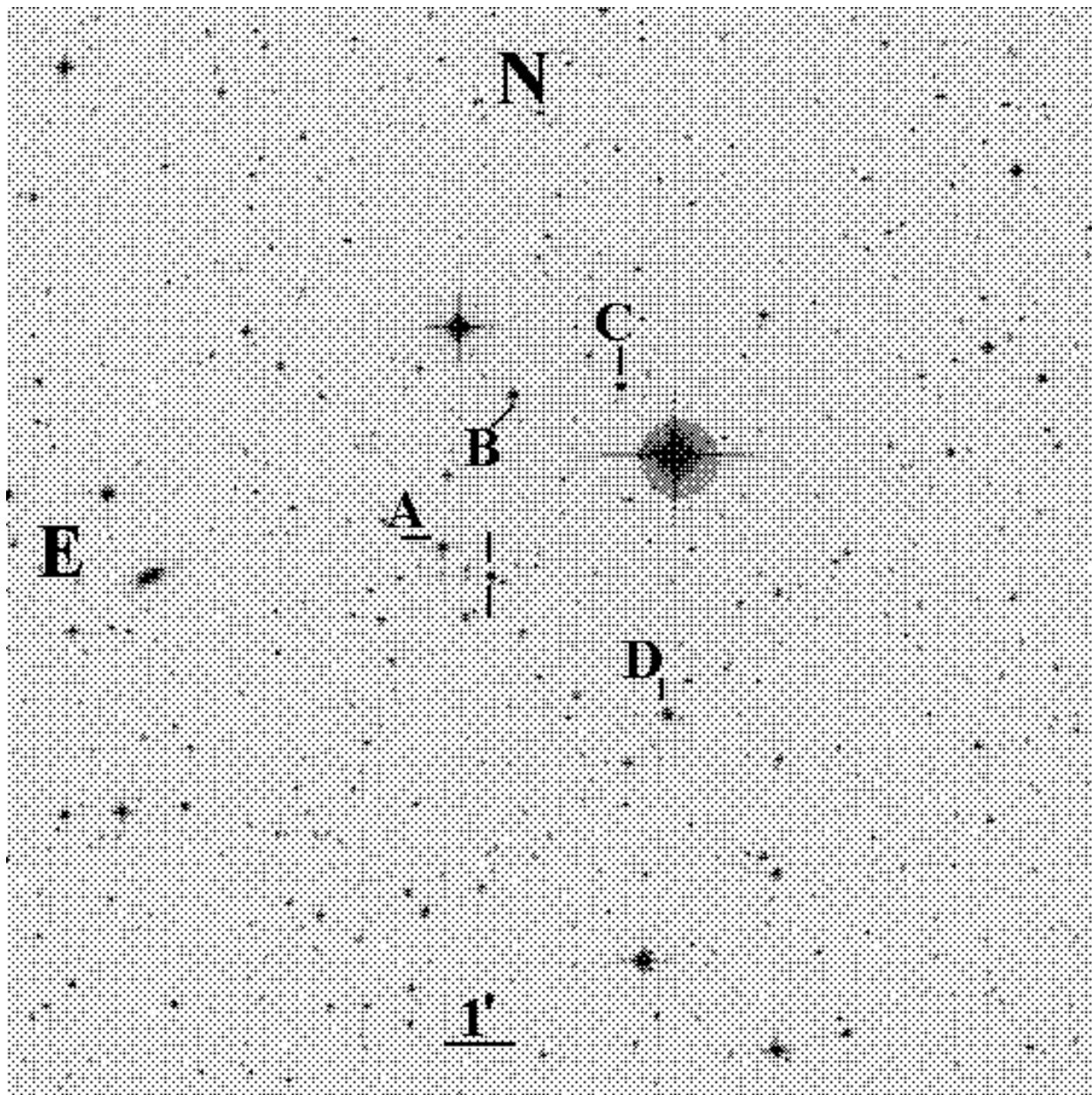


Fig. 21.— Field, 15' on a side, of the sequence in the vicinity of the star WD 1056-384.

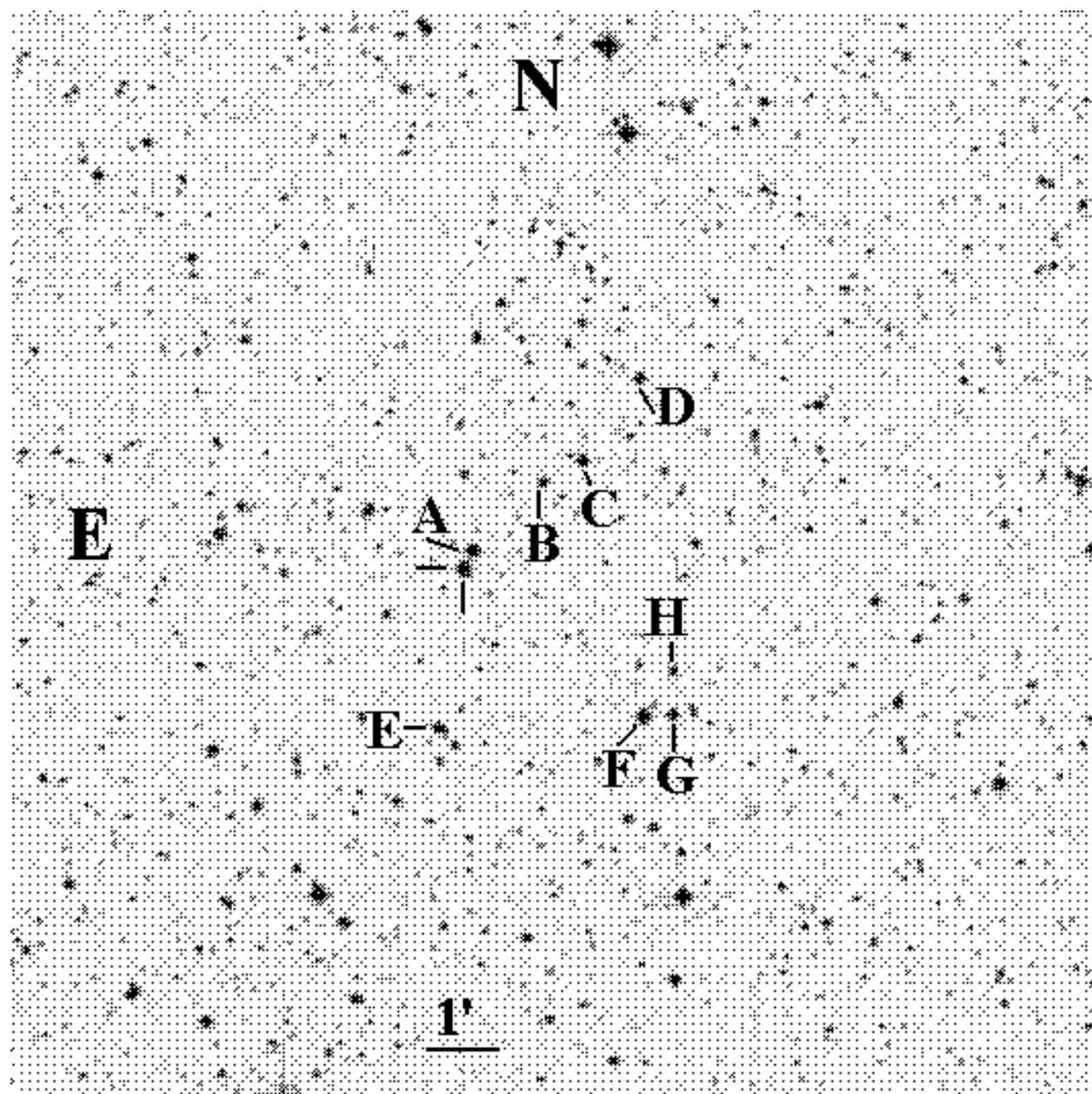


Fig. 22.— Field, 15' on a side, of the sequence in the vicinity of the star WD 1153-484.

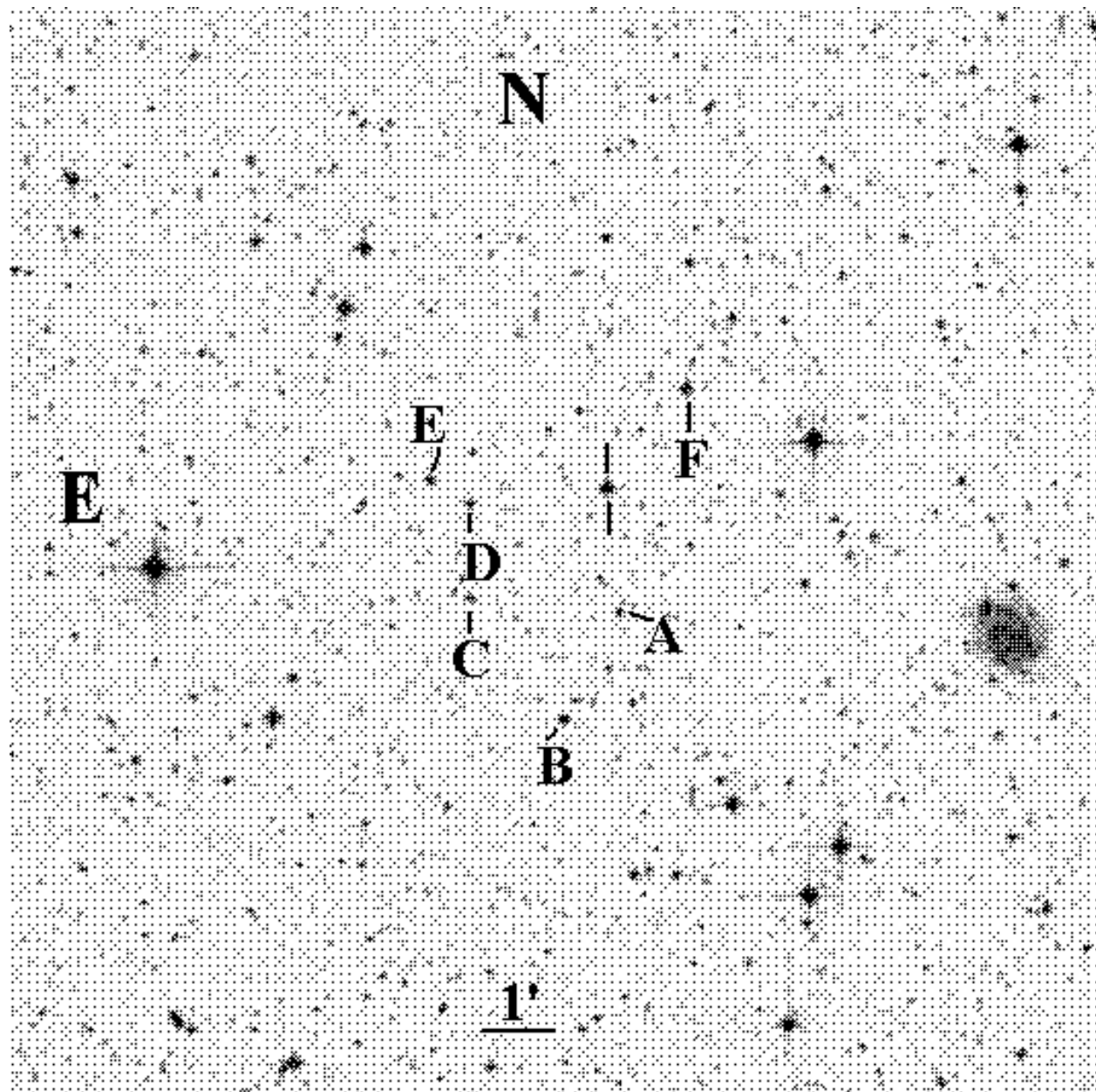


Fig. 23.—Field, 15' on a side, of the sequence in the vicinity of the star LSE 44.

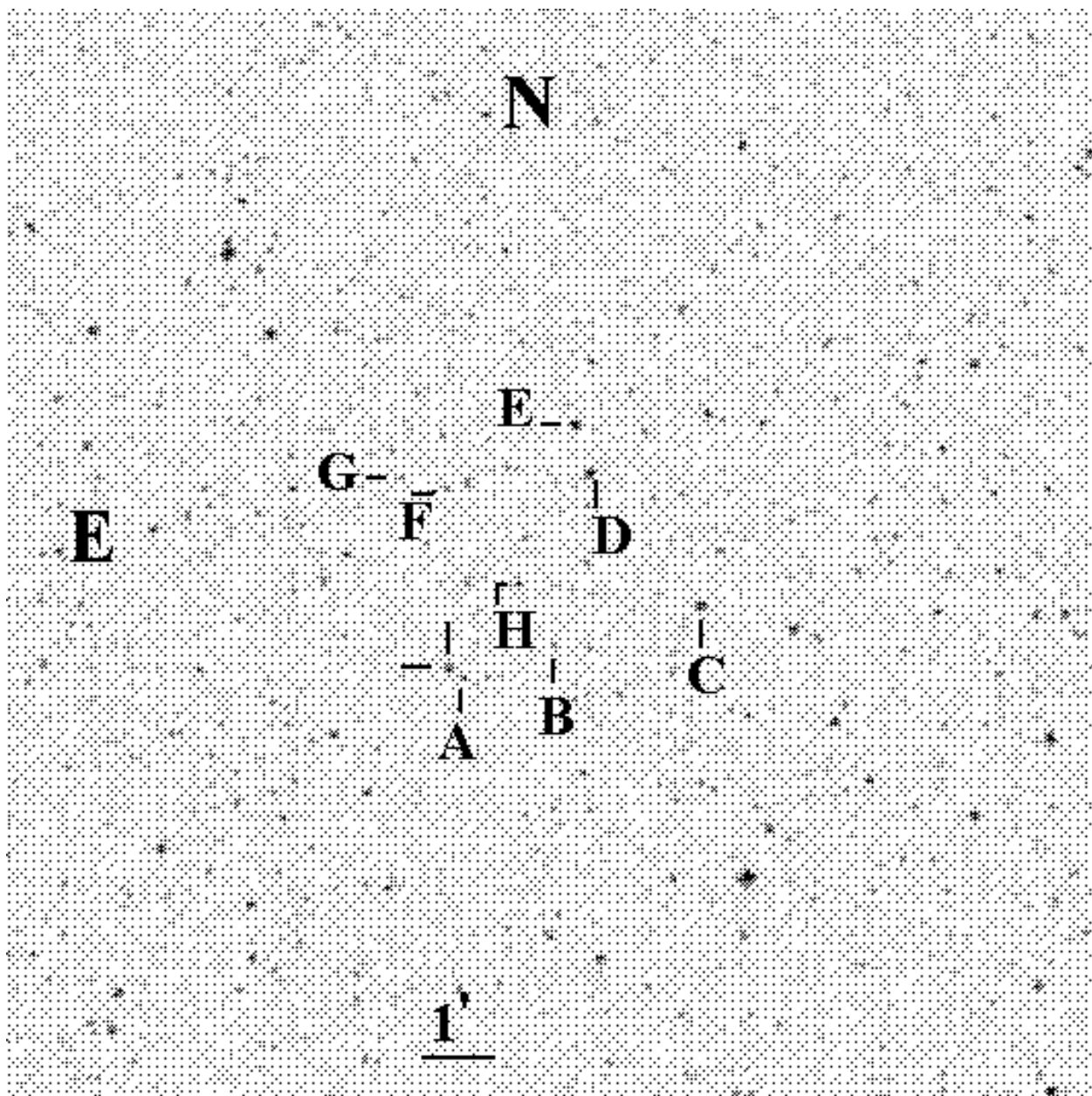


Fig. 24.—Field, 15' on a side, of the sequence in the vicinity of the star LSE 259.

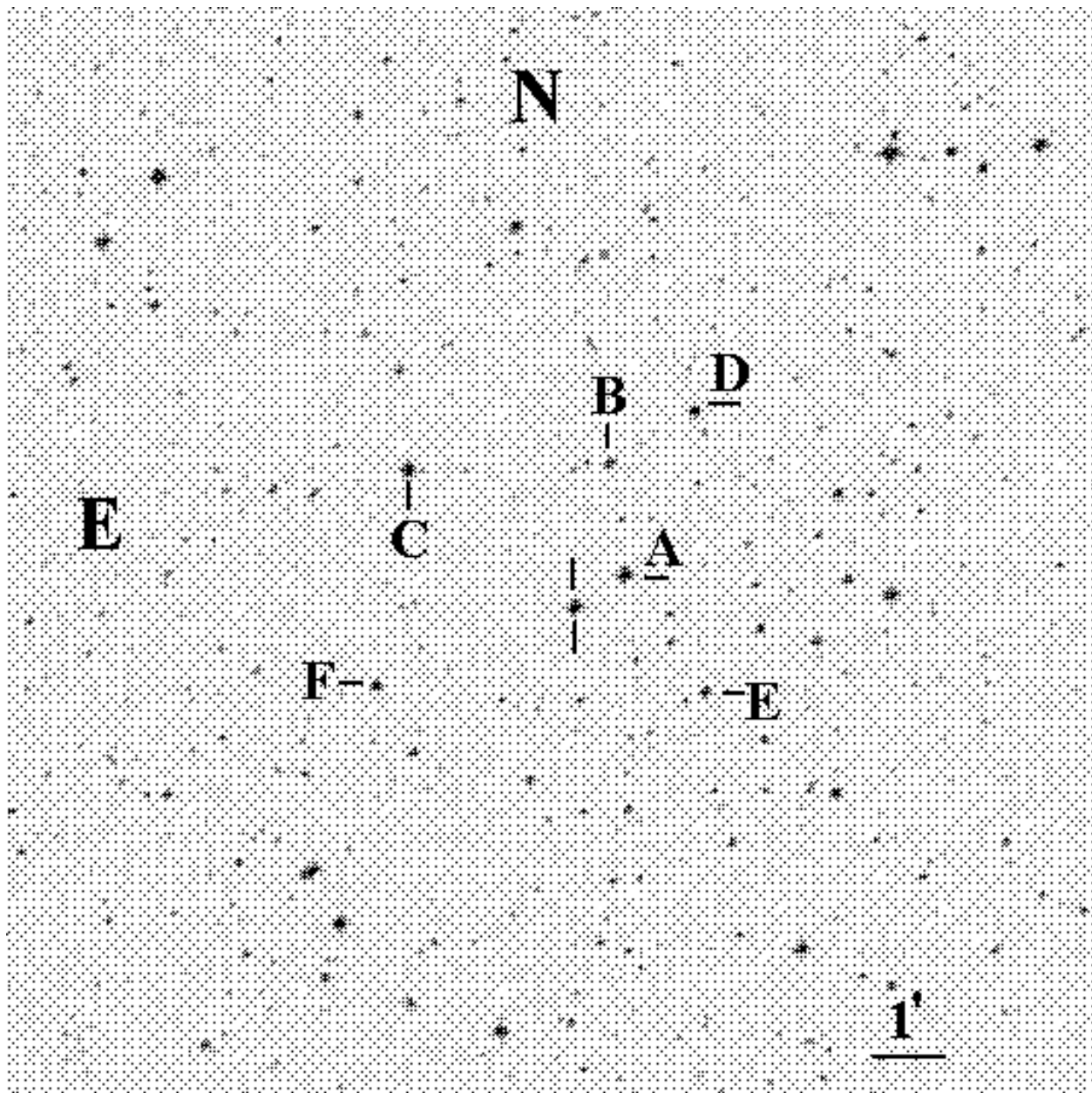


Fig. 25.— Field, 15' on a side, of the sequence in the vicinity of the star MCT 2019-4339.

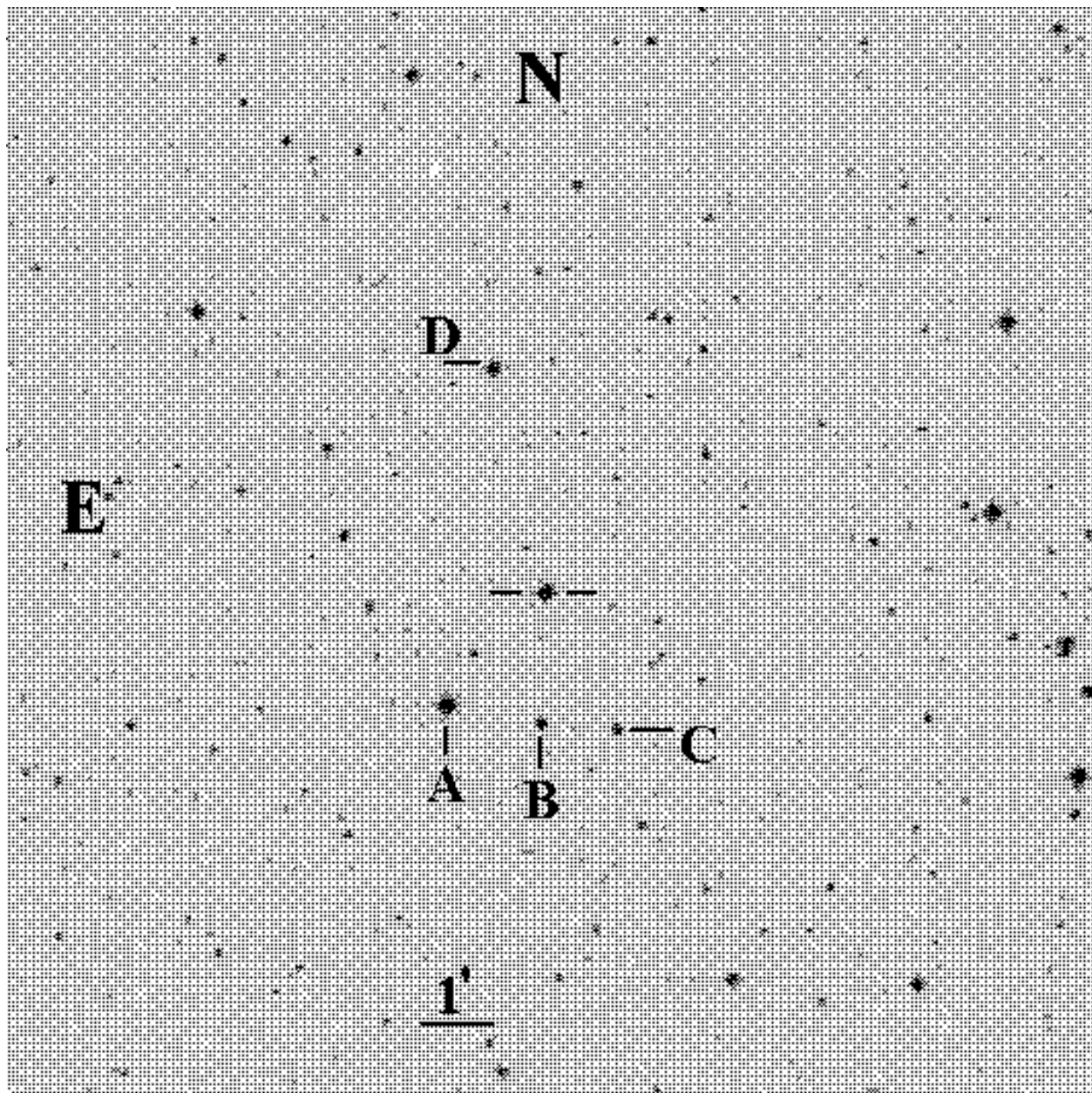


Fig. 26.—Field, 15' on a side, of the sequence in the vicinity of the star JL 82.

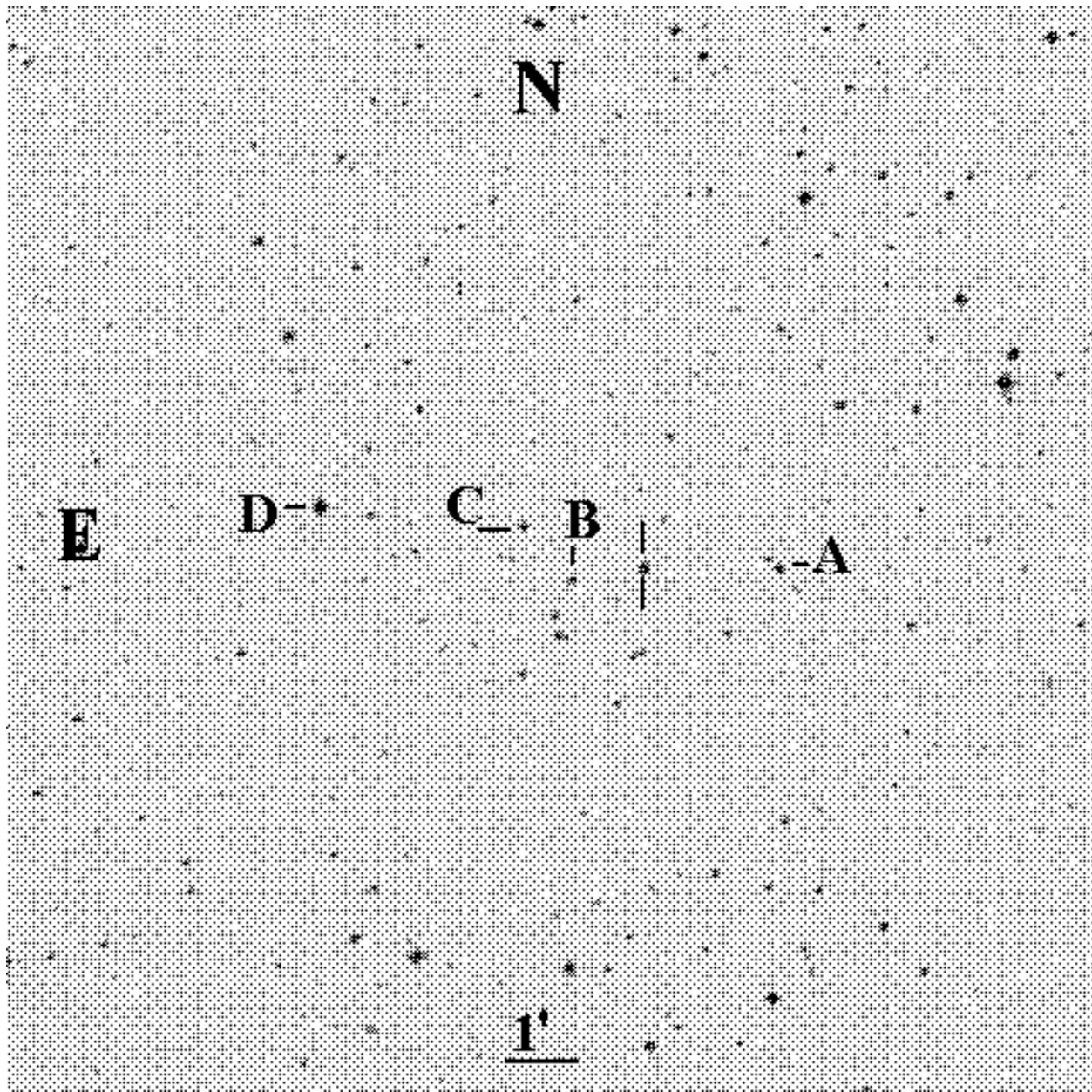


Fig. 27.—Field, 15' on a side, of the sequence in the vicinity of the star JL 117.

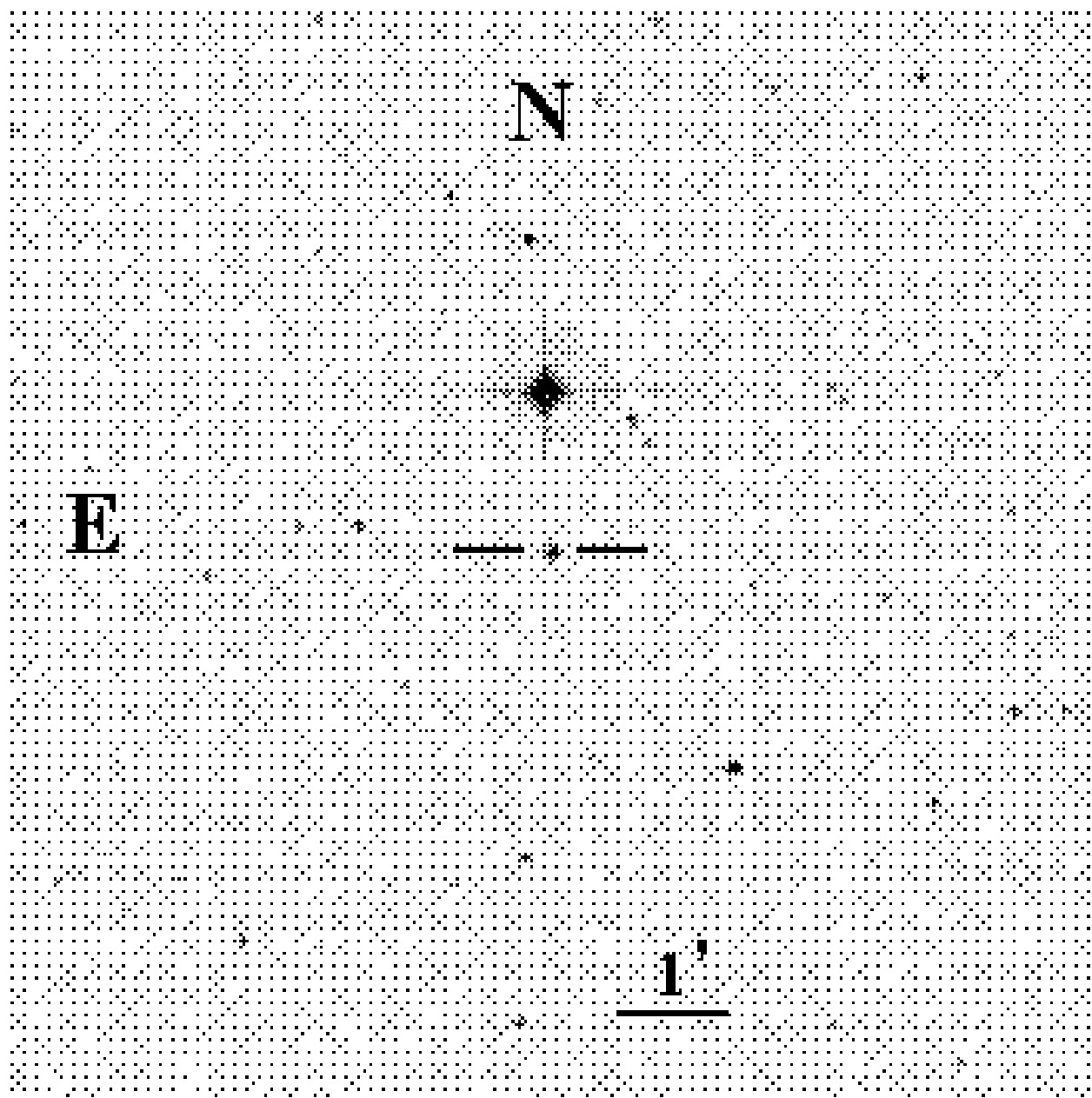


Fig. 28.—Field, 10' on a side, of the star JL 166.

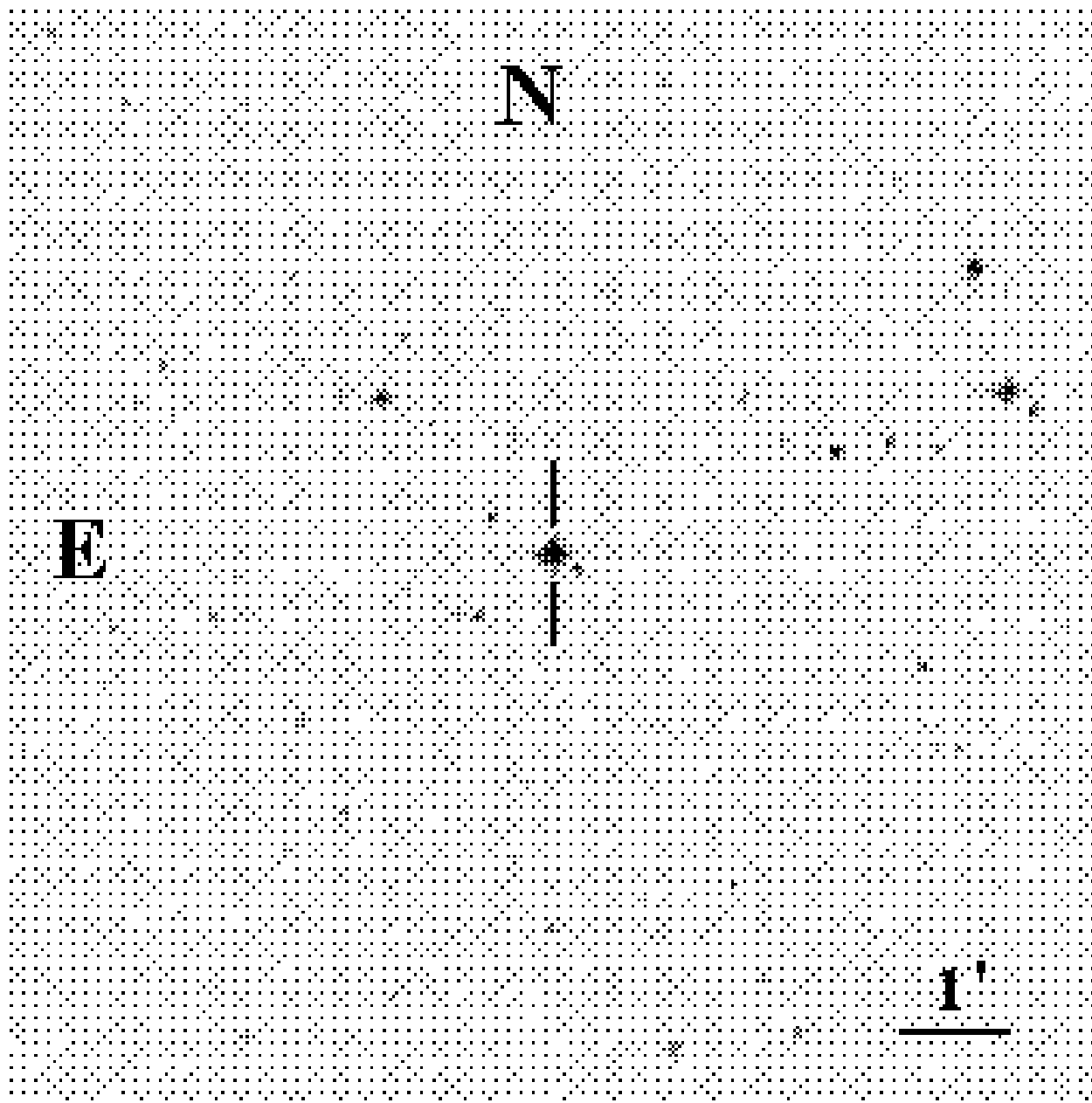


Fig. 29.—Field, $10'$ on a side, of the star JL 194.

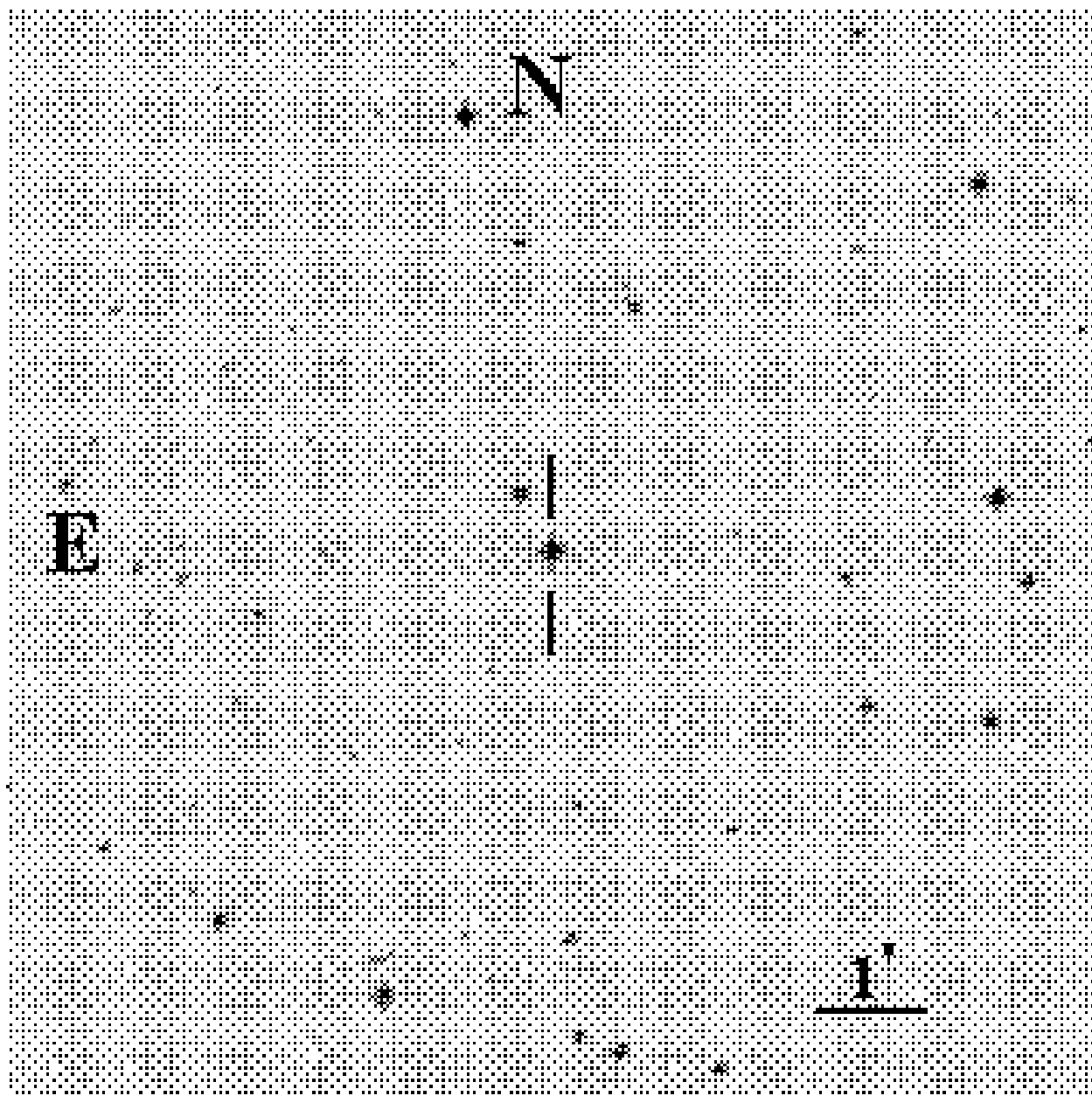


Fig. 30.— Field, $10'$ on a side, of the star JL 202.

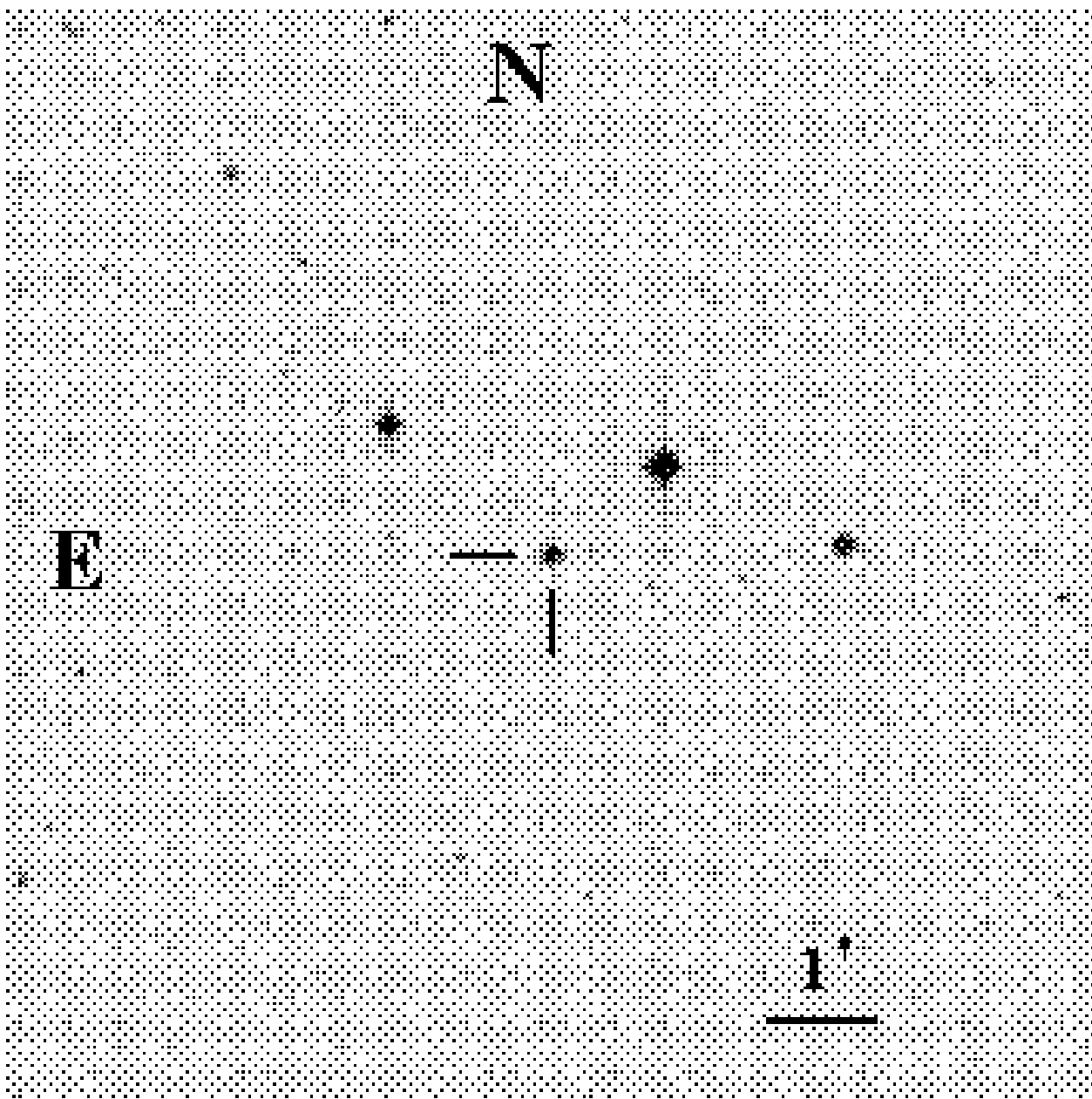


Fig. 31.— Field, 10' on a side, of the star GD 679.

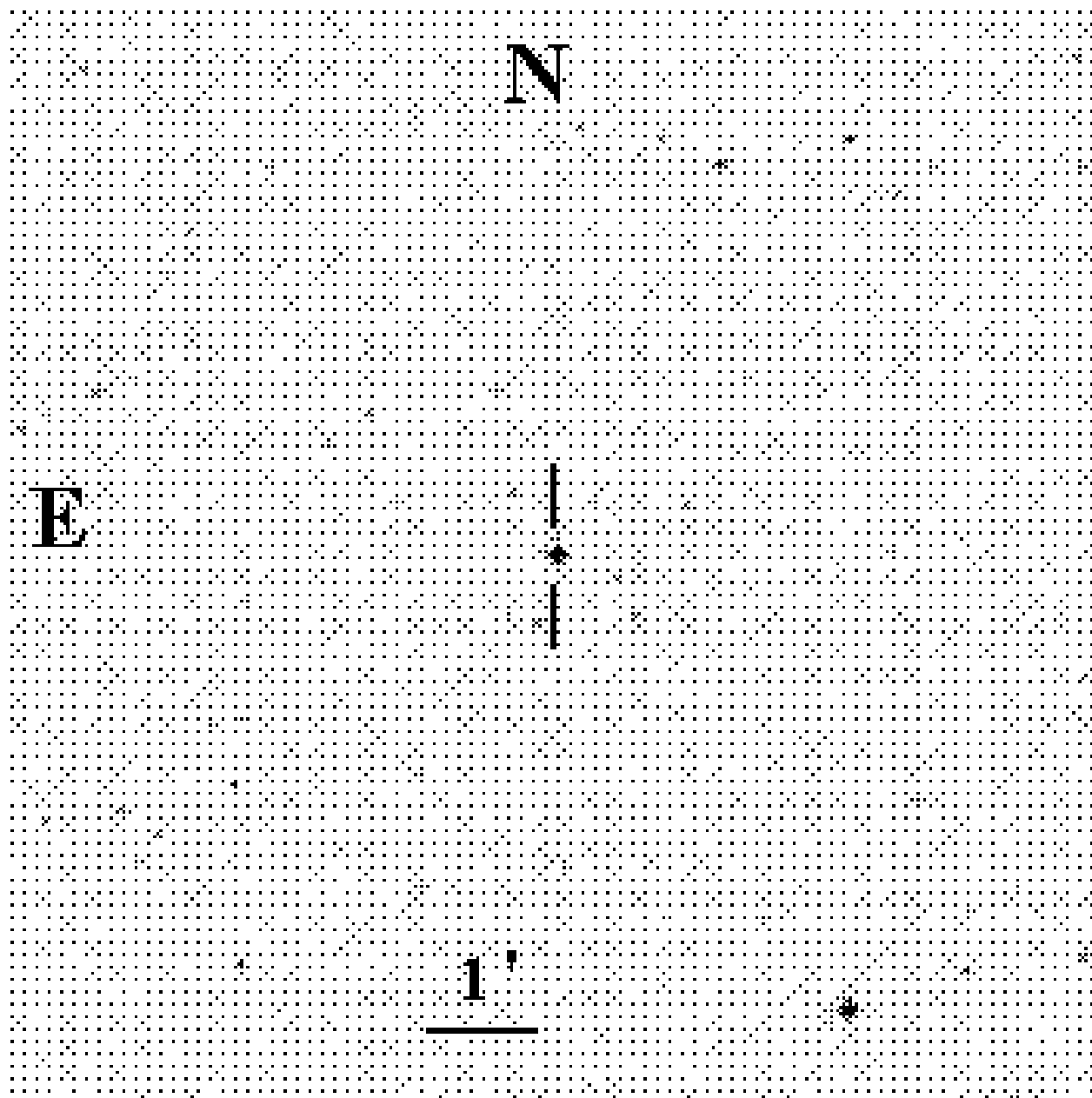


Fig. 32.—Field, 10' on a side, of the star JL 236.

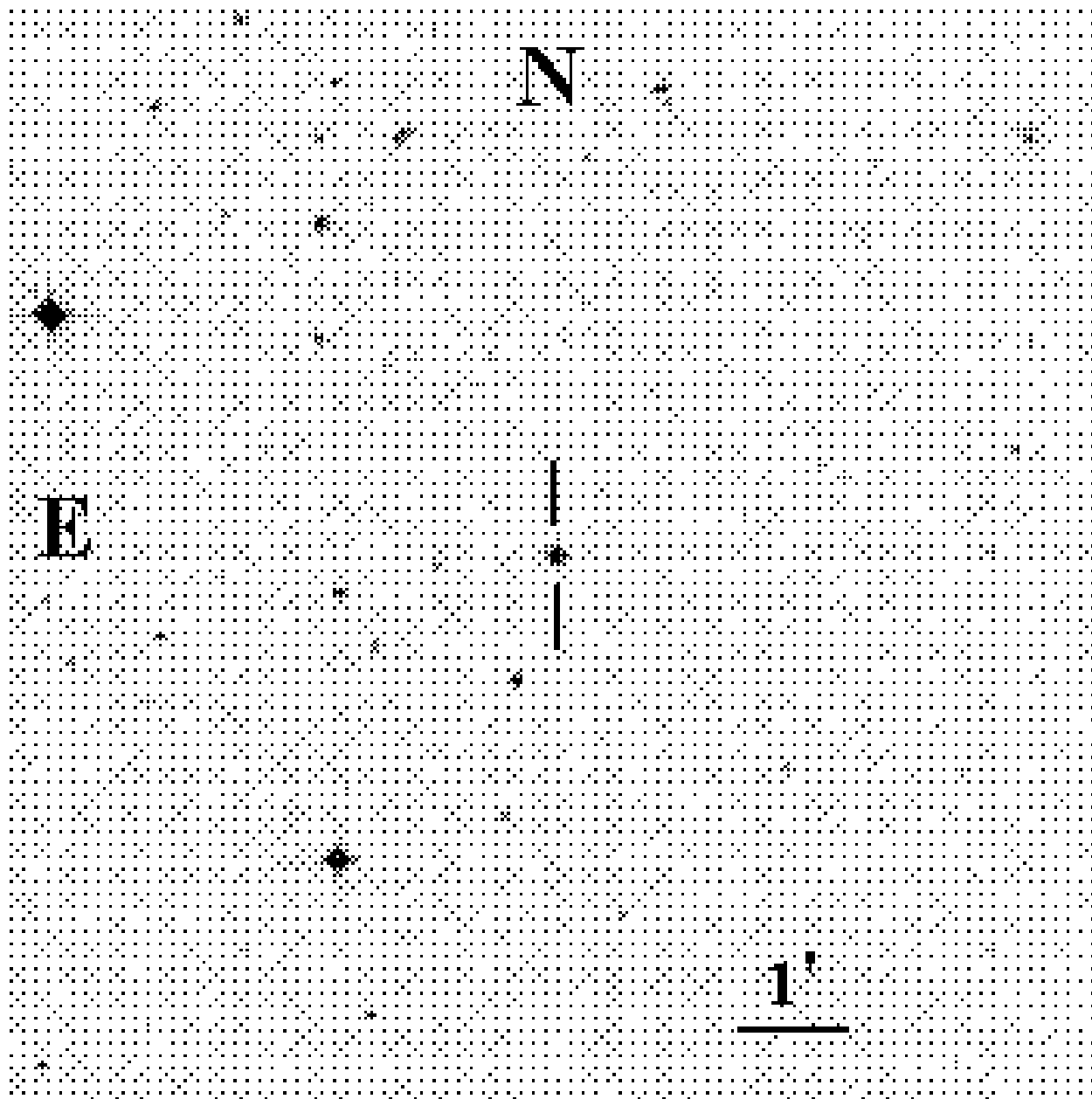


Fig. 33.— Field, 10' on a side, of the star JL 261.

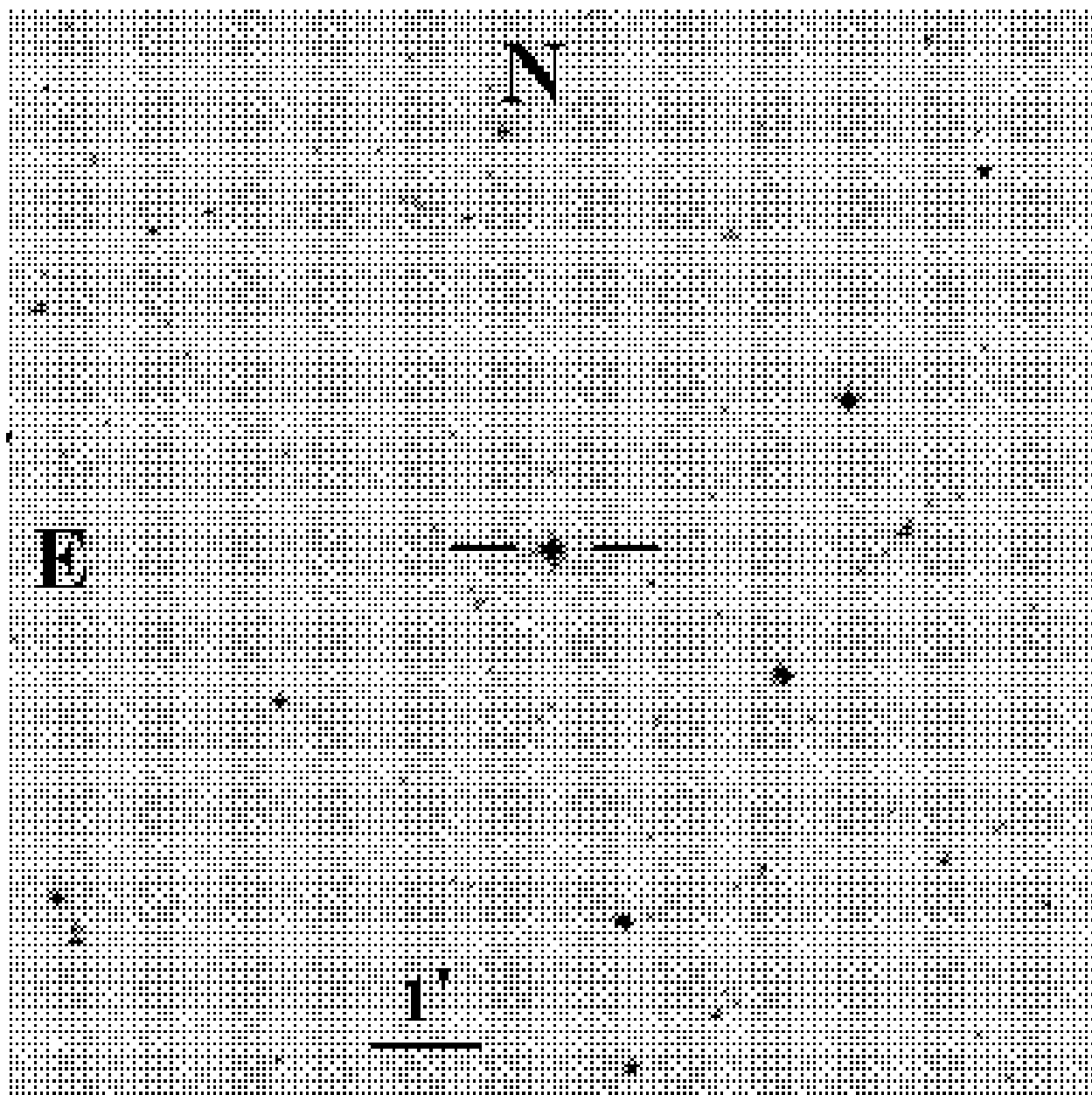


Fig. 34.— Field, $10'$ on a side, of the star LB 3241.

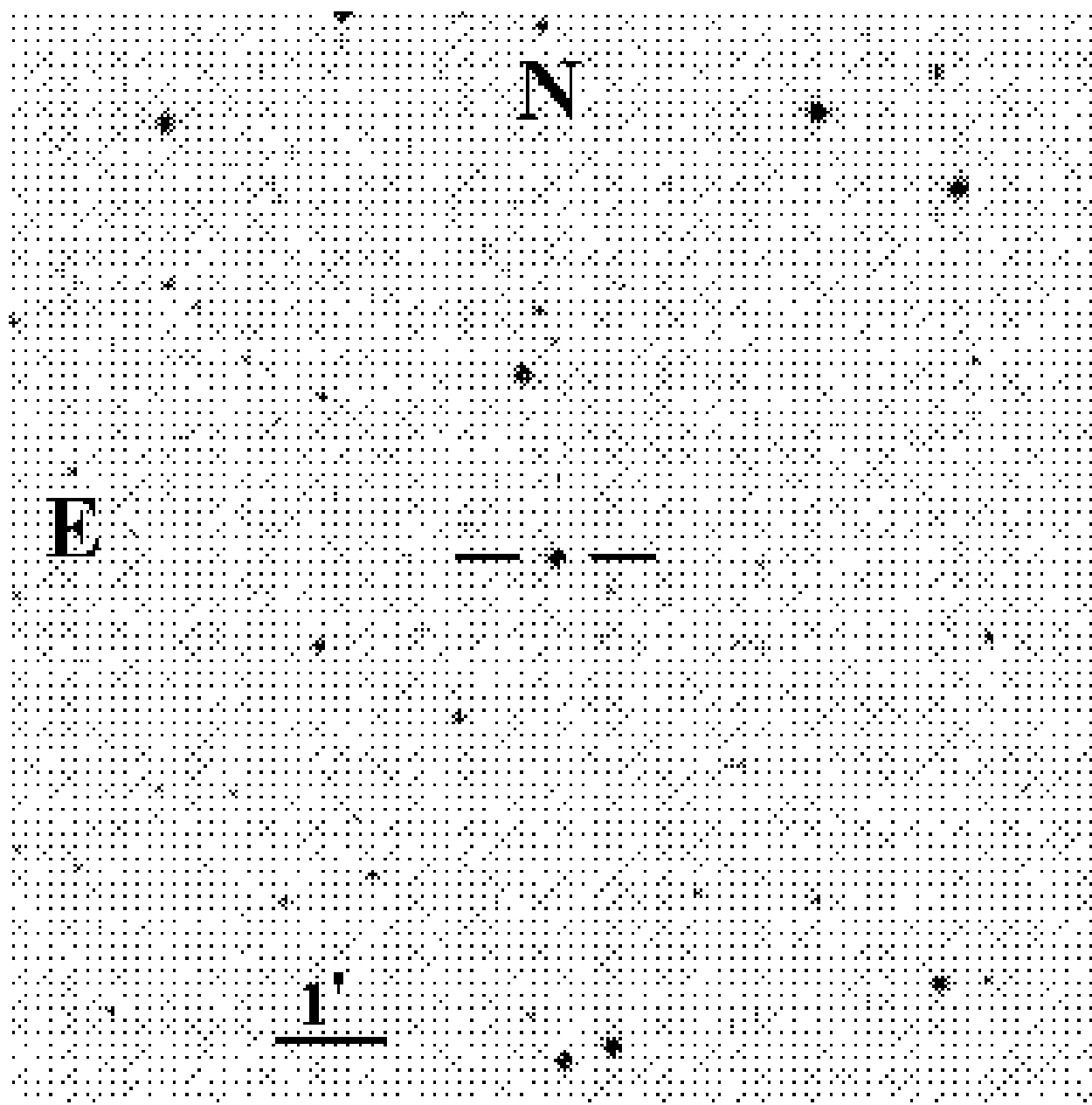


Fig. 35.—Field, 10' on a side, of the star JL 286.

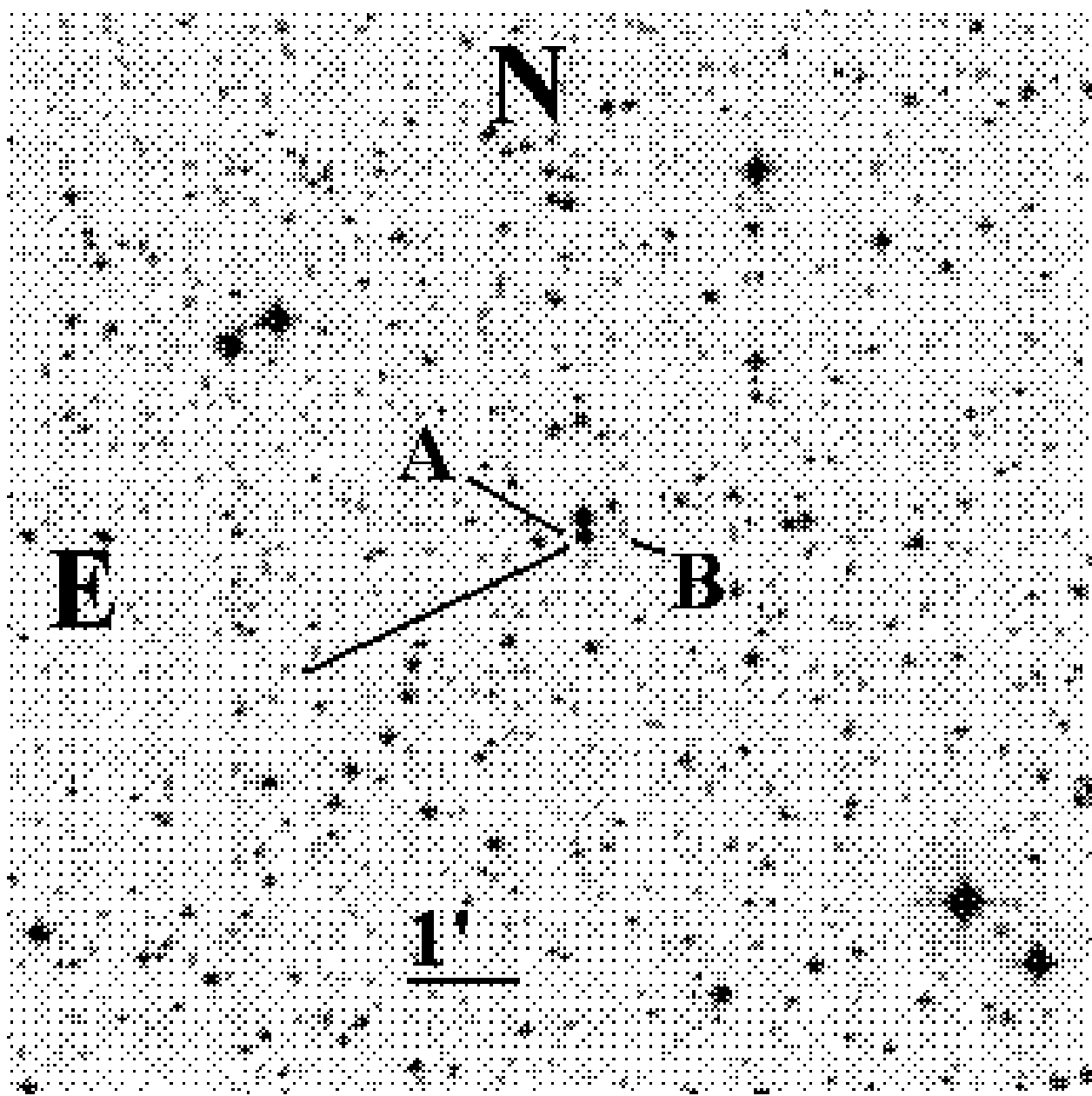


Fig. 36.—Field, 10' on a side, of the star L745-46A (see text, Section 4).

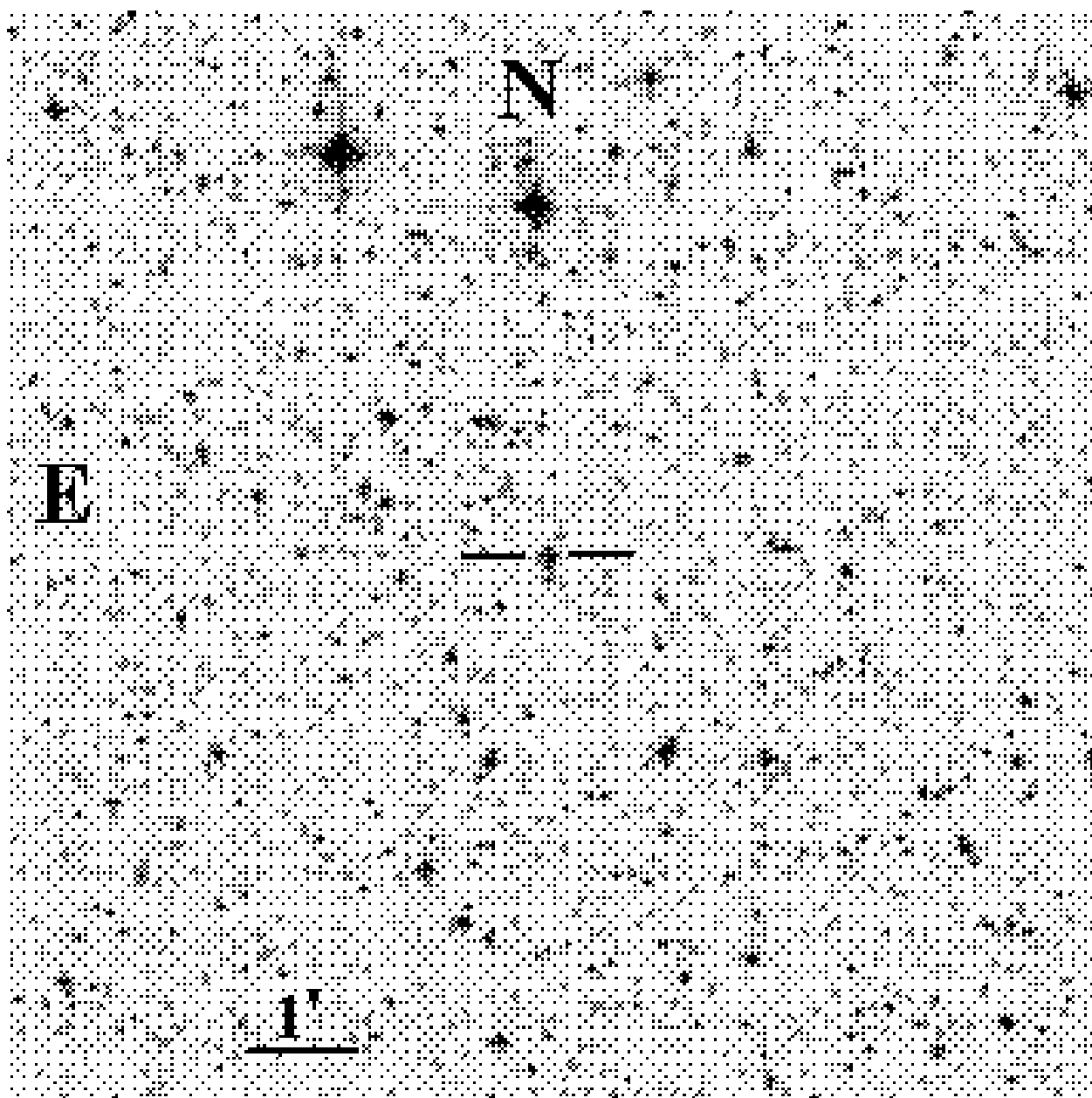


Fig. 37.—Field, 10' on a side, of the star LSS 1274.

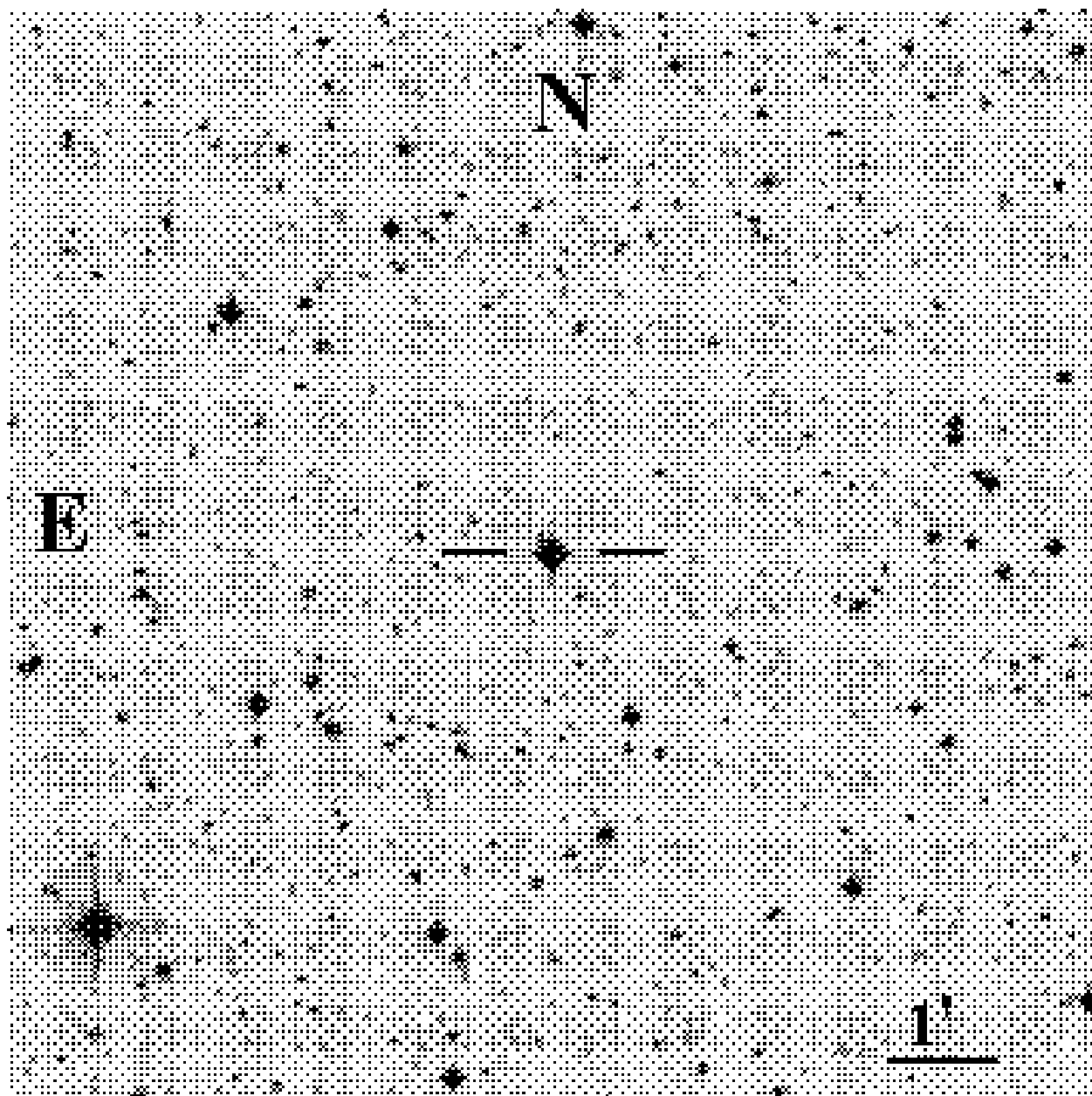


Fig. 38.—Field, 10' on a side, of the star LSS 1275.

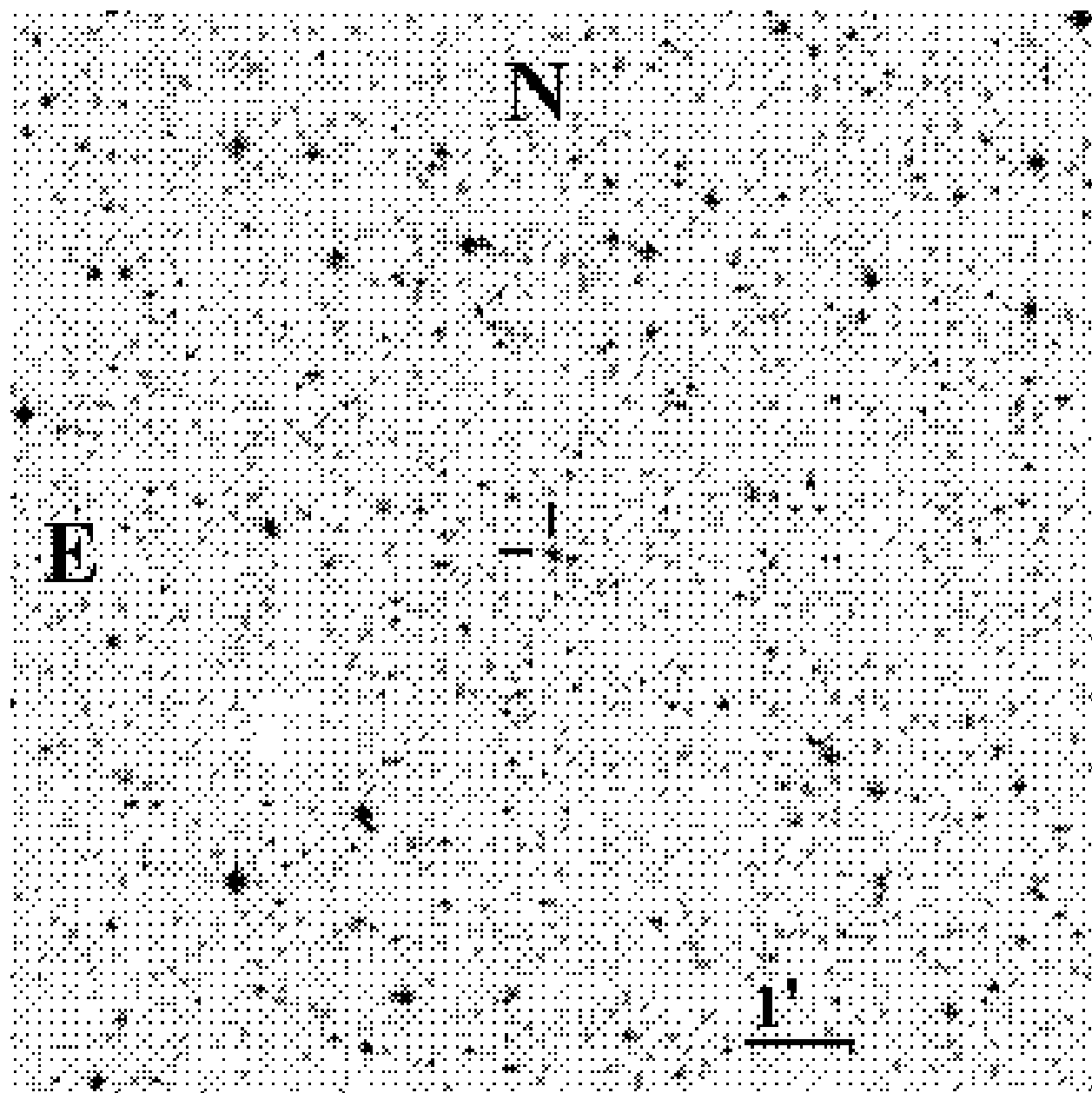


Fig. 39.—Field, 10' on a side, of the star LSS 1349.

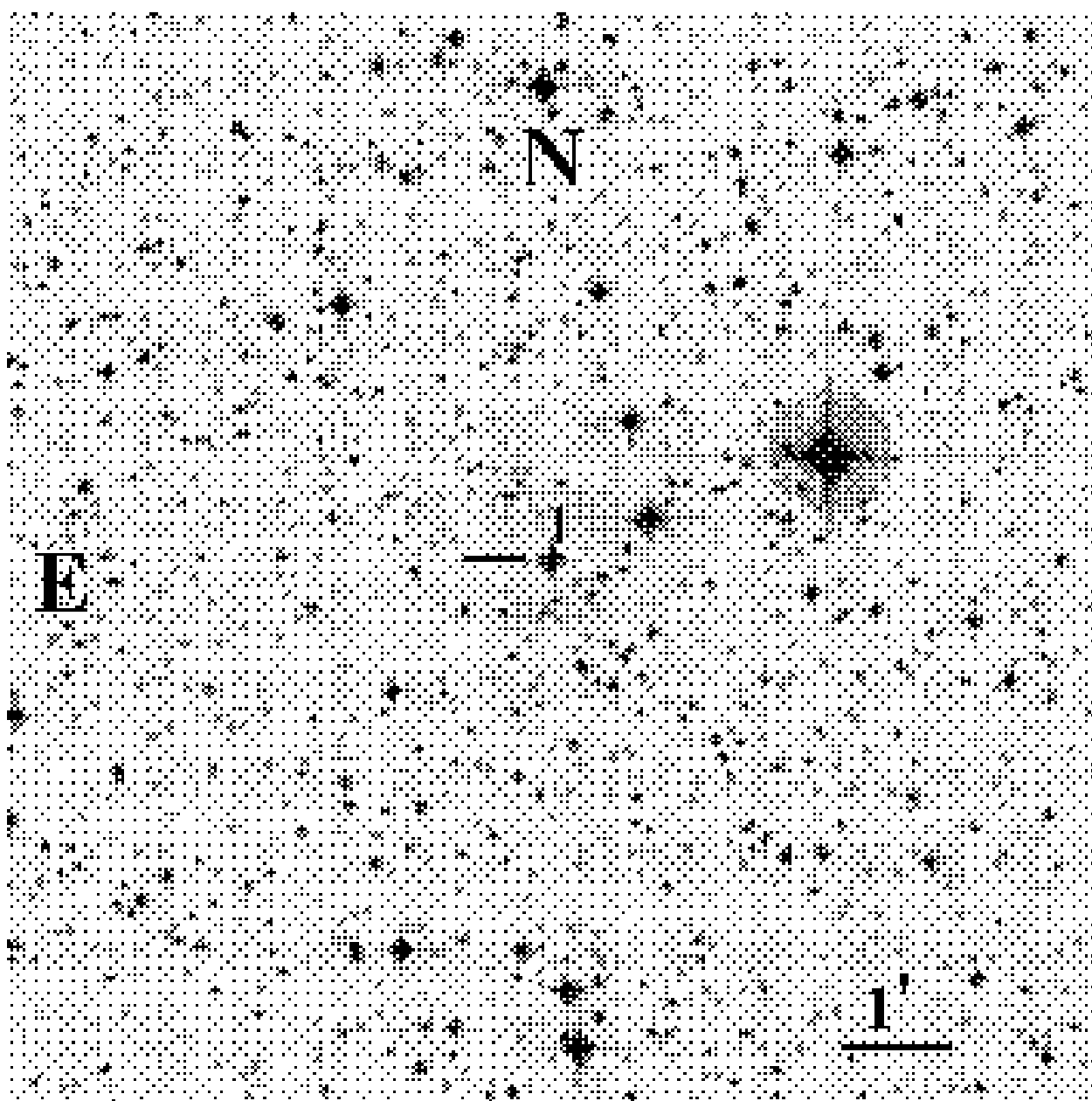


Fig. 40.— Field, 10' on a side, of the star LSS 1362.

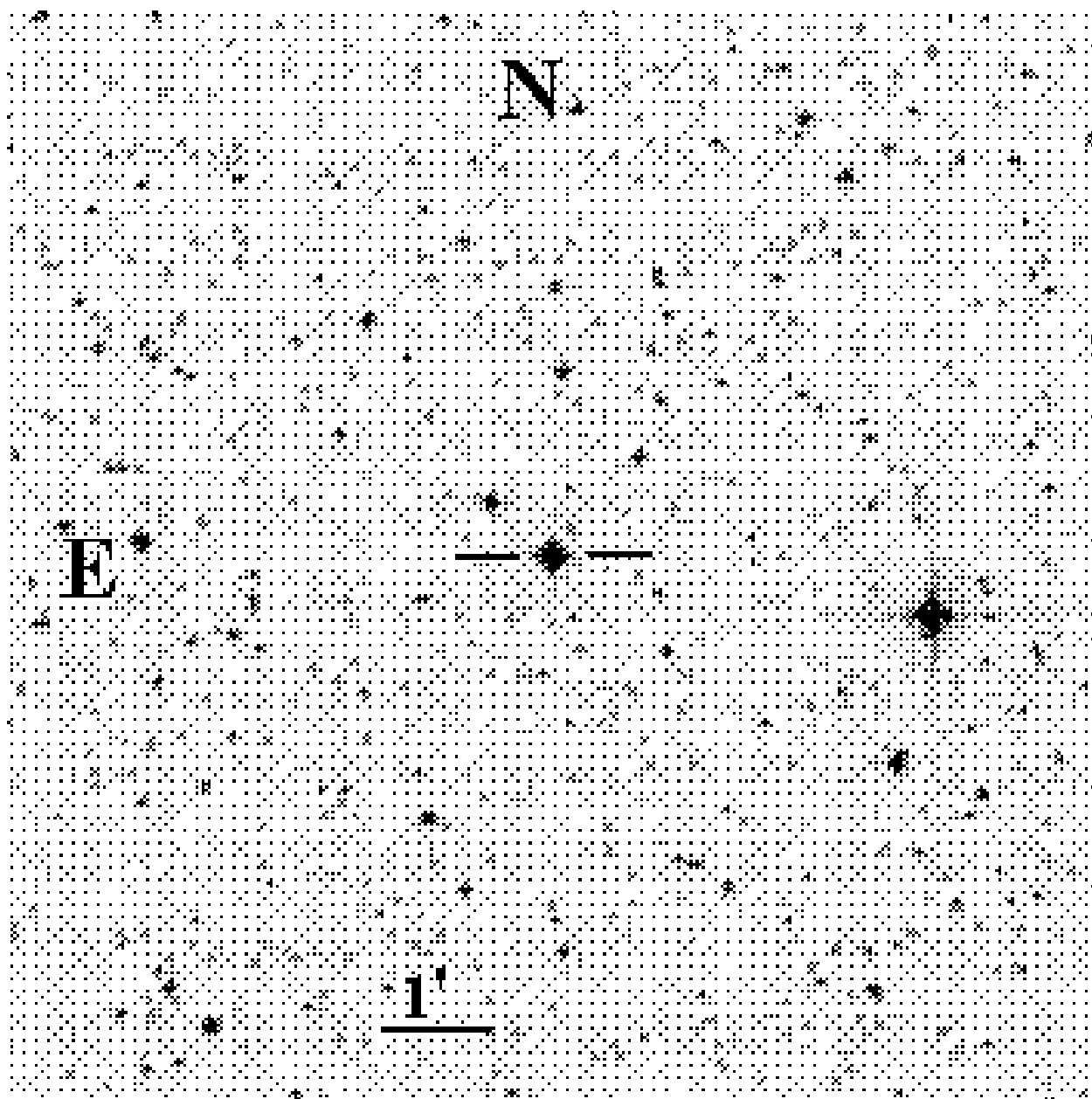


Fig. 41.— Field, 10' on a side, of the star LSE 153.

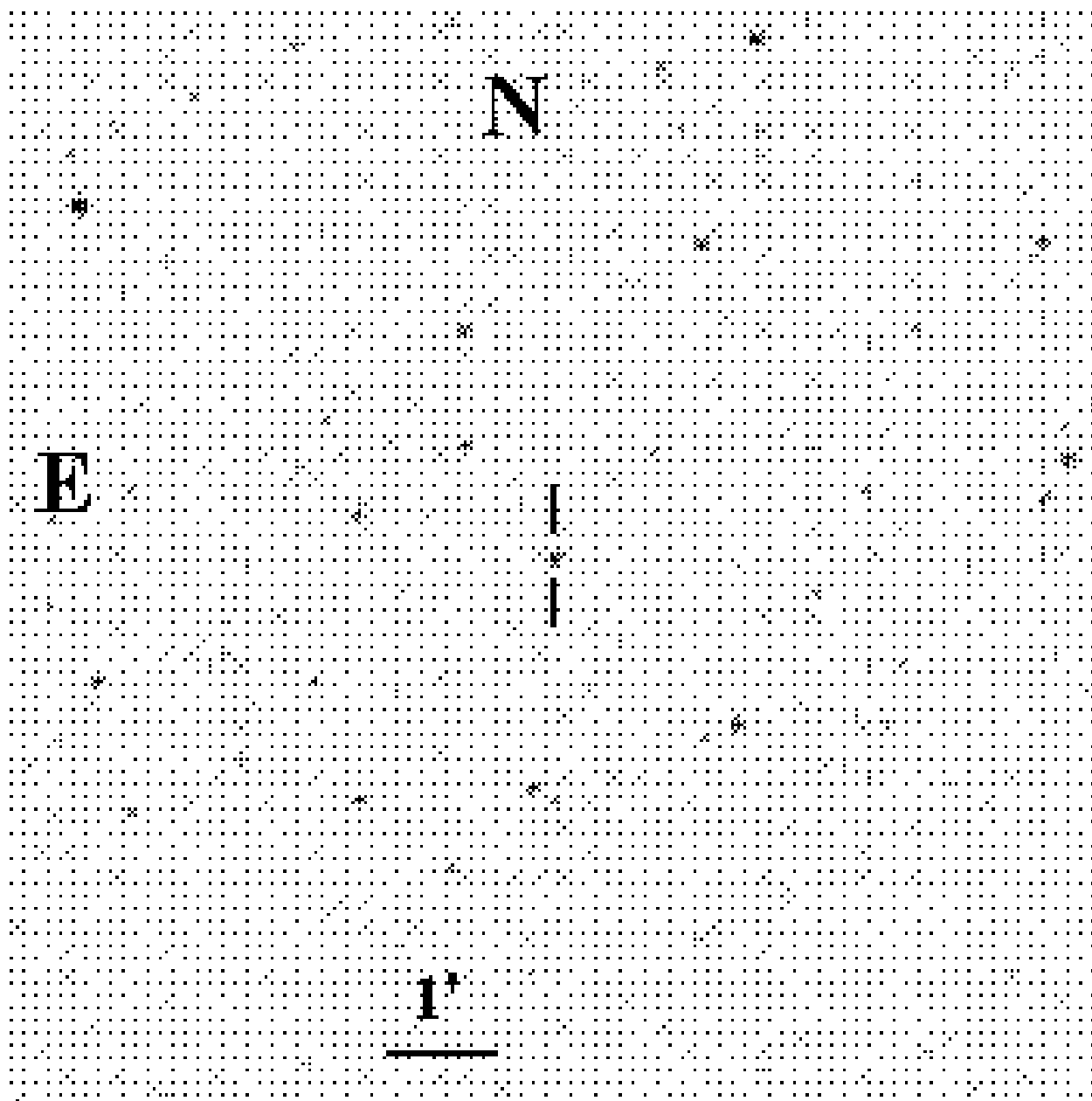


Fig. 42.—Field, 10' on a side, of the star LSE 125.

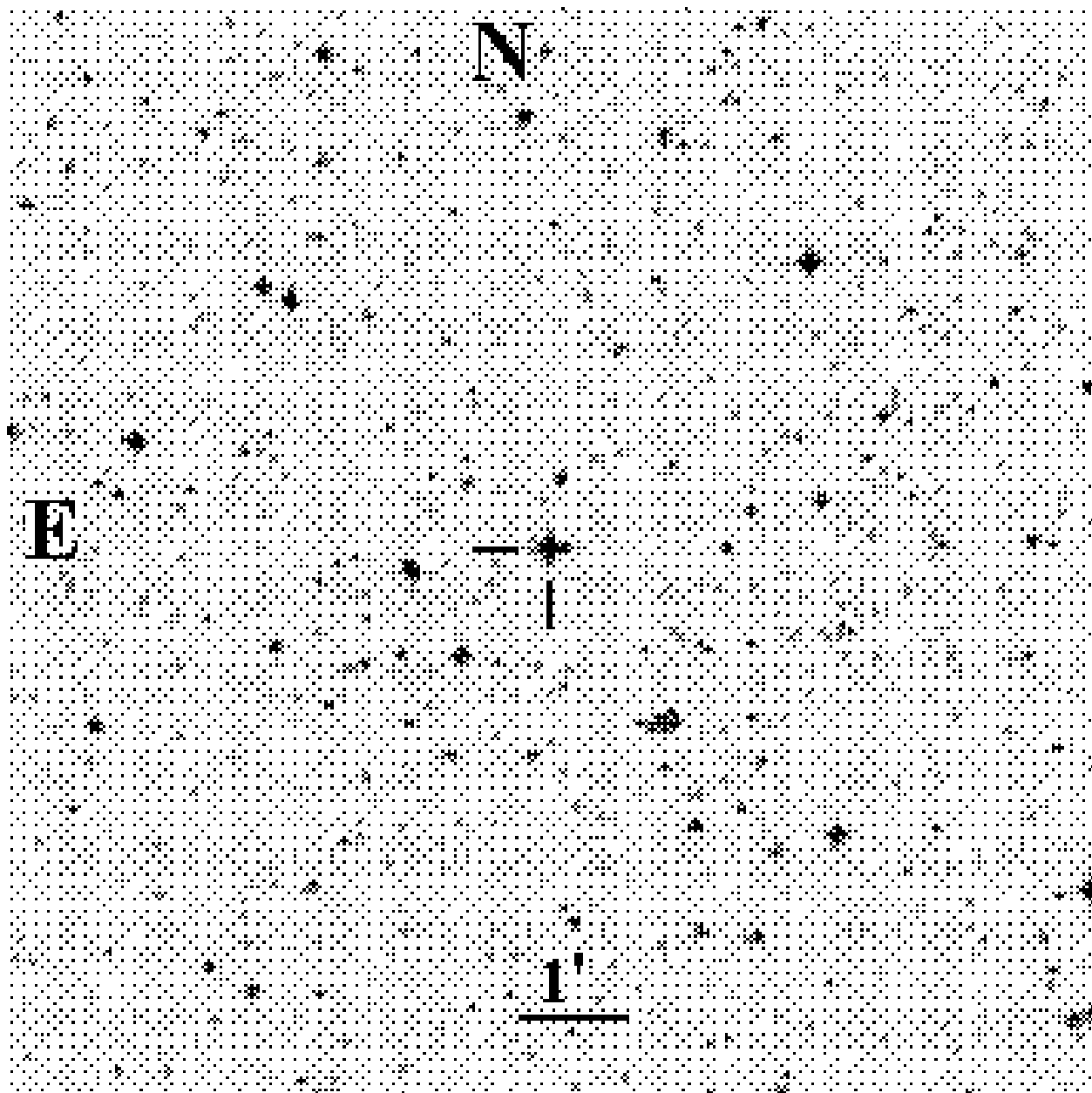


Fig. 43.— Field, 10' on a side, of the star LSE 234.

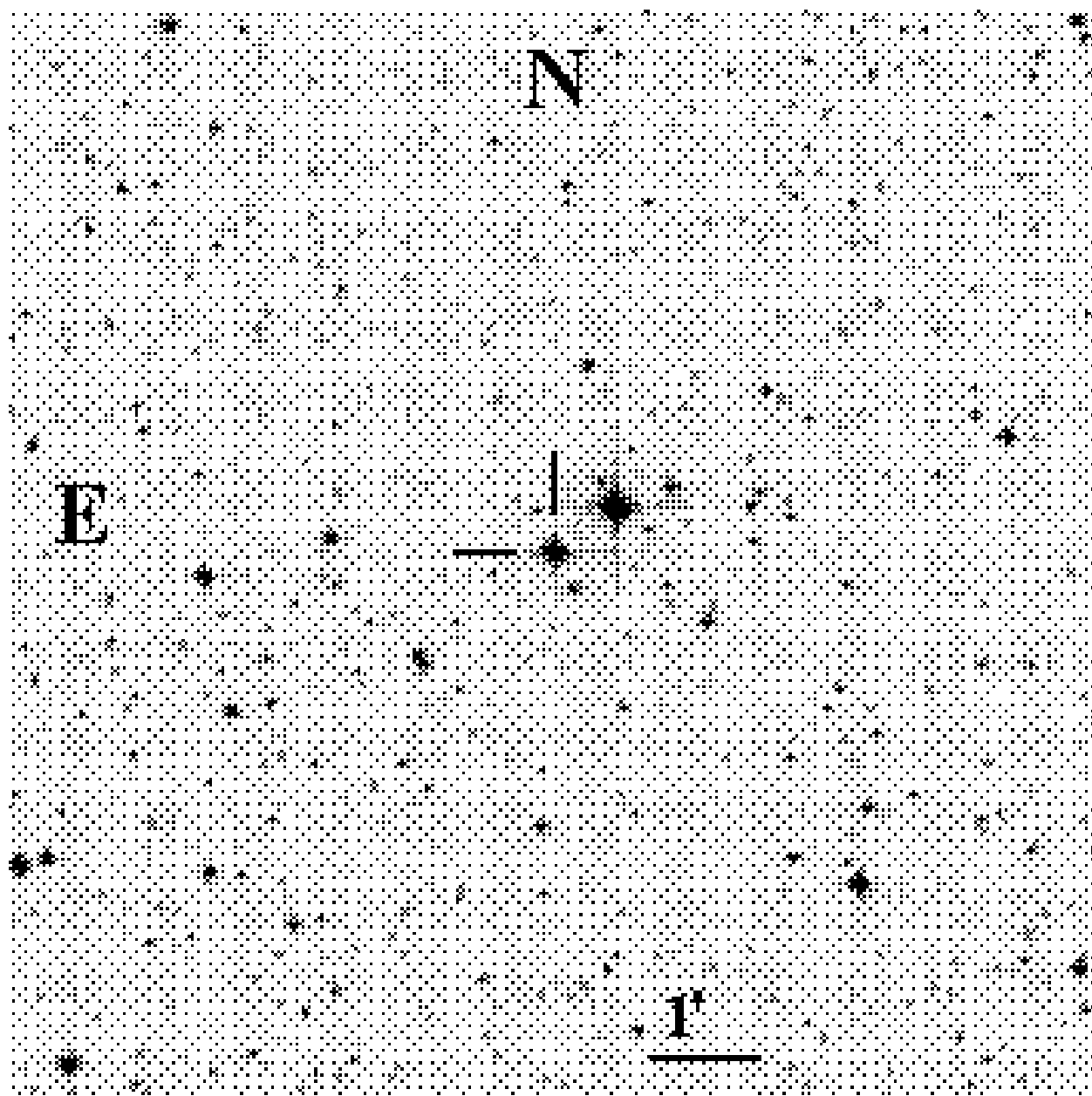


Fig. 44.—Field, 10' on a side, of the star LSE 263.

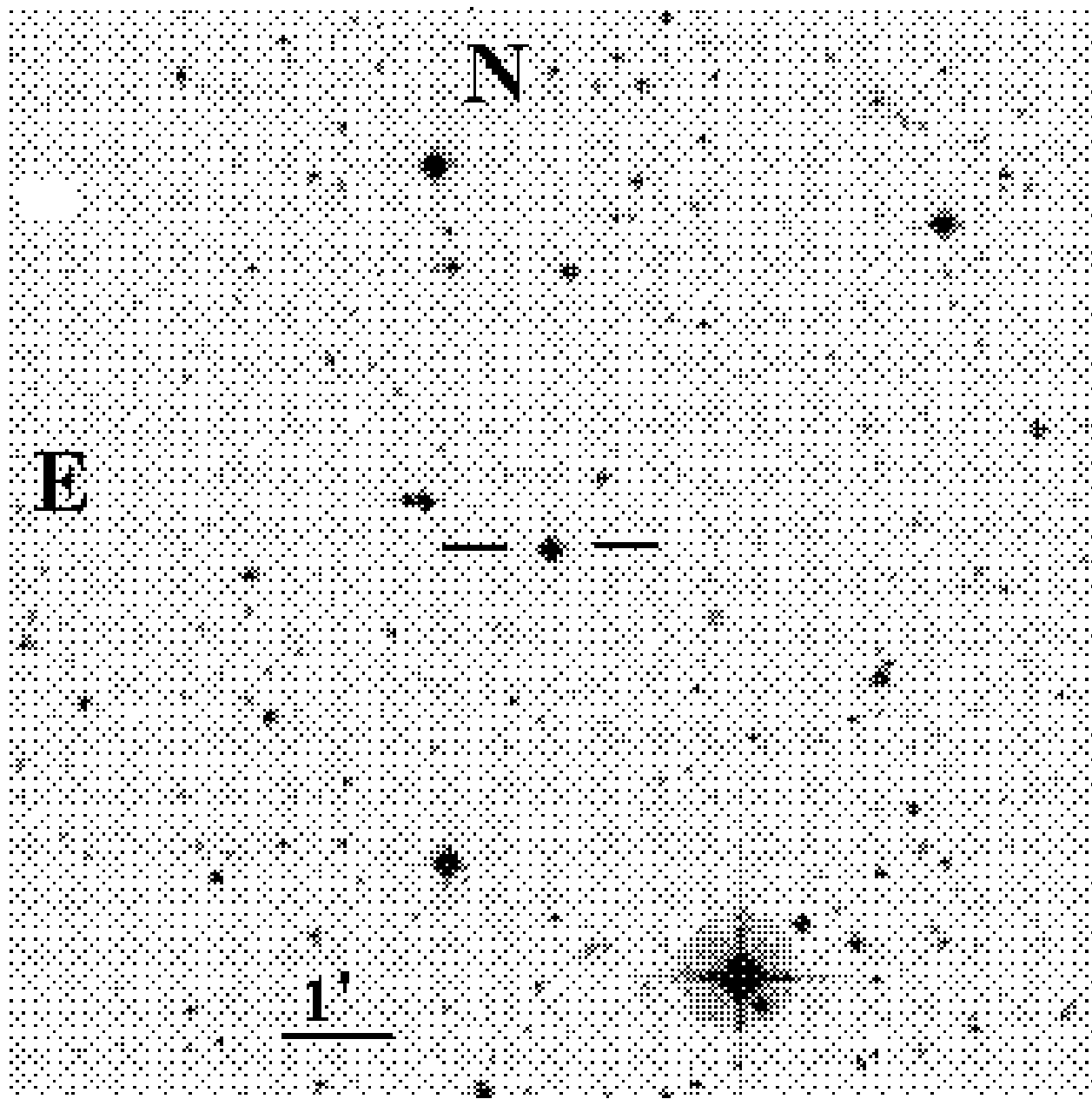


Fig. 45.—Field, $10'$ on a side, of the star JL 25.

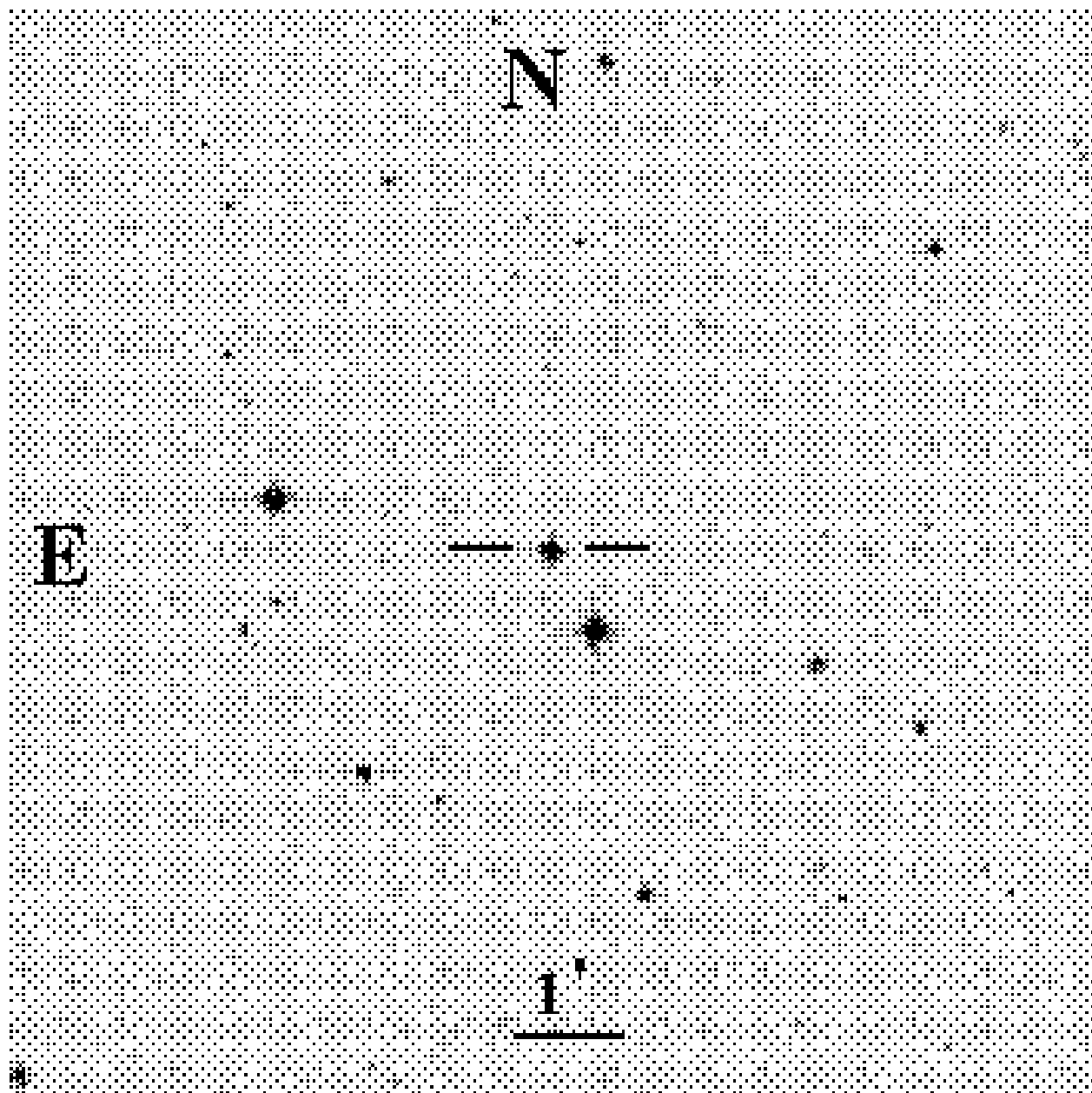


Fig. 46.—Field, 10' on a side, of the star LB 1516.

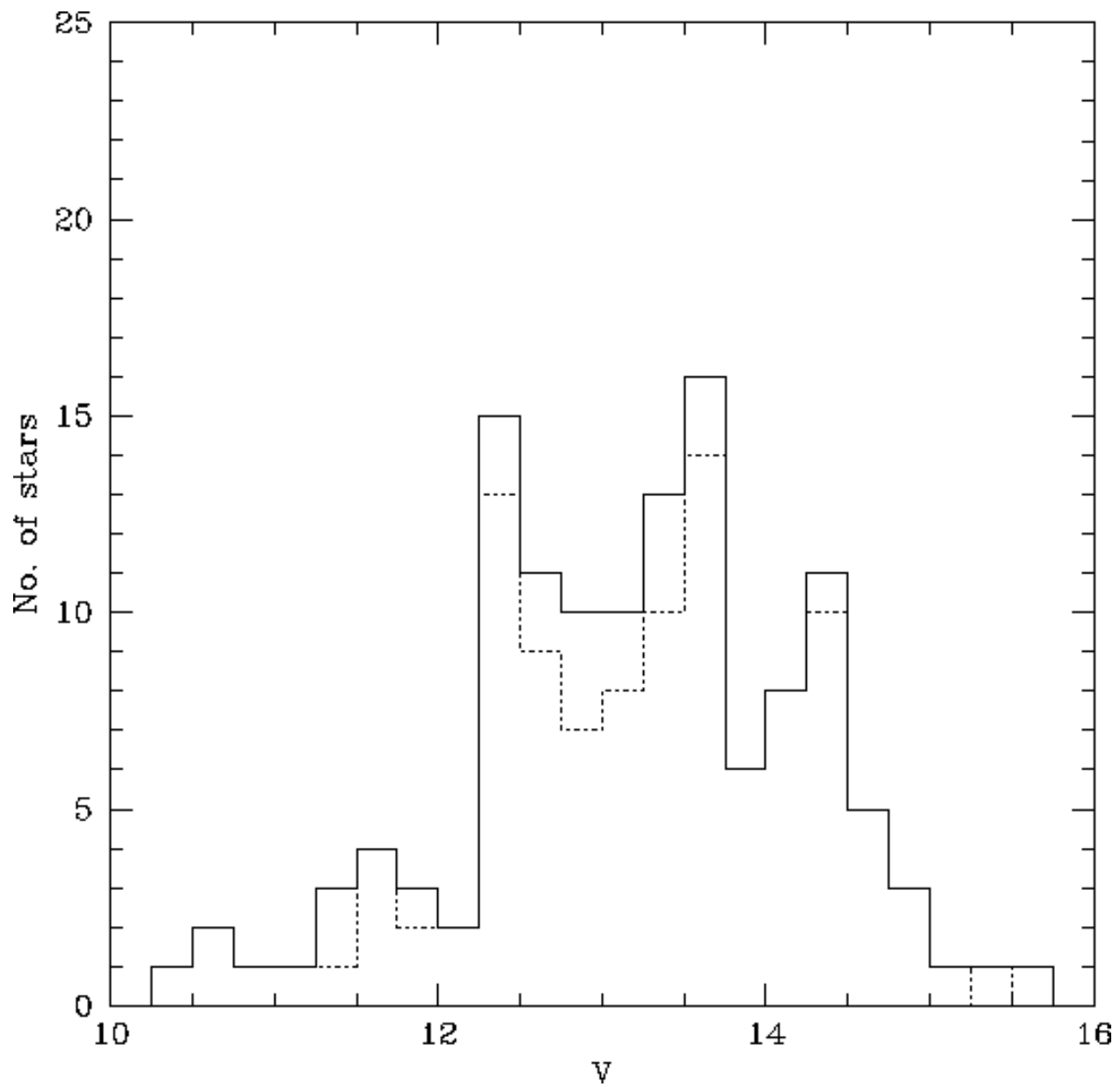


Fig. 47.— The magnitude distribution for the new standards stars listed in Table 1 (dotted line) and all stars in both Tables 1 and 4 (solid line) in intervals of 0.25 V mag.

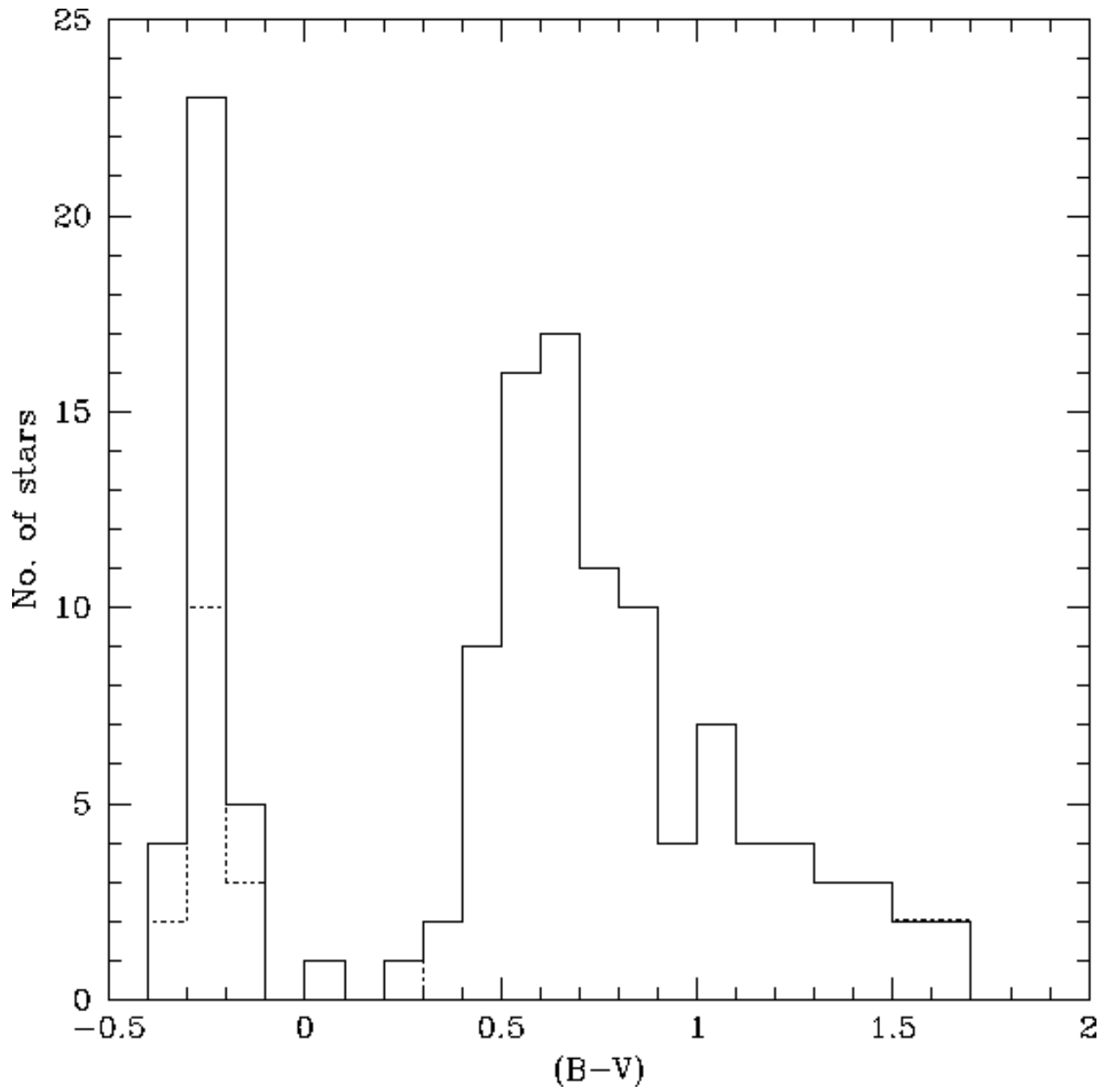


Fig. 48.— The distribution in $(B-V)$ color index for the new standards stars listed in Table 1 (*dotted line*) and all stars in both Tables 1 and 4 (*solid line*) in intervals of 0.1 mag.

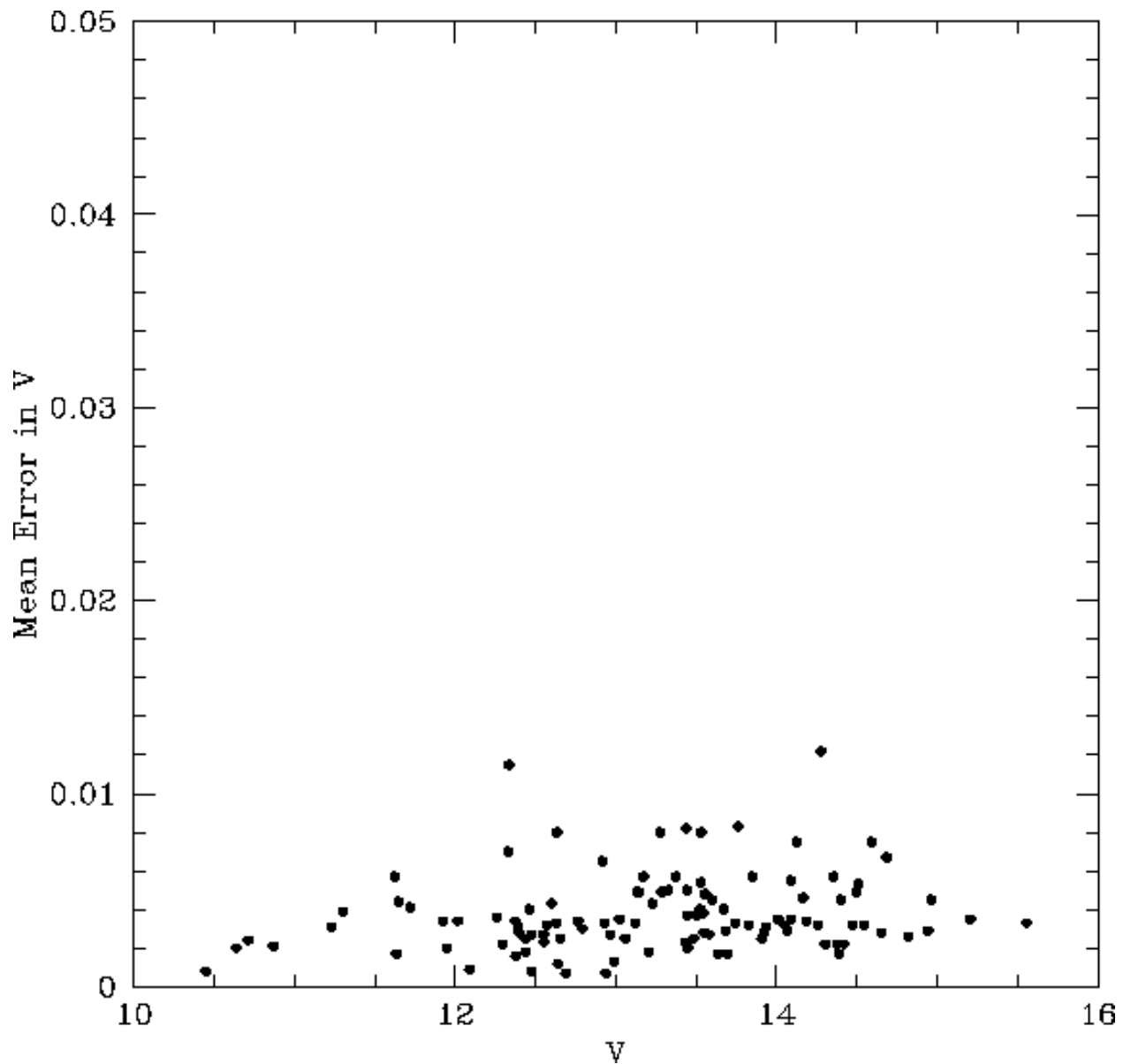


Fig. 49.— The mean error of the mean of a single observation in V for the new standard stars as a function of V .

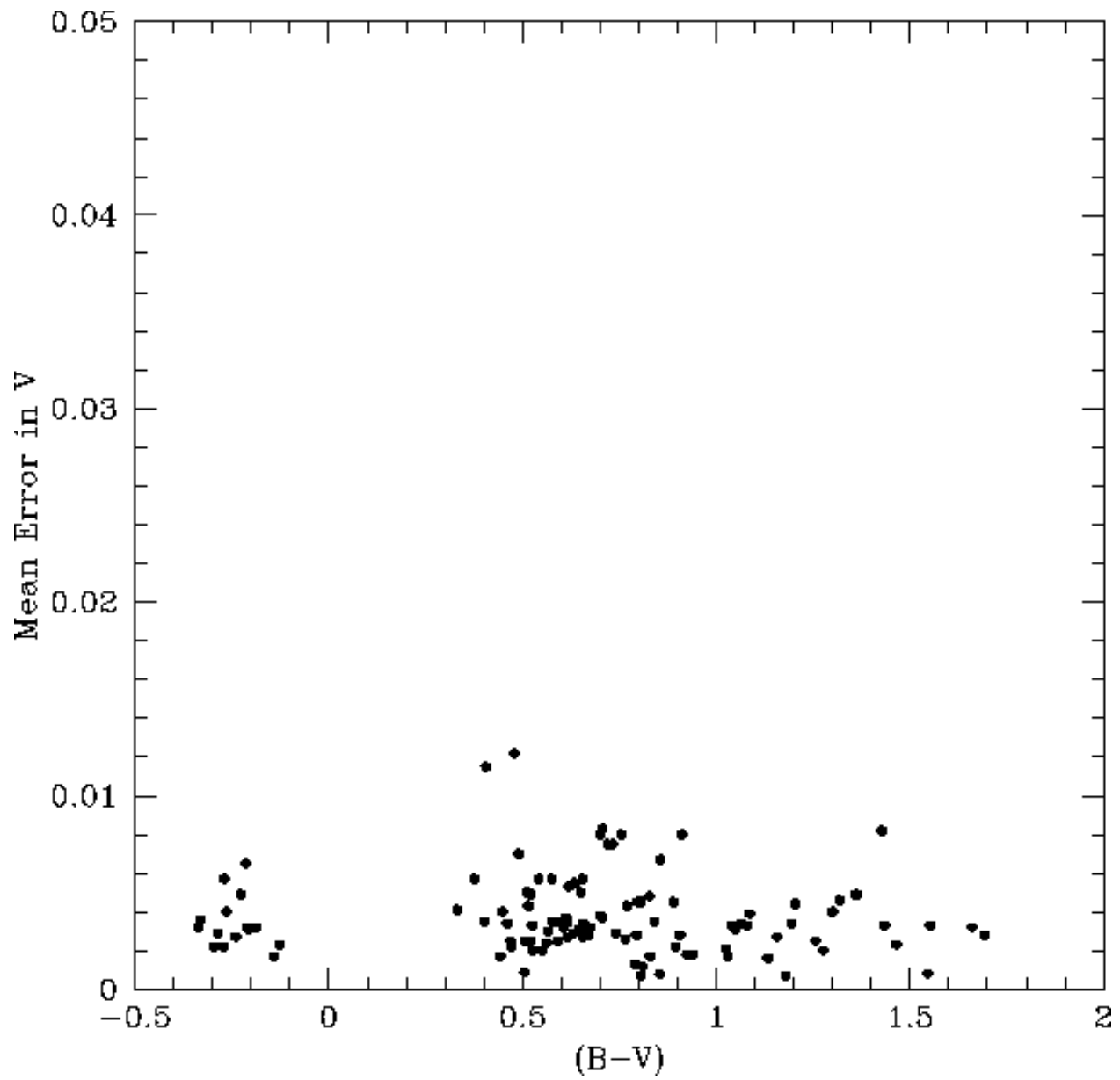


Fig. 50.— The mean error of the mean of a single observation in V for the new standard stars as a function of $(B - V)$.

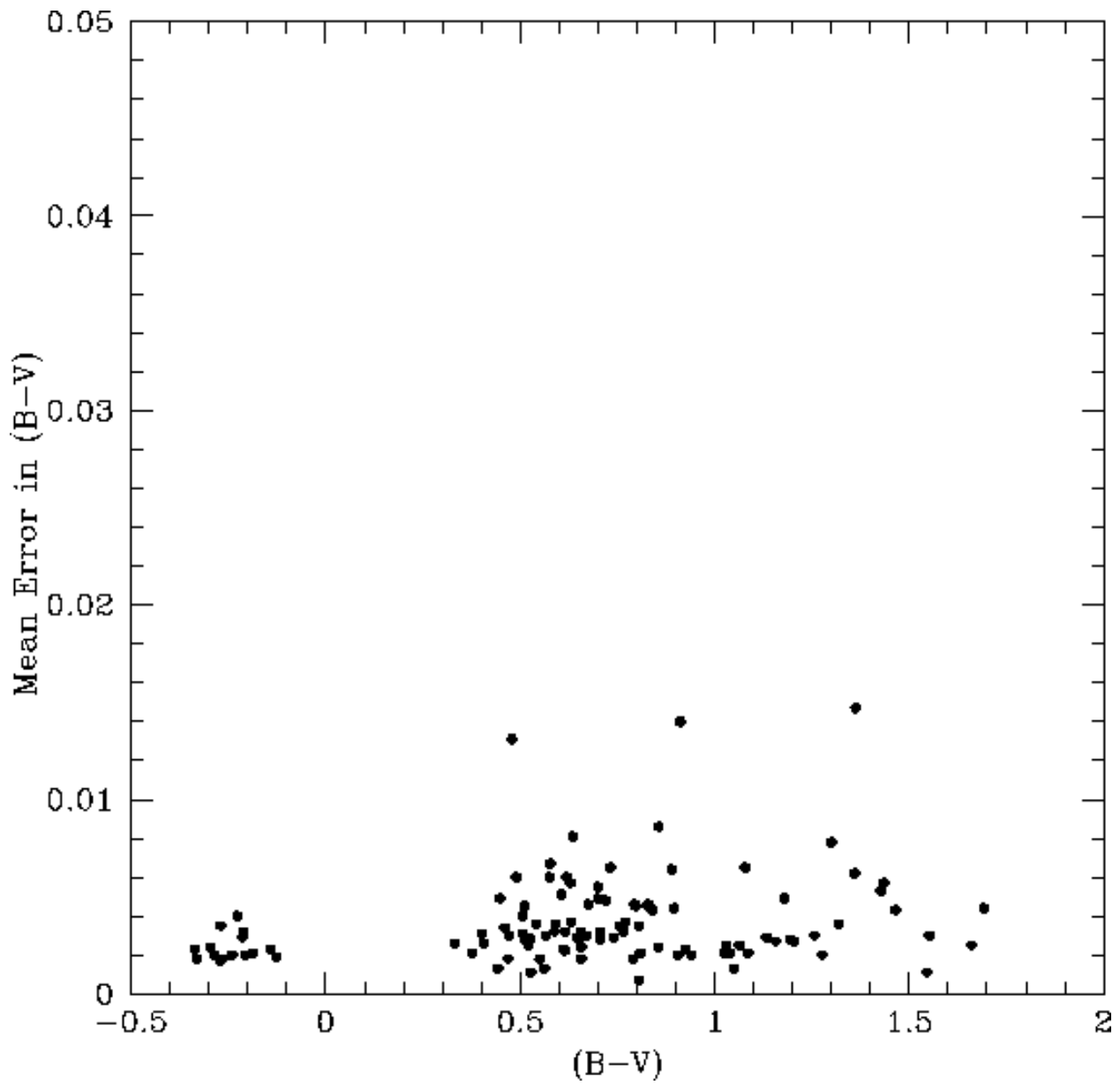


Fig. 51.— The mean error of the mean of a single observation in $(B - V)$ for the new standard stars as a function of $(B - V)$.

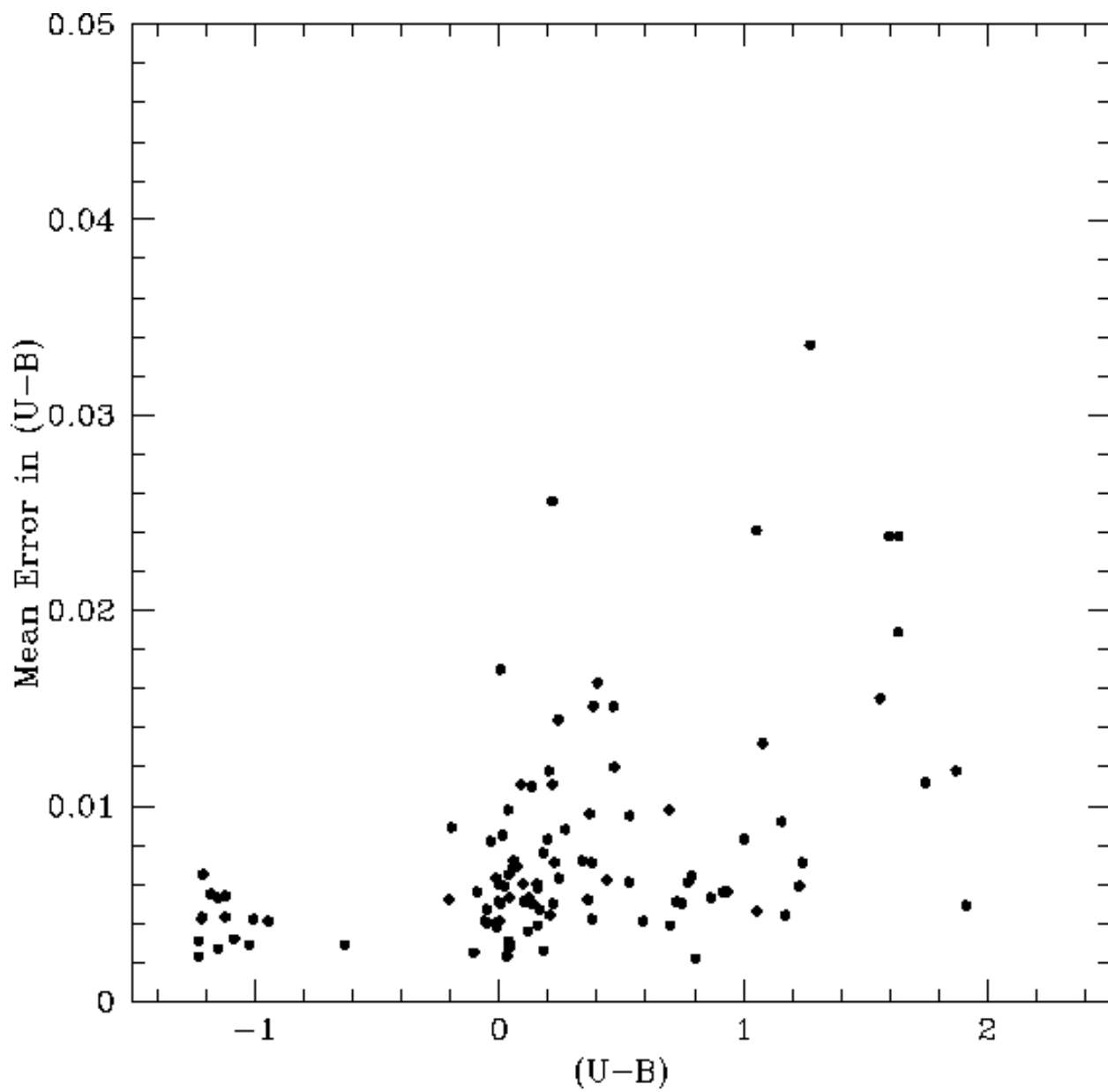


Fig. 52.— The mean error of the mean of a single observation in $(U - B)$ for the new standard stars as a function of $(U - B)$.

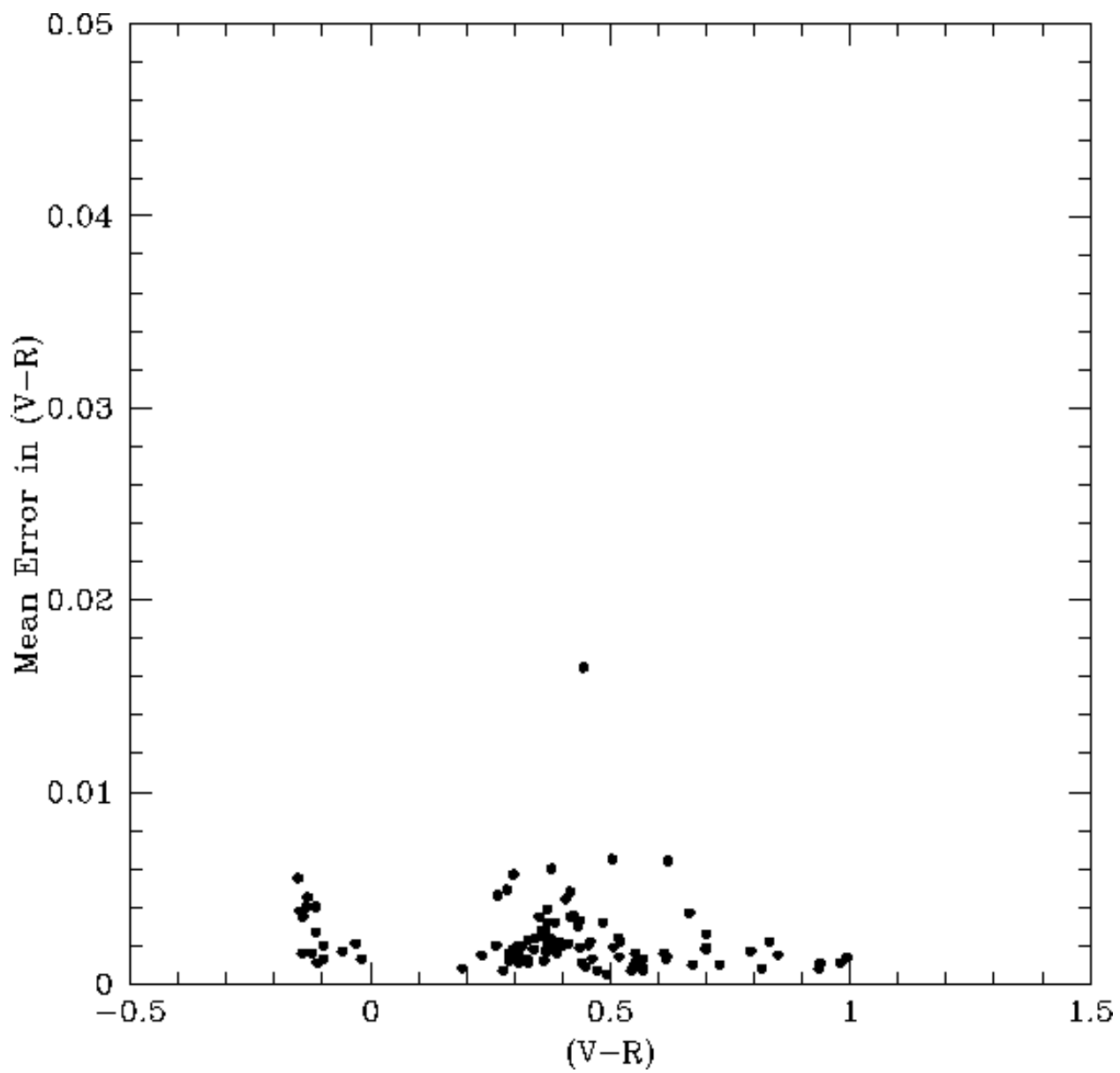


Fig. 53.— The mean error of the mean of a single observation in $(V - R)$ for the new standard stars as a function of $(V - R)$.

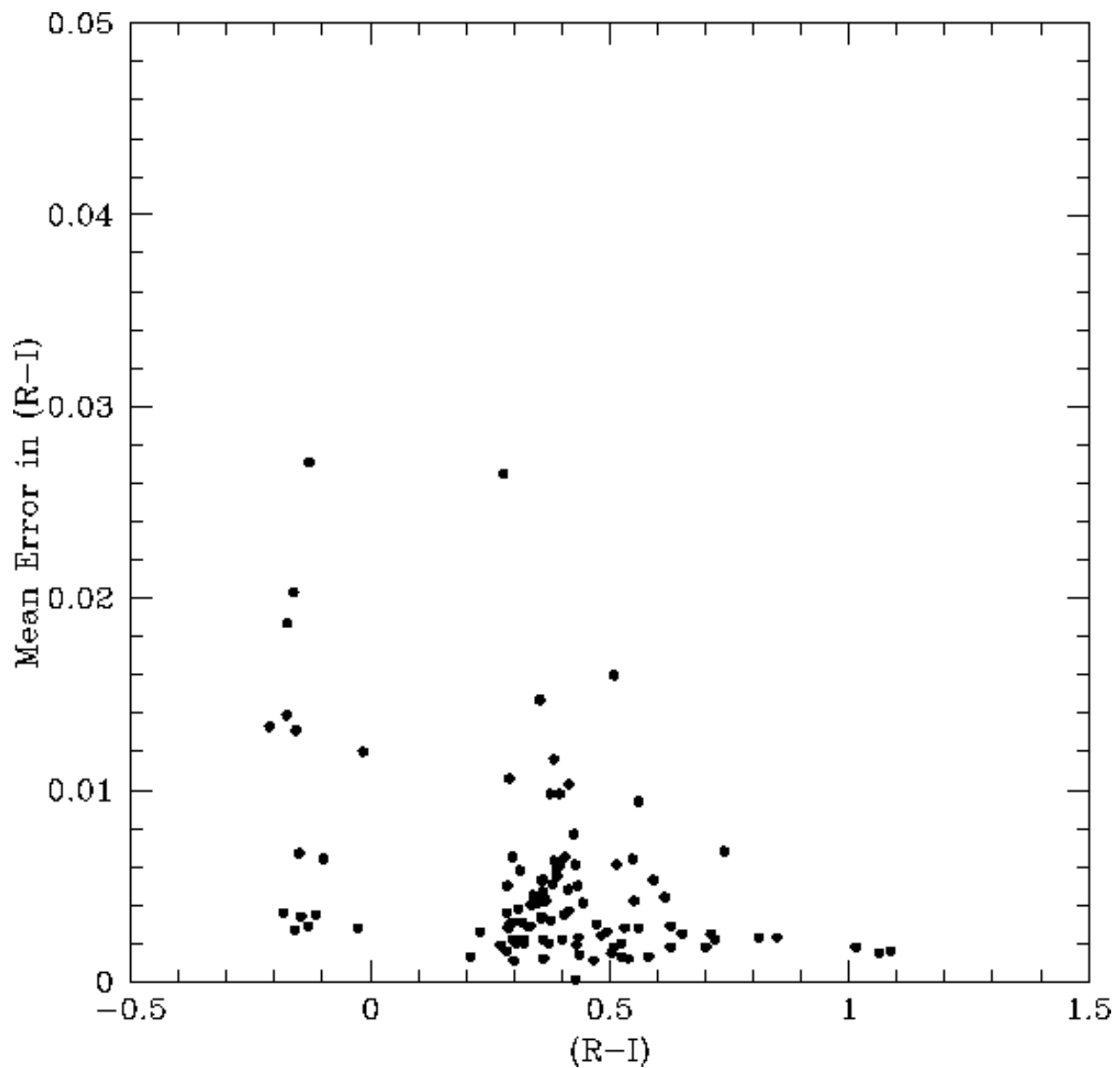


Fig. 54.— The mean error of the mean of a single observation in $(R-I)$ for the new standard stars as a function of $(R-I)$.

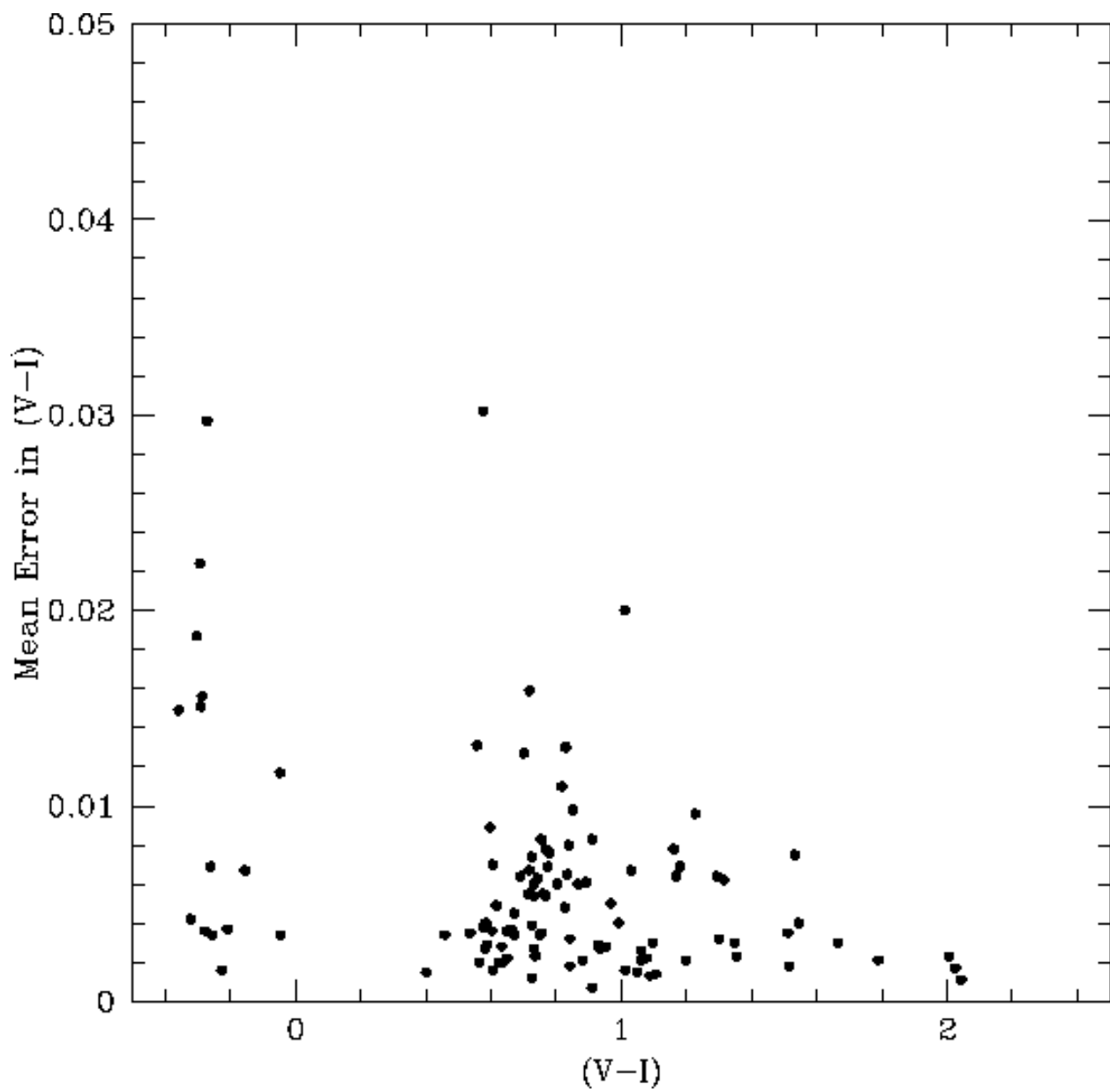


Fig. 55.— The mean error of the mean of a single observation in $(V - I)$ for the new standard stars as a function of $(V - I)$.

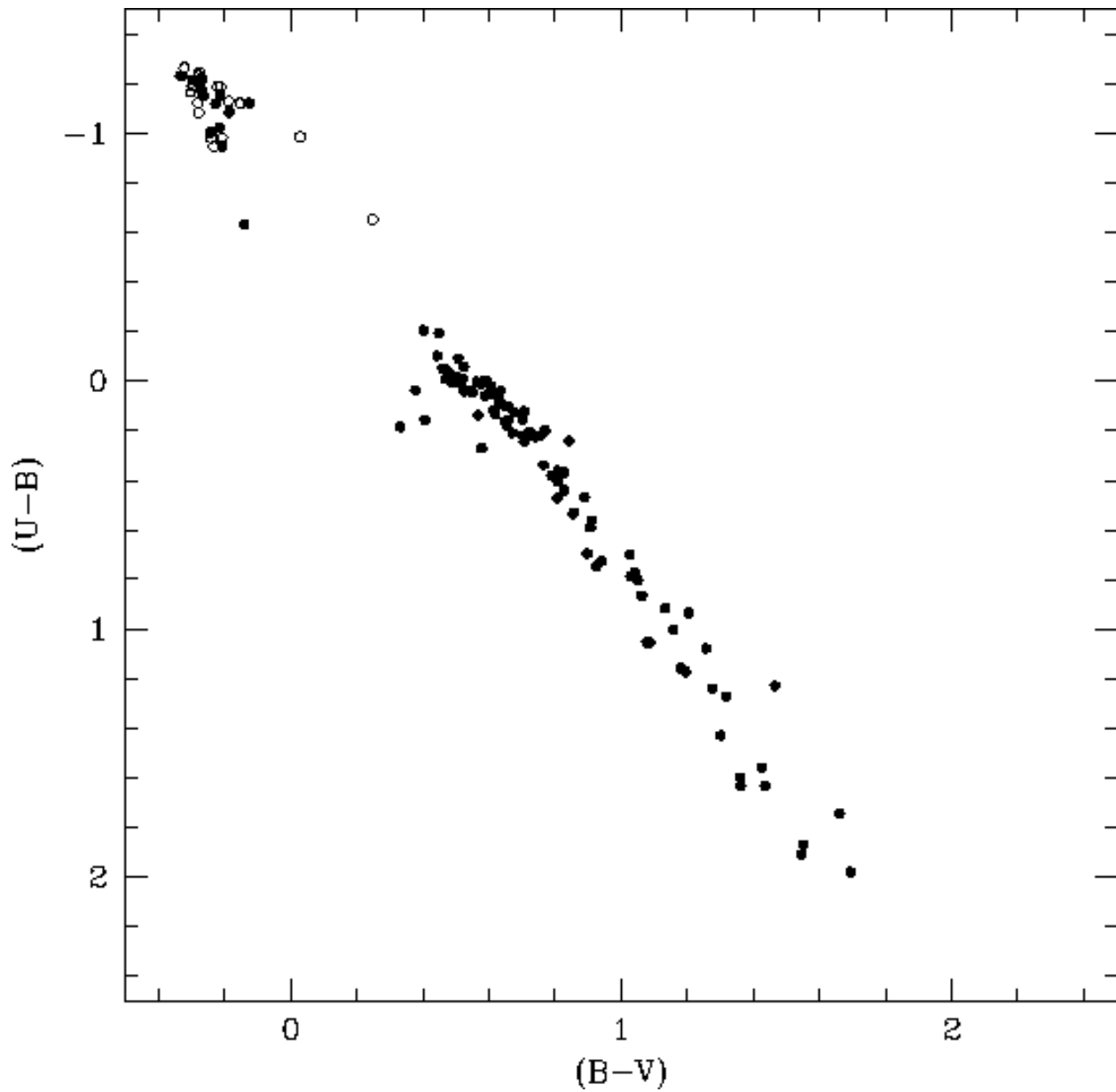


Fig. 56.— The $[(U - B), (B - V)]$ color-color plot for all stars measured in this paper, filled circles from Table 1 and open circles from Table 4.

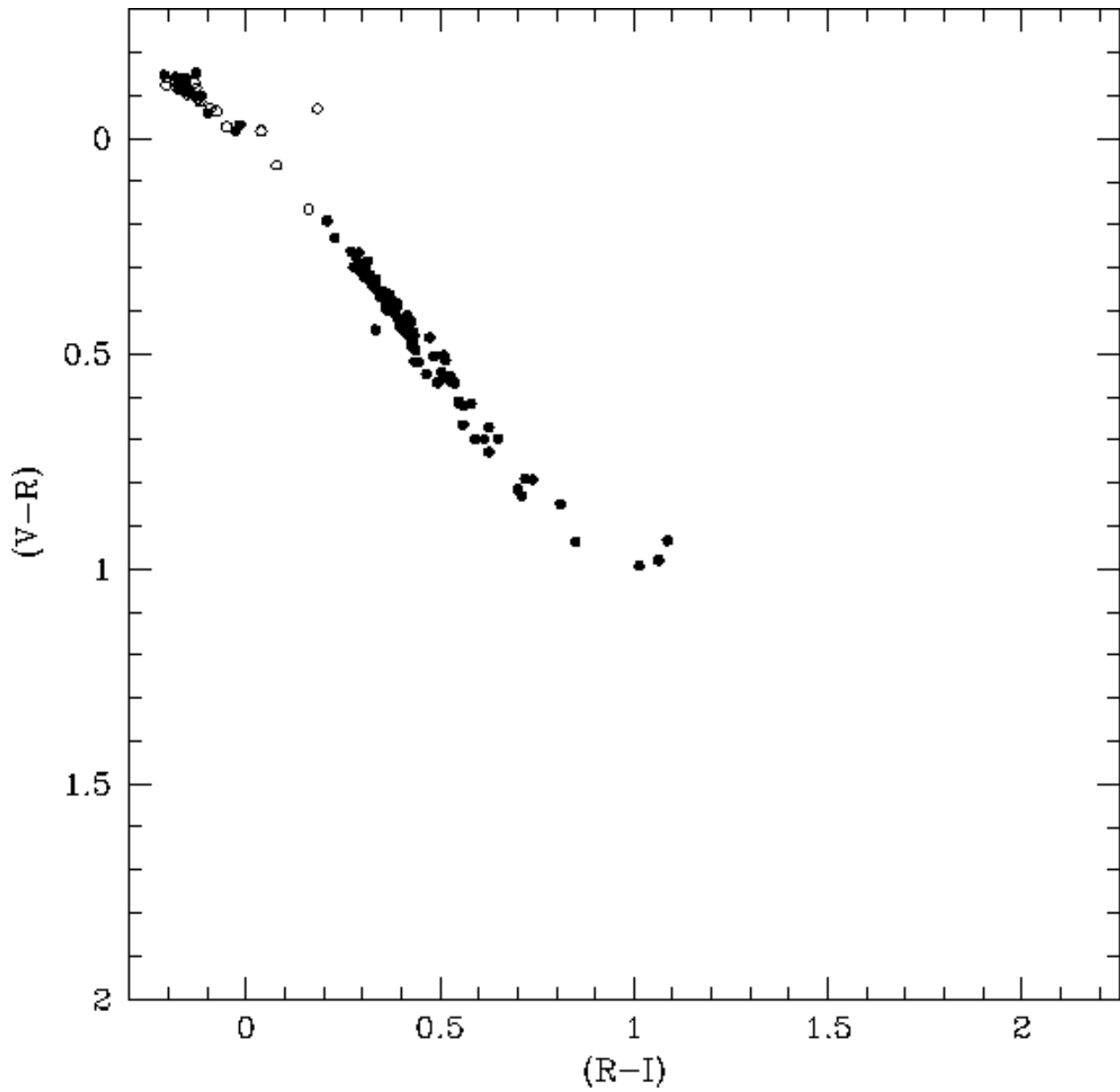


Fig. 57.— The $[(V - R), (R - I)]$ color-color plot for all stars measured in this paper, filled circles from Table 1 and open circles from Table 4.